Seamounts and Ferromanganese Crusts Within and Near the U.S. EEZ Off California– Data for RV *Farnella* Cruise F7-87-SC

By James R. Hein, Jane A. Reid, Tracey A. Conrad, Rachel E. Dunham, David A. Clague, Marjorie S. Schulz, and Alicé S. Davis

Open-File Report 2010–1069

U.S. Department of the Interior
U.S. Geological Survey

U.S. Department of the Interior
KEN SALAZAR, Secretary

U.S. Geological Survey
Marcia K. McNutt, Director

U.S. Geological Survey, Reston, Virginia: 2010

For product and ordering information:
World Wide Web: *http://www.usgs.gov/pubprod*
Telephone: 1-888-ASK-USGS

For more information on the USGS—the Federal source for science about the Earth,
its natural and living resources, natural hazards, and the environment:
World Wide Web: *http://www.usgs.gov*
Telephone: 1-888-ASK-USGS

Suggested citation:
Hein, J.R., Reid, J.A., Conrad, T.A., Dunham, R.E., Clague, D.A., Schulz, M.S., and Davis, A.S., 2010, Seamounts and ferromanganese crusts within and near the U.S. EEZ off California--Data for RV *Farnella* cruise F7-87-SC: U.S. Geological Survey Open-File Report 2010-1069, 124 p. [*http://pubs.usgs.gov/of/2010/1069/*].

Any use of trade, product, or firm names is for descriptive purposes only and does not imply endorsement by the U.S. Government.

Although this report is in the public domain, permission must be secured from the individual copyright owners to reproduce any copyrighted material contained within this report.

Cover: Photograph of cut sample from Ben Seamount; porphyritic basalt with 15-mm-thick Fe-Mn crust (from figure 59 *A*)

Contents

Conversion Factors vii
Introduction 1
Ship-Board Operations 1
Shore-Based Analyses 1
Data Organization 2
Data Description 2
Rodriguez Seamount 2
San Marcos Seamount 3
Adam and Hoss Seamounts 3
Little Joe Seamount 3
Ben Seamount 4
Jasper and Flint Seamounts 4
Rock Mineralogy and Geochemistry 4
Fe-Mn Crust Mineralogy and Geochemistry 5
Acknowledgments 6
References Cited 7

Figures

Figure 1. Map showing islands (green) and seamounts within the Southern California Borderland. Seamounts pertaining to this study are in bold type; the 200 nmi U.S. Exclusive Economic Zone (EEZ) boundary is shown in red 64
Figure 2. Map showing Rodriguez Seamount bathymetry. D, dredge; DSC, deep-sea camera; and R, geophysical line locations; contour interval is 100 m. 65
Figure 3. Map showing Rodriguez Seamount ETOPO bathymetry. D, dredges in red; DSC, deep-sea camera in purple; and R, geophysical lines in black; contour interval is 100 m. 66
Figure 4. Seabed photos of Rodriguez Seamount courtesy of MBARI, collected during the 2004 and 2003 cruises aboard the RV *Western Flyer*. *A*, Bedded volcaniclastic sandstone at 664 m water depth, dive T628. *B*, Cross section of bedded volcaniclastic sandstone at 681 m showing evidence of beach deposition, dive T631 (Paduan and others, 2009). *C*, An eroded volcaniclastic ridge approximately 0.25 m high at 838 m that has trapped basalt talus, dive T661. *D*, Outcrop and perhaps a vent at the summit of a volcanic cone at 755 m, dive T630. *E*, Pitted and eroded pavement typical of volcaniclastic material at 999 m, dive T661. *F*, Ferromanganese crusts on lava flow at 1,694 m, with a pink mushroom coral (*Anthomastus ritteri*), dive T629. 67
Figure 5. Rodriguez Seamount 3.5 kHz bathymetry line R1; VE, vertical exaggeration. 68
Figure 6. Rodriguez Seamount 3.5 kHz bathymetry line R2; VE, vertical exaggeration. 69
Figure 7. Rodriguez Seamount 3.5 kHz bathymetry line R3; VE, vertical exaggeration. 70
Figure 8. Rodriguez Seamount 3.5 kHz bathymetry line R4; VE, vertical exaggeration. 71
Figure 9. Rodriguez Seamount 3.5 kHz bathymetry line R5 with D, dredges 1-4; NR, No Recovery; LB, Lost Bag; VE, vertical exaggeration. 72
Figure 10. Rodriguez Seamount 3.5 kHz bathymetry. DSC1, deep-sea camera line 1. 73
Figure 11. Map showing San Marcos Seamount bathymetry. D, dredge; and SM, geophysical line locations for San Marcos Seamount; contour interval is 100 m. 74

Figure 12. Seabed photos of San Marcos Seamount courtesy of MBARI, collected during a 2004 cruise aboard the RV *Western Flyer*; all photos from dive T669. *A*, pillow lava at 2,334 m. *B*, volcaniclastic deposit of coarse-grained spatter at 2,347 m, with a sea worm, Aphroditidae. *C*, outcrop at 2,029 m thought to be welded volcaniclastic spatter. *D*, light colored probably pelagic sediment pockets with ferromanganese encrusted volcaniclastic spatter at 2,343 m. 75
Figure 13. San Marcos Seamount 3.5 kHz bathymetry line SM1 with D, dredge; VE, vertical exaggeration. 76
Figure 14. San Marcos Seamount 3.5 kHz bathymetry line SM2; VE, vertical exaggeration. 77
Figure 15. San Marcos Seamount 3.5 kHz bathymetry line SM3; VE, vertical exaggeration. 78
Figure 16. San Marcos Seamount 3.5 kHz bathymetry line SM4; VE, vertical exaggeration. 79
Figure 17. San Marcos Seamount 3.5 kHz bathymetry line SM5; VE, vertical exaggeration. 80
Figure 18. Maps showing A, Adam Seamount; and B, Hoss Seamount; bathymetry and D, dredge locations; contour interval for both seamounts is 100 m. 81
Figure 19. Map showing Little Joe Seamount bathymetry, D, dredge; and LJ, geophysical line locations; contour interval is 100 m. 82
Figure 20. Seabed photos of Little Joe Seamount courtesy of MBARI, collected during a 2004 cruise aboard the RV *Western Flyer*; all photos from dive T668. *A*, Pillow basalt at 2,161 m. *B*, A stalked mushroom coral (*Anthomastus ritteri*) on pillow basalt at 2,247 m. *C*, Truncated pillow lava showing cross section of radial jointing due to contraction of the lava during cooling at 2,353 m. *D*, Talus of pillow lava fragments at 2,597 m. *E*, Slabs of volcaniclastic rock and pockets of pelagic sediment at 2,385 m. *F*, Small mound vent or hornito at 2,335 m. 83
Figure 21. Little Joe Seamount 3.5 kHz bathymetry line LJ1 with D, dredges 12-14; NR, No Recovery; VE, vertical exaggeration. 84
Figure 22. Little Joe Seamount 3.5 kHz bathymetry line LJ2; VE, vertical exaggeration. 85
Figure 23. Little Joe Seamount 3.5 kHz bathymetry line LJ3; VE, vertical exaggeration. 86
Figure 24. Little Joe Seamount 3.5 kHz bathymetry line LJ4; VE, vertical exaggeration. 87
Figure 25. Little Joe Seamount 3.5 kHz bathymetry line LJ5; VE, vertical exaggeration. 88
Figure 26. Little Joe Seamount 3.5 kHz bathymetry line LJ6; VE, vertical exaggeration. 89
Figure 27. Map showing Ben Seamount bathymetry, D, dredge; and B, geophysical line locations; contour interval is 100 m…… 90
Figure 28. Map showing Ben Seamount bathymetry, D, dredges in red; and B, geophysical lines in black; contour interval is 100 m. 91
Figure 29. Ben Seamount 3.5 kHz bathymetry line B1; VE, vertical exaggeration. 92
Figure 30. Ben Seamount 3.5 kHz bathymetry line B2. 93
Figure 31. Ben Seamount 3.5 kHz bathymetry line B3; VE, vertical exaggeration. 94
Figure 32. Ben Seamount 3.5 kHz bathymetry line B4. 95
Figure 33. Ben Seamount 3.5 kHz bathymetry line B5; VE, vertical exaggeration. 96
Figure 34. Ben Seamount 3.5 kHz bathymetry line B6. 97
Figure 35. Ben Seamount 3.5 kHz bathymetry line B7 with D, dredges 15-17; NR, No Recovery; LB, Lost Bag; VE, vertical exaggeration. 98
Figure 36. Map showing Jasper and Flint Seamounts bathymetry. D, dredge; DSC, deep-sea camera; and JF, geophysical line locations; contour interval is 100 m; see Figure 37 for close-up of Flint Seamount. 99
Figure 37. Maps showing Jasper and Flint Seamounts bathymetry. D, dredges in red; DSC, deep-sea camera in purple; and JF, geophysical line locations in black; contour interval is 200 m for the seamount map and 100 m for the close-up of Flint Seamount. 100
Figure 38. Jasper Seamount 3.5 kHz bathymetry line JF1; VE, vertical exaggeration. 101
Figure 39. Jasper Seamount single-channel water-gun line JF1; VE, vertical exaggeration. 102
Figure 40. Jasper Seamount 3.5 kHz bathymetry line JF2. 103

Figure 41. Jasper Seamount single-channel water-gun line JF2; VE, vertical exaggeration. 104
Figure 42. Jasper Seamount 3.5 kHz bathymetry line JF3; VE, vertical exaggeration. 105
Figure 43. Jasper Seamount single-channel water-gun line JF3; VE, vertical exaggeration. 106
Figure 44. Jasper and Flint Seamounts 3.5 kHz bathymetry line JF4; VE, vertical exaggeration. 107
Figure 45. Jasper and Flint Seamounts single-channel water-gun line JF4; VE, vertical exaggeration. 108
Figure 46. Flint Seamount 3.5 kHz bathymetry line JF5; VE, vertical exaggeration. 109
Figure 47. Flint Seamount single-channel water-gun line JF5; VE, vertical exaggeration. 110
Figure 48. Flint Seamount 3.5 kHz bathymetry line JF6 with D, dredges 18-22; NR, No Recovery, LB, Lost Bag; VE, vertical exaggeration. 111
Figure 49. Flint Seamount single-channel water-gun line JF6 with D, dredges 18-22; NR, No Recovery, LB, Lost Bag; VE, vertical exaggeration. 112
Figure 50. Flint Seamount 3.5 kHz bathymetry line JF7 with D, dredges 23 and 24; VE, vertical exaggeration. 113
Figure 51. Flint Seamount 3.5 kHz bathymetry DSC2, deep-sea camera line 2. 114
Figure 52. Flint Seamount 3.5 kHz bathymetry DSC3, deep-sea camera line 3. 115
Figure 53. Photographs of dredge hauls. *A*, Dredge D7, Adam Seamount, showing mudstone and Fe-Mn crusts. *B*, Close-up of large center sample from dredge D7 (in *A)* showing Fe-Mn crust coated in places with calcareous mud. *C*, Dredge D8, Adam Seamount, with small rounded Fe-Mn nodules (right half) and basalt with Fe-Mn crust. *D-H*, Dredge D23, Flint Seamount, primarily basalt including pillow fragments with thick Fe-Mn crust, smoothed in places by bottom currents, such as in *E*; the Fe-Mn crust is coated in places with silty mud. 116
Figure 54. Sample photos from Rodriguez (*A*) and San Marcos Seamounts (*B-E*). *A*, D4-1 vesicular basalt with common vesicles. *B*, D5-3B fractured basalt with alteration rims along the fractures, encrusted by cement supported phosphatized carbonate breccia. *C*, D6-32 breccia with vesicular basalt in a phosphate matrix. *D*, D6-30 breccia. *E*, D5-17 basalt with a glass rim. 117
Figure 55. Photographs of cut samples from Adam Seamount. *A*, D8-5, Fe-Mn nodule with a fracture filled with sediment. *B*, D9-25, spherical Fe-Mn nodule with old nodule fragment nucleus and zeolites. *C*, D9-23, nodule with granular Fe-Mn nucleus. *D*, D9-3, volcanic tuff or hyaloclastite mixed with phillipsite-cemented basalt-clast microbreccia; laminated dark-brown Fe-Mn crust averages about 22 mm thick. *E*, D9-9E, 30-mm thick layered Fe-Mn crust on altered hyaloclastite. *F*, D9-9B, 35-mm thick layered Fe-Mn crust on hyaloclastite; a thinner crust occurs on the underside of the sample. *G*, D9-1, crudely bedded, extensively bioturbated, altered (to phillipsite and smectite) volcanic tuff or hyaloclastite. 118
Figure 56. Photographs of cut samples from Hoss (*A-D*) and Little Joe (*E,F*) Seamounts. *A*, D10-3, 25- to 52-mm thick Fe-Mn crust fragment with zeolitic hyaloclastite inclusions. *B*, D10-4, massive 20-mm thick Fe-Mn crust with clasts of hyaloclastite phillipsite and breccia, resting on an altered breccia with Mn cement. *C*, D11-1, laminated and bored calcareous porcellanite. *D*, D11-7, 35- to 55-mm thick Fe-Mn crust with hyaloclastite clasts. *E*, D14-2, massive brown dolomitic mudstone with local dendritic Mn-oxide lining burrows; Fe-Mn crust averages 10 mm thick. *F*, D14-3, phosphorite breccia with a 10-mm thick black Fe-Mn crust. 119
Figure 57. Photographs of cut samples from Ben (*A-C*) and Flint (*D*) Seamounts. *A*, D17-9, porphyritic basalt with 15-mm thick Fe-Mn crust. *B*, D17-14, massive basalt with 16-mm thick Fe-Mn crust. *C*, D17-13, massive basalt with 23- to 35-mm thick Fe-Mn crust. *D*, D23-3C, large massive pillow-basalt fragment with glass rind and 10- to 40-mm thick Fe-Mn crust. 120
Figure 58. REE plots of 2 B, bulk crusts and 2 L, crust layers from dredges D5 and D6, San Marcos Seamount: *A,* Chondrite (Anders and Ebihare 1982) normalized and *B,* PAAS (McLennan 1989) normalized; interval in mm. 121

Figure 59. REE plots of B, bulk crusts from dredges D11, Hoss Seamount; D14, Little Joe Seamount; D17, Ben Seamount; and D21, Flint Seamount; *A,* Chondrite (Anders and Ebihare 1982) normalized, and *B*, PAAS (McLennan 1989) normalized; intervals in mm. 122
Figure 60. REE plots of B, bulk crust and L, crust layer samples from dredges D7, D8, and D9, Adam Seamount; *A*, Chondrite (Anders and Ebihare 1982) normalized, and *B*, PAAS (McLennan 1989) normalized; BN, bulk nodule; interval in mm. 123
Figure 61. Ternary diagram showing A, diagenetic; B, hydrogenetic; and C, hydrothermal fields. 124

Tables

Table 1. Scientific personnel on RV *Farnella* cruise F7-87-SC. 8
Table 2. Station locations and operations for cruise F7-87-SC. 9
Table 3. Bathymetry/geophysics lines, RV *Farnella* cruise F7-87-SC, U.S. Exclusive Economic Zone, California. . 10
Table 4. Deep-sea camera locations for RV *Farnella* cruise F7-87-SC. 11
Table 5. Dredge locations and major rock types for RV *Farnella* cruise F7-87-SC. 12
Table 6. Location and description of dredge hauls, cruise F7-87-SC. 13
Table 7. Foraminifer and calcareous nannofossil ages of sediments and sedimentary rocks. 19
Table 8. X-ray diffraction mineralogy of substrate rocks. 20
Table 9. Whole-rock chemical composition (weight percent) of substrate rocks on six seamounts. 21
Table 10. X-ray diffraction mineralogy of ferromanganese deposits. 22
Table 11. Chemical composition of Fe-Mn crusts and nodules. 24
Table 12. Hygroscopic water-free chemical composition (data in Table 11 normalized to 0% H_2O^-). 35
Table 13. Rare-earth element concentrations (in ppm) of Fe-Mn crust and nodule samples from six seamounts, normalized to 0% H_2O^-. 43
Table 14. Statistics for all crust and nodule data from Tables 12 and 13. 45
Table 15. Statistics for 60 bulk crusts and nodules from Tables 12 and 13. 46
Table 16. Statistics for crust layer data from Tables 12 and 13. 47
Table 17. Statistics for nodule data from Adam Seamount from Table 12. 48
Table 18. Statistics for Fe-Mn crust data from Rodriguez Seamount from Table 12. 49
Table 19. Statistics for Fe-Mn crust data from San Marcos Seamount, from Tables 12 and 13. 50
Table 20. Statistics for Fe-Mn crust data from Adam Seamount, from Tables 12 and 13. 51
Table 21. Statistics for Fe-Mn crust data from Hoss Seamount, from Tables 12 and 13. 52
Table 22. Statistics for Fe-Mn crust data from Little Joe Seamount, from Table 12. 53
Table 23. Statistics for 6 Fe-Mn bulk crusts, Ben Seamount, from Tables 12 and 13. 54
Table 24. Statistics for Fe-Mn crust data from Flint Seamount, from Table 12. 55
Table 25. Correlation matrix for bulk crusts; data from Tables 12 and 13. 56
Table 26. Correlation matrix for crust layers; original data in Tables 12 and 13. 59
Table 27. Correlation matrix for 7 nodules from Adam Seamount, original data in Table 12. 62

Conversion Factors

Multiply	By	To obtain
	Length	
millimeter (mm)	25.4	inch (in)
meter (m)	0.3048	foot (ft)
meter (m)	0.9144	yard (yd)
kilometer (km)	1.852	mile, nautical (nmi)
Kilometer (km)	0.6214	Mile (mi)

Temperature in degrees Celsius (°C) may be converted to degrees Fahrenheit (°F) as follows:
°F = (1.8 x °C) + 32

Abbreviations and Acronyms

EEZ	Exclusive Economic Zone
RV	Research Vessel
m	Meters
mm	Millimeters
Ma	Mega-annum (one million years)
kHz	Kilohertz
s	Second
D	Dredge
REE	Rare-Earth Element

Seamounts and Ferromanganese Crusts Within and Near the U.S. EEZ Off California–Data for RV *Farnella* Cruise F7-87-SC

By James R. Hein[1], Jane A. Reid[2], Tracey A. Conrad[1], Rachel E. Dunham[3], David A. Clague[4], Marjorie S. Schulz[1], and Alicé S. Davis[4]

Introduction

The purpose of this report is to present and briefly describe ship-board and laboratory data for a U.S. Geological Survey (USGS) research cruise aboard the RV *Farnella* that took place December 3-21, 1987 (cruise F7-87-SC; tables 1 and 2, fig. 1). The purpose of the cruise was to survey seamounts and ferromanganese crusts within and near the U.S. Exclusive Economic Zone (EEZ) off California. Eight seamounts were studied–Rodriguez, San Marcos, Adam, Hoss, Little Joe, Ben, Flint, and Jasper. A geophysical survey of Jasper Seamount took place, but that seamount was not sampled; whereas Adam and Hoss Seamounts were sampled, but not surveyed with geophysics lines.

Ship-Board Operations

The two main types of navigation used were RhoRho, which is the name of a software program developed at the USGS to do direct ranging on Loran C stations (Gann, 1988), and partial coverage by the U.S. Navy's Global Positioning System. Ship-board geophysical operations consisted of analog 3.5 kHz and 10 kHz bathymetric surveys and an analog single-channel water-gun survey on Jasper and Flint Seamounts (table 3), which were surveyed together. The 10 kHz system had technical difficulties, and those data are not presented. Bathymetric lines typically crossed each seamount at least twice at nearly right angles, and dredge and camera stations were chosen based on those geophysical records. Geophysical lines were not run on Adam and Hoss Seamounts. A deep-towed camera sled took port and starboard 35 mm still photos at 10-s intervals and continuous 70 mm video. One camera tow was on Rodriguez Seamount, and two camera tows were on Flint Seamount (table 4). Because of rough weather, the camera sled was often too far above bottom to get good photographs. Consequently, the Monterey Bay Aquarium Research Institute (MBARI) kindly allowed us to reproduce several bottom photos from Rodriguez, San Marcos, and Little Joe Seamounts that were taken in 2003 and 2004 using their ROV *Tiburon*. Samples were collected using a 1-m circular chain-bag dredge (tables 5-7). Most dredged samples were cut, described, photographed, and subsampled in the ship's laboratory.

[1]U.S. Geological Survey, Menlo Park, Calif.
[2]U.S. Geological Survey, Santa Cruz, Calif.
[3]Western Washington University, Bellingham, Wash.
[4]Monterey Bay Aquarium Research Institute, Moss Landing, Calif.

Shore-Based Analyses

Mineralogy was determined with x-ray diffraction on powdered samples using CuKα radiation and a carbon monochromator on a Philips diffractometer (tables 8 and 10). The abundances of major oxides of substrate rocks were determined by x-ray fluorescence and H_2O and CO_2 by wet-chemical techniques; loss on ignition was at 900º Celsius (table 9; Taggart and others, 1987). For ferromanganese oxides, most major and minor elements were determined by inductively coupled plasma-atomic emission spectrometry (ICP) on air-dried samples (table 10; Aruscavage and others, 1989). Potassium, Zn, and Pb were determined by flame atomic-absorption (FAA) and As, Cd, Co, and Cr were determined by graphite-furnace atomic absorption (GFAA). Platinum-group elements (PGEs) were determined by fire assay (FA) and ICP-mass spectrometry (ICP-MS), rare-earth elements (REEs) were determined by ICP-MS, and Au was determined by FA and GFAA (tables 10-24; Lichte and others, 1987a,b).

Data Organization

The data are organized by first showing a bathymetric map for each seamount [figs. 2 (Rodriguez), 11 (San Marcos), 18 (Adam-Hoss), 19 (Little Joe), 27 (Ben), and 36 (Jasper-Flint)] that displays the locations of operations. Three seamounts (Rodriguez, Ben, Jasper-Flint) have an ETOPO1 (satellite-based digital bathymetry) bathymetric map (figs. 3, 28 and 37, respectively; Amante and Eakins, 2009) in addition to the map that was used originally during the cruise. Those original maps were modified from the Chase and Menard (1973) atlas. Following the maps are bottom photographs for Rodriguez (fig. 4), San Marcos (fig. 12), and Little Joe (fig. 20) Seamounts. Otherwise, the 3.5 kHz lines follow the maps (figs. 5-10, 13-17, 21-26, and 29-35). Water-gun lines follow respective 3.5 kHz lines for the Jasper-Flint Seamounts pair (figs. 38-52). Photographs of examples of the dredge hauls and cut-rock samples are shown in figures 53-57. REE plots are shown in figures 58-60 and a ternary diagram of chemical composition is shown in figure 61. Rock mineralogy and chemistry data are presented in tables 8 and 9, and Fe-Mn crust mineralogy data is presented in table 10. Fe-Mn crust data chemistry is in tables 11 through 27.

Data Description

Rodriguez Seamount

Rodriguez Seamount sits on the continental slope at the northern boundary of the borderland. Five geophysical lines crossed the seamount, and one camera survey was completed up the northwest flank (figs. 2 and 3; tables 2-4). The shallowest point crossed is at about 615 m, and the seamount shows a central peak with a gently sloping terrace to the southwest. The 3.5 kHz lines show little sediment cover on the seamount and thin sediment layers at the base of the seamount and off structure. The seamount may be partly surrounded by a moat. Seabed photographs (fig. 4) and dredged samples (table 6) show bedded volcaniclastic deposits, lava flows, and lava spatter.

Recent analysis of geomorphology indicates a broadly domed, smooth, sediment-draped summit platform that contains evidence of subaerial exposure (Paduan and others, 2009). Bedded clastic deposits are common along the summit (fig. 4*A*, *B*).

Four dredging attempts resulted in two recoveries (table 5). Less than 20 percent of the rocks, mostly breccia and basalt (for example, fig. 54*A*), are coated with Fe-Mn crusts, which are generally thin (maximum 22 mm; table 6). The deeper water dredge haul had the thickest crusts. Most rocks

contained only a Fe-Mn oxide patina. The thin Fe-Mn crusts are consistent with a relatively young age of the seamount, about 9.4 Ma, possibly as old as 12 Ma (Davis and others, 1995, 2002).

San Marcos Seamount

This seamount rises from a depth of about 4,000 m to about 1,900 m based on the Chase and Menard (1973) bathymetric map (fig. 11), but 3.5 kHz line SM3 (fig. 15) shows the seamount to be much shallower, about 1,350 m. San Marcos is elongate NE-SW and has several small deep-water volcanic edifices located just off structure. The geophysical lines (figs. 13-17) show that little sediment occurs on this seamount, but that well-bedded abyssal sediments occur adjacent to the southeast flank. Slump deposits also characterize the lower flanks. Seabed photographs (fig. 12) and dredged samples (table 6) show well-developed pillow flows and bedded volcaniclastic deposits and lava spatter (fig. 54*B*-*E*).

Two dredging attempts both recovered samples (table 5). Less than 15 percent of the rocks are coated with Fe-Mn crusts, which are generally moderately thick (maximum 50 mm; table 6). The shallower water dredge haul, D4, had the thickest crusts, which occur mostly on basalt. Most rocks contained only a Fe-Mn oxide patina. These thin to moderately thick crusts are consistent with a seamount age of between 11 and 16 Ma (Davis and others, 1995)

Adam and Hoss Seamounts

This pair of adjacent small seamounts (fig. 1) rises from a depth of about 4,000 m to 2,200 m for Adam and 2,500 m for Hoss. Both seamounts are roughly conical. Geophysical lines were not run across these volcanic edifices.

Three dredging attempts all recovered samples on Adam Seamount, predominantly hyaloclastite/volcaniclastic rocks, mudstone, and basalt (table 6; fig. 53*A*-*C*). The mudstone is hyaloclastite or volcanic ash altered to zeolites and smectite (fig. 55*D*, *G*). Some kelp-rafted exotic rocks were recovered, such as dolostone in dredge D9 (see Paduan and others, 2007 for discussion of exotic rocks on California margin seamounts). Fe-Mn nodules were collected in dredges D8 and D9 (fig. 55*A*-*C*). Fe-Mn oxides encrusted all the rocks in D8 and D9 and 25 percent of the rocks in D7 (for example, fig. 55*D*-*G*). The Fe-Mn crusts are among the thickest collected during cruise F7-87-SC, up to 120 mm (table 6). The thick crusts are consistent with a seamount age of about 17 Ma (Davis and others, 1995), but suggest that the seamount may be as old as the oceanic crust on which it sits, about 22 Ma.

Two dredging attempts both recovered samples on Hoss Seamount, predominantly breccia, limestone, and basalt (table 6). Some kelp-rafted exotic rocks were recovered, such as porcellanite in dredge D11 (fig. 56C) of Miocene age (table 7). Fe-Mn oxides encrusted 95-100 percent of the rocks. The Fe-Mn crusts are also among the thickest collected during cruise F7-87-SC, up to 83 mm (table 6; fig. 56*A*, 56*B*, 56*D*). Rocks from Hoss Seamount have not been dated, but the thick crusts suggest an age similar to that of Adam Seamount.

Little Joe Seamount

This northeast-southwest elongate seamount occurs just west of the Patton Escarpment and rises from about 3,600 m water depth to a summit near 2,400 m (fig. 19). However, the 3.5 kHz lines show that the summit is near 2,160 m water depth (figs. 21 and 25). The geophysical lines (figs. 21-26) show that little sediment occurs on this seamount or around its base, but that a thin sediment layer occurs adjacent to the east flank (figs. 24 and 25). Slump deposits occur along the lower flanks. Seabed photographs (fig. 20) and dredged samples (table 6) indicate predominantly well-developed pillow and

massive lava flows and volcaniclastic breccia. Phosphorite breccia and mudstone are minor rock types (fig. 56*E*, 56*F*).

Three dredging attempts resulted in two recoveries of samples (table 5). All of the rocks are coated with Fe-Mn crusts, which are generally moderately thick (maximum 65 mm; table 6). The thicker crusts collected are not consistent with the poorly constrained seamount age of <7±3 Ma (Davis and others, 1995).

Ben Seamount

This northeast-southwest elongate seamount occurs west of Little Joe Seamount and rises from about 3,800 m water depth to a summit near 2,700 m (figs. 27 and 28). The 3.5 kHz lines show only slightly shallower depths, near 2,600 m (fig. 29). The geophysical lines (figs. 29-35) show that little sediment occurs on this seamount, but well-bedded sediment layers occur adjacent to the north flank (fig. 30). Slump deposits occur along the lower flanks. Dredged samples (table 6) indicate predominantly massive and pillow lavas with abundant glass (fig. 57*A*-*C*) and lesser amounts of volcaniclastic breccia, sandstone, siltstone, and mudstone, and minor phosphorite.

Three dredging attempts resulted in one recovery of samples (table 5). All of the rocks are coated with Fe-Mn crusts, which are generally thin to moderately thick (maximum 42 mm; table 6). The Fe-Mn crusts are generally thin considering a seamount age of about 20 Ma (Davis and others, 1995). Nannofossils from sample D17-3 indicate a questionable Miocene age (table 7).

Jasper and Flint Seamounts

These two seamounts were surveyed together, but only Flint was sampled because dredging proved to be difficult and, therefore, time consuming, leaving no time to sample Jasper (figs. 36 and 37). The seamounts occur just west of the U.S. EEZ (fig. 1) and rise from a base of about 4,000 m to a summit at about 1,700 m for Flint and 600 m for Jasper. The shallowest depths on the 3.5 kHz records are 1,380 m for Flint (fig. 48) and 853 m for Jasper (fig. 42). Both seamounts are nearly conical, and smaller volcanic edifices surround Jasper. The geophysical lines (figs. 38-52) show that little sediment occurs on Jasper seamount, but well-bedded sediment layers occur in the trough between Jasper Seamount and the volcanic edifice to the south (figs. 42 and 44) and possibly to the northwest, of Flint Seamount (fig. 46). Slump deposits occur along the lower flanks. Dredged samples from Flint Seamount (table 6; fig. 53*D*-*H*) indicate predominantly massive and pillow lavas with moderate amounts of glass (fig. 57*A*-*C*).

Seven dredging attempts on Flint Seamount resulted in two with recoveries of rock samples, and one with solely biota (table 5). All of the rocks are coated with Fe-Mn crusts, which are generally thin to somewhat moderately thick (maximum 40 mm; table 6). The Fe-Mn crusts are generally in agreement with a seamount age of ≤11 Ma (Pringle and others, 1991, assuming that Flint is of a similar age as Jasper. Mud from sample D23-1 on Flint Seamount has an age of late Pleistocene or younger (table 7).

Rock Mineralogy and Geochemistry

Detailed mineralogy, petrography, petrology, major-and minor-element chemistry, isotopes, and age dating of the basalts collected during this cruise is reported by Davis and others (1995). Davis and others dealt with the least altered rocks, and here we present data on altered basalts, as well as other rock types. Exotic rocks brought to the seamounts by kelp rafting include dolostone (D3-11, D9-33, D9-34, and D14-2), porcellanite (D11-1), and quartzite (D17-30) (tables 8 and 9). Those rocks will not be further discussed.

The main rock types include basalt, breccia, altered hyaloclastite, pyroclastic rocks, and fine-grained (siltstone, mudstone) pyroclastic and volcaniclastic rocks. The primary minerals include

predominantly plagioclase and pyroxene, and the volcanogenic rocks are invariably altered to phillipsite and smectite, which replace grains and provide cement for clastic rocks (table 8). Other alteration products and cements include calcite, carbonate fluorapatite (CFA), todorokite, birnessite, δ-MnO_2, and rarely zeolites other than phillipsite (natrolite, erionite). Quartz, illite, and chlorite are most likely detrital, but quartz may also be in part an alteration product. CFA forms both a cement and clasts for some breccia samples (for example, D14-3A) thereby producing a nearly pure phosphorite (table 9); the low total oxides for that sample and for D17-8 are due to the absence of F, Cl, and S in those totals, which are typically high in marine phosphorite but were not analyzed here. Barite occurs in at least one sample (D10-4; table 8) and accounts for the low total oxides in that sample (table 9).

Fe-Mn Crust Mineralogy and Geochemistry

All Fe-Mn crust and nodule samples are composed predominantly of δ-MnO_2, 61-98 percent (table 10). Sample D13-1B, a Mn-oxide cemented breccia, is made up predominantly of goethite ironstone and volcanogenic clasts. Ironstones have been found on many seamounts throughout the central Pacific (Hein and others, 1994), but this is the first example from a continental-margin seamount. Sample D13-2A has a similar chemical composition as D13-1B (table 12), but a much different mineralogy because the Fe phase is x-ray amorphous; therefore it is not included in table 10. Todorokite and, to a lesser extent, birnessite occur in many samples (table 10). These Mn oxides occur only rarely (<2 percent of samples) in open-ocean Fe-Mn crusts (Hein and others, 2000), which emphasize a fundamental difference with continental-margin deposits (49 percent of samples; table 10). This difference indicates either a diagenetic input, or more likely, lower oxygen conditions under which the continental-margin crusts formed. None of the Fe-Mn crusts contain CFA, which is common in the older parts of thick crusts from the open ocean (Hein and others, 2000). Another major phase is x-ray amorphous Fe oxyhydroxide, which crystallized to goethite in 18 percent of the samples; this contrasts with only 6 percent of open-ocean Pacific Fe-Mn crusts containing goethite (Hein and others, 2000). Three crust samples (D10-3, D10-4A, and D13-2C) contain significant barite (table 10), which is reflected in the highest three Ba concentrations (table 12). Detrital plagioclase, quartz, phillipsite, smectite, dolomite, and illite occur in many of the crust samples.

Chemical data are presented in two ways–table 11 gives the raw data, which includes sorbed (hygroscopic) water content, and tables 12 and 13 present the data on a hygroscopic water-free basis. Hydroscopic water can vary up to 32 weight percent and thereby affects the concentrations of all other elements. Compositions normalized to 0 percent H_2O^- (hygroscopic water) can be more meaningfully compared and also more closely represent the grade of the potential ore. All analyses of the chemical data are made on the water-free data set. The Fe/Mn ratios vary widely from 0.4 to 11, with a mean of 1.6 (table 14). These Fe-Mn crusts are generally Fe rich compared to open-ocean crusts, where Fe/Mn ratios are typically less than 1. Some samples are very rich in detrital material with Si contents up to 25 percent and Al contents up to about 5 percent. Si is enriched relative to Al compared to the detrital component in many samples, especially samples D9-21A-C, indicating a nondetrital source for some of the Si, probably biogenic. Other indicators of biogenic input include Ba and P concentrations. Ba is greater than 0.5 percent in some samples from San Marcos (to 0.56 percent), Adam (to 0.66 percent), Hoss (to 2.4 percent), and Little Joe (to 6.6 percent) Seamounts, the latter of which may also have a hydrothermal component (see below). Although none of the samples are phosphatized, the P contents, especially of Rodriguez Seamount samples, are quite high, to 0.89 percent. The mean Pb content is highest for Fe-Mn crusts from Rodriguez Seamount (table 18), the seamount closest to the continental-margin zone of upwelling and high biological productivity. This high Pb content may reflect the high

biological input as should the As contents. High Cr concentrations (up to 180 ppm) in Rodriguez Seamount crusts likely reflect input from the nearby continental margin.

Individual samples may have high Co (up to 1.05 percent), Ni (up to 0.91 percent), or Cu (up to 0.38 percent) contents, the elements generally considered of most economic interest, but the mean values for the entire data set are relatively low (0.28 percent, 0.31 percent, and 0.08 percent, respectively) compared to open-ocean Fe-Mn crusts (Hein and others, 2000). Our limited data sets for Ben (table 23) and Flint (table 24) Seamounts suggest that additional sampling to determine resource potential is warranted. Fe-Mn nodules generally have higher mean Cu and Ni contents (table 17) than do the Fe-Mn crusts, and this may indicate a diagenetic contribution to the nodules. REEs are also of economic interest, and total REEs (up to 0.29 percent for bulk crusts; table 13) and Ce concentrations (up to 0.20 percent; tables 12 and 13) indicate that further studies are warranted for this potential resource on Ben, Flint, and possibly Rodriguez and San Marcos Seamounts. PGEs are low in all samples compared to open-ocean Fe-Mn crusts, with a maximum Pt concentration of 141 ppb, which is for a bulk crust from Flint Seamount.

The REE concentrations normalized to mean chondrite and shale compositions and plotted in figures 58-60 generally show patterns typical of hydrogenetic Fe-Mn crusts. For example, all samples show a positive Ce* anomaly, albeit that for sample D8-3D is very small (table 13, fig. 60). All samples also show light REE enrichments on chondrite-normalized plots. For the two crusts in which layers were analyzed (D8-3 and D9-16) the Ce* anomaly increases with time, such as from the oldest layers to the youngest layers. This may indicate that the redox potential of the bottom waters and/or growth rates of the crusts changed consistently during the past approximately 10 Ma, becoming more oxidizing.

A ternary plot of (Co+Cu+Ni)x10:Mn:Fe is shown in figure 61. About half of the data fall within field B, which is typical of hydrogenetic Fe-Mn crusts. The other half defines a trend toward more Fe-rich compositions, and several samples plot near the hydrothermal C field. Since field B is defined by open-ocean Fe-Mn crusts, the continental-margin crust hydrogenetic field likely includes much of the data to the lower left of the field B. However, several samples may have a hydrothermal component, especially the D13 group of samples from Little Joe Seamount, which include the 4 points closest to the Fe apex. The next two sample points closest to the Fe apex are from Rodriguez Seamount, with high aluminosilicate fractions that dilute the metals, especially the Mn, Ni, and Cu contents.

A correlation coefficient matrix for bulk samples (table 25) shows that Fe has positive correlations with Pb, As, P, V, Y, and the REEs (except Ce), and we interpret those elements to be part of the FeOOH phase. Mn has positive correlations with Mo, Ca, Cd, Ni, Pt, Co, Zn, Y, and V, and we interpret those elements to be part of the δ-MnO_2 phase. V and Y are partitioned between both phases, which are consistent with sequential leaching studies of open-ocean Fe-Mn crusts (Koschinsky and Hein, 2003). Cu and the middle REEs increase in crusts with increasing water depth of occurrence, whereas P, Pb, As, Cr, and V decrease with increasing water depth of crust occurrence (table 25). Correlation coefficients for crust layers and nodules show similar relationships with only minor variations (tables 26, 27).

Acknowledgments

We thank the Captain and crew of the RV *Farnella* cruise F7-87-CP. We thank Paula Quinterno, USGS retired, for the micropaleontology ages and Mike Torresan, USGS, and Jennifer Paduan, MBARI, for helpful reviews of this open-file report.

References Cited

Amante, C. and Eakins, B.W., 2009, ETOPO1 1 Arc-Minute Global Relief Model–Procedures, data sources and analysis: National Oceanographic and Atmospheric Administration Technical Memorandum NESDIS NGDC-24, 19 p.

Anders, E., and Ebihare, M., 1982, Solar-system abundances of the elements: Geochimica et Cosmochimica Acta, v. 46, p. 2363-2380.

Aruscavage, P.J., Kirschenbaum, H., and Brown, F., 1989, Analytical methods–The determination of 27 elements in ferromanganese materials, *in* Manheim, F.T. and Lane-Bostwick, C.M., eds. Chemical composition of ferromanganese crusts in the world ocean–A review and comprehensive database: U.S. Geological Survey Open-File Report 89-020, 200 p., 3 appendices.

Chase, T.E., and Menard, H.W., compilers, 1973, Bathymetric atlas of the north Pacific Ocean: Washington, D.C., U.S. Naval Oceanographic Office, Publication 1301-2-3.

Cook, H.E., Johnson, P.D., Matti, J.C., and Zemmels, I., 1975, Methods of sample preparation and x-ray diffraction data analysis (x-ray mineralogy laboratory, Deep Sea Drilling Project, University of California Riverside), *in* Hays, D.E., Frakes, L.A., and others, Initial Reports of the Deep Sea Drilling Project: Washington, D.C., U.S. Government Printing Office, v. 28, p. 999-1007.

Davis, A.S., Gunn, S.H., Bohrson, W.A., Gray, L-B., and Hein, J.R., 1995, Chemically diverse, sporadic volcanism at seamounts offshore southern and Baja California: Geological Society America Bulletin, v. 107, p. 554-570.

Davis, A.S., Clague, D.A., Bohrson, W.A., Dalrymple, G.B., and Greene, H.G., 2002, Seamounts at the continental margin of California–A different kind of oceanic intraplate volcanism: Geological Society America Bulletin, v. 114, p. 316-333.

Gann, J.T., 1988, Integrated GPS, range-range and hyperbolic Loran C marine navigation system for use on IBM AT or compatible microcomputer: U.S. Geological Survey Open-File Report 88-562.

Hein, J.R., Schwab, W.C., and Davis, A.S., 1988, Cobalt- and platinum-rich ferromanganese crusts and associated substrate rocks from the Marshall Islands: Marine Geology, v. 78, p. 255-283.

Hein, J.R., Yeh, H.-W., Gunn, S.H., Gibbs, A.E., and Wang, C.-H., 1994, Composition and origin of hydrothermal ironstones from central Pacific seamounts: Geochimica et Cosmochimica Acta, v. 58, p. 179-189.

Hein, J.R., Koschinsky, A., Bau, M., Manheim, F.T., Kang, J.-K., and Roberts, L., 2000, Cobalt-rich ferromanganese crusts in the Pacific, *in* Cronan, D.S., ed., Handbook of marine mineral deposits: Boca Raton, Florida, CRC Press, p. 239-279.

Koschinsky, A., and Hein, J.R., 2003, Uptake of elements from seawater by ferromanganese crusts–Solid-phase associations and seawater speciation: Marine Geology, v. 198, p. 331-351.

Lichte, F.E., Golightly, D.W., and Lamothe, P.J., 1987a, Inductively coupled plasma-atomic emission spectrometry, *in* Baedecker, P.A., ed., Methods for geochemical analysis: U.S. Geological Survey Bulletin 1770, p. B1-B10.

Lichte, F.E., Meier, A.L., and Crock, J.G., 1987b, Determination of rare earth elements in geological materials by inductively coupled plasma-mass spectrometry: Analytical Chemistry, v. 59, p. 1150-1157.

McLennan, S.M., 1989, Rare earth elements in sedimentary rocks: Influence of provenance and sedimentary processes, *in* Lipin, B.R., and McKay, G.A., Geochemistry and mineralogy of rare earth elements: Mineralogical Society of America's Reviews in Mineralogy, v. 21, p. 169-200.

Paduan, J.B., Clague, D.A., and Davis, A.S., 2007, Erratic continental rocks on volcanic seamounts off the U.S. west coast: Marine Geology, v. 246, p. 1-8.

Paduan, J.B., Clague, D.A., and Davis, A.S., 2009, Evidence that three seamounts off southern California were ancient islands: Marine Geology, v. 265, p. 146-156.

Pringle, M.S., Staudigel, H., and Gee, J., 1991, Jasper Seamount–Seven million years of volcanism: Geology, v. 19, p. 364-368.

Taggart, J.E., Lindsay, J.R., Scott, B.A., Vivit, D.V., Bartel, A.J., and Stewart, K.C., 1987, Analysis of geologic materials by wavelength-dispersive x-ray fluorescence spectrometry, *in* Baedecker, P.A., ed., Methods for geochemical analysis: U.S. Geological Survey Bulletin 1770, p. E1-E19.

Table 1. Scientific personnel on RV *Farnella* cruise F7-87-SC.

Name	Position
James R. Hein	Chief Scientist
John Barber	Geologist
Laura M. Benninger	Geologist
Hank Chezar	Camera Technician
Walt Friesen	Geologist
Marjorie Morrison (Schulz)	Geologist
Kevin O'Toole	Marine Technician
Corky (Ward) Ozanne	Marine Technician
Leda Beth Gray Pickthorn	Geologist
Byron Ruppel	Navigator
Barbara Seekins	Watch Stander
Joe Thomas	Electronics Technician
Mike Torresan	Geologist
Jim Vaughan	Electronics Technician

Table 2. Station locations and operations for cruise F7-87-SC.

[D, dredge; DSC, deep-sea camera]

Station	Location	Operation
01	Rodriguez Seamount	D1
02	Rodriguez Seamount	D2
02	Rodriguez Seamount	D3
03	Rodriguez Seamount	D4
04	Rodriguez Seamount	DSC1
05	San Marcos Seamount	D5
06	San Marcos Seamount	D6
07	Adam Seamount	D7
08	Adam Seamount	D8
09	Adam Seamount	D9
10	Hoss Seamount	D10
11	Hoss Seamount	D11
12	Little Joe Seamount	D12
13	Little Joe Seamount	D13
14	Little Joe Seamount	D14
15	Ben Seamount	D15
16	Ben Seamount	D16
16	Ben Seamount	D17
17	Flint Seamount	D18
18	Flint Seamount	D19
19	Flint Seamount	D20
20	Flint Seamount	DSC2
21	Flint Seamount	D21
22	Flint Seamount	D22
23	Flint Seamount	D23
24	Flint Seamount	D24
25	Flint Seamount	DSC3

Table 3. Bathymetry/geophysics lines, RV *Farnella* cruise F7-87-SC, U.S. Exclusive Economic Zone, California.
[no., number; OD, ordinal day; GMT, Greenwich mean time; °N, degrees north; °W, degrees west; nmi, nautical miles; km, kilometers; kHz, kilohertz; SCWG, single-channel water gun]

	START				END				Comments		
Line no.	Day (OD)	Time (GMT)	Latitude (°N)	Longitude (°W)	Day (OD)	Time (GMT)	Latitude (°N)	Longitude (°W)	Length (nmi)	Length (km)	Type (kHz)
Rodriguez Seamount											
R1	338	1716	34°08.13’	121°07.10’	338	1826	34°02.02’	120°59.56’	11	20	3.5, 10
R2	338	1830	34°01.80’	120°59.68’	338	1921	34°02.90’	121°07.50’	7	13	3.5, 10
R3	338	1924	34°02.80’	121°07.65’	338	2010	33°57.50’	121°04.75’	6	11	3.5
R4	338	2012	33°57.50’	121°04.65’	338	2039	34°02.30’	121°03.37’	5	9	3.5
R5	338	2043	34°02.30’	121°03.17’	338	2117	33°59.24’	121°00.50’	4	7	3.5
Transit to San Marcos Seamount											
TRAN	339	2319	33°57.58’	121°10.78’	340	0934	32°41.96’	121°41.17’			
San Marcos Seamount											
SM1	340	0934	32°41.70’	121°40.90’	340	1124	32°31.17’	121°27.82’	16	30	3.5, 10
SM 2	340	1138	32°31.15’	121°28.64’	340	1315	32°31.40’	121°36.92’	4	7	3.5, 10
SM 3	340	1321	32°31.63’	121°36.85’	340	1806	32°46.10’	121°22.82’	20	37	3.5, 10
SM 4	340	1817	32°46.60’	121°22.36’	340	1927	32°45.16’	121°27.54’	5	9	3.5, 10
SM 5	340	1929	32°45.05’	121°27.61’	340	2223	32°31.26’	121°27.78’	15	28	3.5, 10
Transit to Hoss Seamount											
TRAN	342	0910	32°05.22’	121°17.51’	342	1030	31°59.84’	121°27.99’			
Transit to Little Joe Seamount											
TRAN	342	1957	31°59.59’	121°28.48’	343	0230	31°54.28’	120°01.70’			
Little Joe Seamount											
LJ1	343	0257	31°56.53’	120°05.89’	343	0402	31°53.41’	119°59.83’	5	9	3.5, 10
LJ2	343	0406	31°53.11’	119°59.83’	343	0513	31°49.83’	120°05.23’	5	9	3.5, 10
LJ3	343	0516	31°50.20’	120°05.50’	343	0716	32°00.00’	120°00.00’	11	20	3.5, 10
LJ4	343	0720	32°00.00’	120°00.00’	343	0824	31°56.20’	119°55.90’	6	11	3.5, 10
LJ5	343	0832	31°56.20’	119°55.90’	343	1049	31°53.90’	120°07.20’	9	17	3.5, 10
LJ6	343	1053	31°53.90’	120°07.20’	343	1236	31°53.35’	119°59.55’	6	11	3.5, 10
Transit to Ben Seamount											
TRAN	344	0530	31°54.63’	120°02.44’	344	0902	31°46.71’	120°39.49’			
Ben Seamount											
B1	344	0910	31°45.67’	120°42.26’	344	1215	31°40.80’	120°54.82’	13	24	3.5, 10
B2	344	1219	31°40.89’	120°55.01’	344	1321	31°46.26’	120°53.50’	5	9	3.5, 10
B3	344	1325	31°46.14’	120°53.31’	344	1513	31°39.55’	120°49.55’	7	13	3.5, 10
B4	344	1517	31°39.55’	120°49.55’	344	1542	31°40.68’	120°47.02’	2	4	3.5, 10
B5	344	1543	31°40.75’	120°47.05’	344	1701	31°45.35’	120°49.53’	5	9	3.5, 10
B6	344	1706	31°45.67’	120°49.04’	344	1742	31°46.83’	120°45.75’	3	6	3.5, 10
B7	344	1747	31°46.83’	120°45.75’	344	1903	31°42.61’	120°43.19’	4	7	3.5, 10
Transit to Jasper/Flint Seamounts											
TRAN	345	1400	31°43.38’	120°46.31’	346	0400	30°51.44’	121°57.85’			
Jasper/Flint Seamounts											
JF1	346	0425	30°37.40’	122°24.50’	346	0915	30°19.70’	122°54.20’	29	54	3.5, 10, SCWG
JF2	346	1000	30°19.46’	122°54.70’	346	1301	30°34.01’	122°46.18’	16	30	3.5, 10, SCWG
JF3	346	1305	30°33.87’	122°46.00’	346	1950	30°05.97’	122°43.95’	27	50	3.5, 10, SCWG
JF4	346	2006	30°05.50’	122°43.55’	347	0621	30°45.40’	123°18.94’	62	115	3.5, 10, SCWG
JF5	347	0630	30°45.70’	123°19.27’	347	0715	30°41.37’	123°20.04’	3	6	3.5, 10, SCWG
JF6	347	0719	30°40.96’	123°19.90’	347	1021	30°34.97’	123°06.28’	16	30	3.5, 10, SCWG
JF7	349	1254	30°36.50’	123°13.00’	349	1428	30°33.00’	123°11.50’	4	7	3.5, 10, SCWG

Table 4. Deep-sea camera locations for RV *Farnella* cruise F7-87-SC.

[DSC1, Rodriguez Seamount; DSC2, 3, Flint Seamount; °N, degrees north; °W, degrees west; hrs, hours; s, seconds; DSC, deep sea camera; m, meters; ft, feet; mm, millimeter; --, no data; ~, approximately; ‘, feet]

DSC number	Station number	Latitude (°N)	Longitude (°W)	Water depth, in meters	Video	Still pictures port	Still pictures starboard
DSC1	4	34°02.6’	121°03.8’	650	4.5 hrs	6 hrs 37 min., 35mm format, 10 s interval	
		31°05.8’	121°07.1’	2,028	3-7 m off bottom	~250' exposed film 100' developed film	~300’exposed film 100 ft developed film
DSC2	20	30°37.08’	123°13.26’	1,340	4.5 hrs	6 hrs 30 min., 35mm format, 10 s interval	
		30°39.32’	123°14.63’	2,195	3-7 m off bottom	~300' exposed film 100' developed film	288' exposed film 50' developed film
DSC3	25	30°37.15’	123°13.08’	1,345	4.5 hrs	6 hrs with DSC2, 35mm format, 8 s interval	
		--	--	2,830	3-7 m off bottom	~150' exposed film, 45' developed film	135' exposed film 90' developed film

Table 5. Dredge locations and major rock types for RV *Farnella* cruise F7-87-SC.
[^{O} N, degrees north; ^{O} W, degrees west.]

Dredge number	Latitude (°N)	Longitude (°W)	Water depth, in meters	Seamount	Major rock types
D1	33°59.32’ 34°00.58’	120°59.97’ 121°01.36’	2,095-1,500	Rodriguez	No recovery
D2	34°00.22’ 34°00.90’	121°00.70’ 121°02.30’	1,060-1,015	Rodriguez	Lost bag
D3	34°00.3' 34°00.9'	121°01.7' 121°02.3'	1,150-1,050	Rodriguez	Volcaniclastic breccia, basalt
D4	34°01.4' 34°01.6'	121°02.7' 121°02.7'	900-860	Rodriguez	Fe-Mn crusts, basalt, volcaniclastic breccia
D5	32°33.21' 32°32.9'	121°30.39' 121°30.2'	3,435-3,385	San Marcos	Fe-Mn crusts, olivine basalt, volcaniclastic breccia
D6	32°34.30' 32°34.66'	121°31.76' 121°32.20'	2,250-2,155	San Marcos	Vesicular basalt, volcanic breccia, mudstone
D7	32°02.68' 32°02.87'	121°13.72' 121°13.96'	3,775-3,610	Adam	Fe-Mn crusts, mudstone, basalt, volcaniclastic breccia
D8	32°03.42' 32°03.27'	121°14.44' 121°15.02'	3,270-3,250	Adam	Fe-Mn crusts and nodules, vesicular basalt
D9	32°06.06' 32°05.09'	121°16.06' 121°16.66'	2,300-2,235	Adam	Fe-Mn crusts, hyaloclastite, dolomite, vesicular basalt
D10	31°59.1' 31°58.8'	121°28.8’ 121°28.7'	2,850-2,790	Hoss	Fe-Mn crusts, breccia, phosphorite
D11	31°59.4' 31°59.39'	121°28.5' 121°28.6'	2,560-2,540	Hoss	Fe-Mn crusts, laminated porcellanite, basalt
D12	31°53.60’ 31°53.96’	120°00.19’ 120°00.79’	3,250-2,675	Little Joe	No Recovery
D13	31°54.38' 31°54.27'	120°01.73' 120°01.49'	2,580-2,520	Little Joe	Fe-Mn crusts, breccia
D14	31°54.63' 31°54.47'	120°02.21' 120°01.89'	2,445-2,225	Little Joe	Fe-Mn crusts, basalt, dolomitic mudstone, phosphorite breccia
D15	31°43.29’ 31°42.95’	120°43.11’ 120°43.38’	3,445-3,400	Ben	No Recovery
D16	31°44.50’ 31°44.75’	120°44.30’ 120°45.19’	2,950-2,895	Ben	Lost 540 meter wire and bag
D17	31°44.20' 31°44.54'	120°44.12' 120°44.17'	2,925-2,875	Ben	Fe-Mn crusts, basalt, volcaniclastic breccia, mudstone
D18	30°36.47’ 30°36.56’	123°14.00’ 123°14.01’	1,700-1,570	Flint	Lost Bag
D19	30°36.55’ 30°36.29’	123°13.33’ 123°13.01’	1,450-1,325	Flint	No Recovery
D20	30°37.06’ 30°37.33’	123°13.52’ 123°13.71’	1,450-1,325	Flint	Lost Bag
D21	30°36.57' 30°36.51'	123°13.12' 123°13.11'	1,470-1,455	Flint	Fe-Mn crusts, basalt
D22	30°36.53' 30°36.52'	123°13.17' 123°12.23'	1,470-1,450	Flint	All biology
D23	30°33.56' 30°33.67'	123°11.27' 123°10.91'	2,890-2,855	Flint	Fe-Mn crusts, basalt
D24	30°34.99’ 30°34.30’	123°11.71’ 123°11.50’	2,670-2,411	Flint	No recovery

Table 6. Location and description of dredge hauls, cruise F7-87-SC.

[CFA, carbonate fluorapatite; kg, kilogram; %, percent; --, no data; mm, millimeter]

Dredge	Total (kg)	% from Outcrop	% Talus	% Encrusted	Ferromanganese oxides	Substrate rocks
D1	0	--	--	--	No recovery	--
D2	0	--	--	--	Lost bag	--
D3	150	50	50	80 patina	Botryoidal, smooth to granular surface textures; most rocks with a patina, brown to black: layering in the thicker crusts with thin CFA layers between crust and substrate; maximum thickness: 22 mm average thickness: 8 mm	74% volcaniclastic breccia with olive-green and black, subrounded, cobble to sand size, vesicular basalt clasts in yellow-ochre CFA cement and fine-grained volcanic debris matrix; minor poorly consolidated, highly altered breccia with CFA cement; 25% black vesicular basalt: some vesicles filled with sediment; <1% brown dolostone with burrows and borings; encrusting forams on rocks
D4	80	5	95	75 patina 5 crust	Smooth and lizard skin botryoids maximum thickness: 6 mm average thickness: 3 mm	75% dark blue-gray basalt, aphanitic, vesicular to amygdaloidal, boulder to cobble sizes; 24% volcaniclastic breccia: boulders to pebbles, with blocky basalt clasts, small altered rounded clasts in orange-yellow zeolite cement and altered sand-sized grains; encrusting organisms on upper and lower surfaces
D5	255	5	95	85 patina 15 crust	Dominantly smooth surface texture, subdued botryoids, granular on the sides; laminated black to brown massive outer layer; porous, Fe stained between crust layers; maximum thickness: 35 mm average thickness: 8 mm	98% grayish blue and beige, massive olivine basalt cobbles; some vesicular, one small boulder with a black glass rind, pale-brown mud in fractures and fractured surfaces of some basalts; 1% volcaniclastic breccia: gray basalt clasts and few basaltic glass clasts in a zeolite matrix; encrusting forams on surface

Table 6 continued

Dredge	Total (kg)	% from Outcrop	% Talus	% Encrusted	Ferromanganese Oxides	Substrate Rocks
D6	500	10	90	95 patina	Minor small sized botryoids, smooth to granular, few with eroded surface, 2 to 4 layers: 1) outer, brown laminated, porous, some with inclusions of vesicular basalt clasts and dolostone, vugs, and/or Fe staining; 2) black, or metallic gray-black laminated or wavy laminated, massive, porous, occasional Fe stained and carbonate lenses; 3) black, massive with volcanic clasts, some altered clasts; 4) inner, thin carbonate layer maximum thickness: 50 mm average thickness: 8 mm	75% gray vesicular basalt; carbonate and/or mud in vesicles, chill rinds on cobbles and boulders with Mn cement, few altered basalt; 24% volcanic breccia; subangular to subrounded, poorly sorted, cobble- to sand-sized vesicular basalt clasts with zeolite or Mn cement or in a orange-yellow or green-gray sand matrix; alteration rim of palagonite in large clasts; <1% sandstone and mudstone; burrows in mudstone filled with Mn oxides
D7	80	95	5	25	Botryoidal, granular, smooth surface textures; black, brown, yellow-brown; massive to laminated; occasional inclusions of tiny basalt fragments with yellow iron-oxide rims maximum thickness: 30 mm average thickness: 15 mm	93% yellowish-white or greenish-brown mudstone; yellowish-white mudstone has many borings lined with black Mn oxides and filled with brown mud; some small green grains; some borings in the greenish-brown mudstone; 2% gray basalt: sparsely vesicular, few blebs of carbonate; 2% volcaniclastic breccia; poorly sorted, dark-gray vesicular basalt clasts, some with Mn or Mn-Fe oxide rims; 2% encrusting forams, worm tubes, glass sponges on top crust; <1% trachyte
D8	20	100	0	100	Smooth, modified botryoids, lizard skin and granular surfaces; few crusts without substrate; 2 to 3 layers: 1) outer, laminated brown, massive; 2) black, wavy laminated with carbonate blebs and laminae, massive; and/or 3) inner, massive brown with carbonate filling fractures and between basalt fragments; 58% nodules: lobate and spherical, combination of layer 1 and 2, also with carbonate in fractures maximum thickness: 68 mm average thickness: 18 mm	65% finely vesicular basalt, mudstone layer between crust and basalt; 35% nodules–nuclei vary from angular old crust fragments, volcaniclastic fragments, sandstone, hyaloclastite, and carbonate; carbonate blebs common in volcaniclastic sandstone and hyaloclastite; Mn and/or zeolite cement common

Table 6 continued

Dredge	Total (kg)	% from Outcrop	% Talus	% Encrusted	Ferromanganese Oxides	Substrate Rocks
D9	150	90	10	100	Large bulbous botryoids, smooth and lizard skin; some granular on sides and bottom; many small crust and nodule fragments without substrate; 1 to 5 layers: 1) outer, massive to laminated layers or wavy laminated; 2) reddish brown to gray; 3) inner layers, submetallic gray to gray, common fracturing in inner crust; 4) innermost, some with disseminated carbonate ± basalt fragments; 20% nodules maximum thickness: 120 mm average thickness: 45 mm	60% hyaloclastite; pale-brown, soft poorly indurated, extensive burrows filled with hyaloclastite; some mixed with carbonate-cemented microbreccia and angular clasts of sand-sized basalt in zeolite cement; Mn impregnations and in fractures; 15% dolostone, large burrows exposed at surface; 1-3 cm infilled by Mn and some filled with cream mud; 10% altered vesicular basalt; 6% gray cross-bedded sandstone; 5% burrowed mudstone, Mn dendrites and burrow fill; 4% nodules, nuclei mainly carbonate, few old crust fragments, hyaloclastite, and chert
D10	2.5	90	10	100	Smooth to granular, botryoidal surfaces, one with high-relief botryoids; some crusts with no substrate; 2 to 3 layers: 1) outer, reddish-brown, massive to laminated, some with thin outer crust; 2) inner, black, laminated to massive and fractured; 3) innermost, barite and altered volcanic rock fragments in Mn cement maximum thickness: 52 mm average thickness: 20 mm	58% breccia; angular clasts, granules to very coarse sand, made up of crust fragments, volcaniclastic and sedimentary rocks; Mn-oxide cement; 38% carbonates with abundant Mn dendrites; 2% old crust fragments; 1% hyaloclastite; 1%-one rounded quartz-feldspathic sandstone with hematite grains; clean, moderately well sorted; encrusting forams on surface
D11	20	100	0	95	Surfaces mostly smooth, botryoidal, and some granular on sides and bottom; most without substrate; 2 to 3 layers: 1) outer, thin, porous, laminated reddish-brown Fe-stained layer or laminated brown; 2) black massive or laminated to wavy laminated, some with fractures; 3) inner, brown laminated to massive; 1, massive to granular and disrupted layer; few with carbonate rounded to angular clasts and dendrites maximum thickness: 83 mm average thickness: 30 mm	75%-one slab of bored, brown, laminated porcellanite; 25%-2 basalt cobbles; pale-brown and gray, chill rind on some margins; encrusting forams on surface
D12	0	--	--	--	No recovery	--

Table 6 continued

Dredge	Total (kg)	% from Outcrop	% Talus	% Encrusted	Ferromanganese Oxides	Substrate Rocks
D13	3	100	0	100	Smooth, subtly botryoidal, granular on sides and bottom, some crust fragments without substrate; 2 to 3 layers: 1) outer, laminated to massive red-brown or black; 2) inner, black, massive, one laced with barite; middle, laminated pale-brown; 3) inner, massive to laminated dark brown maximum thickness: 26 mm average thickness: 18 mm	100% breccia, 2 cobbles; clasts of tabular basalt, old crusts, and carbonate in Mn-Fe oxide cement; aligned tabular basalt clasts, fractures filled with carbonate; encrusting forams on surface
D14	25	100	0	100	Smooth, subtly bulbous botryoids, granular on bottom and/or sides, some with lizard skin; 2 layers: 1) outer, brown to black laminated to massive; 2) inner, gray-black or submetallic black, massive to occasionally laminated; one cobble with alternating layers of submetallic black and matte black maximum thickness: 65 mm average thickness: 18 mm	85% blue-gray porphyritic basalt with common phenocrysts of pyroxene and feldspar, a chill margin with a thin, dark-colored, glassy aphanitic outer edge; 9% massive pale-brown dolomitic mudstone, many filled burrows, Mn dendrites around burrows and infilled with Mn or mud; 4% phosphorite breccia: pale-brown, extremely poorly sorted, subangular to subrounded phosphorite clasts and minor basalt fragments in grain-supported CFA cement, undulatory layers; 2% laminated crust on basalt pebbles
D15	0	--	--	--	No recovery	--
D16	0	--	--	--	Lost bag	--

Table 6 continued

Dredge	Total (kg)	% from Outcrop	% Talus	% Encrusted	Ferromanganese Oxides	Substrate Rocks
D17	900	50	50	100	Dominantly smooth, granular, some small, bulbous or angular botryoids and lizard skin surfaces; 2 to 3 layers: 1) outer, mostly massive, black to brown, few laminated with or without carbonate; 2) middle, black to brown, laminated or massive; and/or 3) inner, carbonate lenses, laminae ± minor clasts maximum thickness: 42 mm average thickness: 8 mm	90% basalt, 2 main types: 1) blue-gray aphanitic basalt with 1 to 2 chill rinds, brown to glassy black, some altered yellowish basalt and chill rinds, minor vugs and fractures filled with CFA and Mn; 2) blue-gray to brown basalt with phenocrysts of feldspar ± pyroxene, some altered phenocrysts, minor CFA in fractures; some flow structures, pillows and sheets; one large, boulder-size massive flow basalt with hyaloclastite layer containing oriented tabular basalt and glass fragments mixed with white CFA; 2 large boulders, one massive with a glass rim, the other massive, brown, heavily fractured; 7% volcaniclastic breccia; basalt clasts cemented by CFA; basalt and hyaloclastite clasts in Mn cement, and basaltic glass clasts in a hyaloclastite matrix; 2% sandstone and mudstone; one very hard, blue-gray quartzite, one slab of graded, cross-bedded volcaniclastic siltstone to sandstone; minor cross-bedded sandstone abundant glass chips; <1% breccia clast-supported phosphorite in CFA cement
D18	0	--	--	--	Lost bag	--
D19	0	--	--	--	No recovery	--
D20	0	--	--	--	Lost bag	--
D21	2.5	100	0	100	Botryoidal, granular, vitreous, 4 crust fragments without substrate, 1 layer: black, massive maximum thickness: 15 mm average thickness: 8 mm	100% basalt: 2 cobbles, 1) vesicular to scoriaceous, vesicles filled with mud or alteration minerals; 2) olivine-feldspathic basalt, vesicles with glassy margin
D22	2	2	0	0	None	All Biology: 7-10 large brittle stars; 3 wrapped around coral stems; 3 types of corals: golden, gorgonian and unknown; 1 small spiderlike crab, corals are opalescent

Table 6 continued

Dredge	Total (kg)	% from Outcrop	% Talus	% Encrusted	Ferromanganese Oxides	Substrate Rocks
D23	150	100	0	100	Botryoidal, granular on sides and bottom, smooth, and lizard skin surfaces; one boulder with 2 crust layers: 1) laminated dark brown; 2) massive dark brown; two boulders with one crust layer: one with carbonate and basalt clasts in the crust maximum thickness: 40 mm average thickness: 20 mm	99% basalt - 3 boulders: 1) 66%: four large pieces of basalt including 2 pillow fragments with a small granitic erratic in Mn cement; 2) 23% olivine basalt, some alteration of olivine to iddingsite; vugs and fractures; 3) 10% a large basalt cobble; <1% greenish-brown silty hemipelagic mud, scraped off the bottom of a basalt sample
D24	0	--	--	--	No recovery	--

Table 7. Foraminifer and calcareous nannofossil ages of sediments and sedimentary rocks.

[Identifications by Paula Quinterno; EDAX, energy dispersive analysis by x-rays attachment to scanning electron microscope; --, no data]

Sample	Lithology	Microfossils	Age	Comments
		Adam Seamount		
D7-1	Mudstone	Barren	--	--
D7-2A	Mudstone	Barren	--	--
D7-2B	Mud filling boring	Barren	--	--
D9-1A	Tuff	Barren	--	--
		Hoss Seamount		
D11-1	Porcellanite	*Cyclicargolithus floridanus* *Dictyococcites scrippsae??* *Discoaster* spp. *Helicosphaera acissura* *Reticulofenestra* sp. *Sphenolithus* sp.	Probably Miocene	sparse flora, poorly preserved (EDAX shows nannos are probably replaced by apatite)
		Little Joe Seamount		
D14-2G	Mud from burrows	Barren	--	--
		Ben Seamount		
D17-3B	Hyaloclastite	*Discoaster* sp. aff. *D. kugleri* *Discoaster* sp.	Very questionably Miocene	Nannos are sparse and very poorly preserved
D17-5B	Mudstone	Barren	--	--
		Flint Seamount		
D23-1	Mud	*Ceratolithus cristatus* *C. simplez* *C. telesmus* *Coccolithus pelagicus* *Calcidiscus leptoporus* *Emiliania huzleyi* *Gephyrocapsa* spp. *Helicosphaera hyalina??* *Rhabdosphaera* sp. aff. *R. claviger*	Late Pleistocene or younger	Nannos are abundant, but poorly preserved

Table 8. X-ray diffraction mineralogy of substrate rocks.

[Major >25%, Moderate 5% - 25%, Minor <5%; All breccias are sedimentary, and most are volcaniclastic; CFA, carbonate fluorapatite; --, no data; δ, delta]

Sample	Rock/Sediment	Major	Moderate	Minor/Trace
D3-5B	Breccia	Plagioclase, quartz	Illite, ilmenite	--
D3-11	Dolostone	Dolomite	CFA	Smectite, plagioclase, quartz
D4-3B	Breccia matrix	Phillipsite, plagioclase	Smectite	--
D4-4	Basalt	Plagioclase	Pyroxene	Smectite
D5-1D	Basalt	Plagioclase	Pyroxene	--
D5-3C	Breccia matrix	Phillipsite	--	Smectite
D5-17B	Altered basalt	Smectite	Phillipsite, plagioclase	--
D7-1	Mudstone	Plagioclase	Quartz, smectite, illite	Phillipsite
D7-2A	Mudstone	Phillipsite	Smectite, quartz	--
D7-2B	Brown mud infilling	Quartz, illite	Phillipsite, smectite	--
D8-1B	Basalt	Plagioclase	Pyroxene	--
D8-9	Altered vesicular basalt	Amorphous, plagioclase, quartz	Smectite, amphibole	Pyroxene
D9-1A	Altered volcanic tuff	Phillipsite, smectite	K-feldspar, quartz	--
D9-1B	Mn-impregnated hyaloclastite	δ-MnO_2	Todorokite, plagioclase, birnessite, smectite	K-feldspar
D9-3	Altered hyaloclastite	Phillipsite	Smectite	Plagioclase, erionite(?)
D9-8C	Altered hyaloclastite	Phillipsite, calcite	Smectite	--
D9-8D	Cross-bedded sandstone	Plagioclase, quartz	Phillipsite, illite	Smectite, natrolite
D9-9D	Altered hyaloclastite	Smectite, phillipsite	--	Todorokite, birnessite
D9-33A	Dolostone	Dolomite	--	Plagioclase, quartz, illite, chlorite
D9-33B	Burrow mud infill	Illite	Smectite, plagioclase, quartz, chlorite	--
D9-34B	Dolostone	Dolomite	--	Phillipsite, quartz
D10-4B	Mn-cemented breccia	Phillipsite	Illite, todorokite, barite, smectite	Quartz
D11-1	Laminated calcareous porcellanite	Opal-CT	Calcite	Halite, quartz, plagioclase, smectite
D13-2B	Altered basalt	Phillipsite, plagioclase	Goethite, smectite, quartz	--
D14-2A	Dolomitic mudstone	Quartz, plagioclase	Dolomite, phillipsite	Illite, smectite
D14-3A	Phosphorite (breccia)	CFA	--	Quartz, plagioclase
D17-3B	CFA-cemented hyaloclastite	Phillipsite	CFA, smectite	--
D17-5B	Mudstone	Phillipsite, smectite	Plagioclase	--
D17-5C	Fine-grained hyaloclastite	Phillipsite, smectite	--	Plagioclase
D17-5D	Coarse-grained hyaloclastite	Phillipsite, plagioclase	Smectite	--
D17-5E	Mn-rich hyaloclastite	Phillipsite	Plagioclase, smectite	Todorokite
D17-7	Hyaloclastite	Phillipsite, smectite	--	--
D17-8	Phosphorite (breccia)	CFA	--	Smectite, quartz
D17-25	Basalt	Plagioclase	Pyroxene	--

Table 8 continued

Sample	Rock/Sediment	Major	Moderate	Minor/Trace
D17-29	Basalt	Plagioclase	--	Pyroxene
D17-30	Quartzite	Quartz	--	--
D23-1	Foraminiferal mud	Calcite	Quartz	Phillipsite, illite, smectite

Table 9. Whole-rock chemical composition (weight percent) of substrate rocks on six seamounts.

[Chemical composition determined by X-ray fluorescence (XRF); LOI, Loss on ignition at 900˚C; --, no data]

	Rodriguez		San Marcos		Adam				
	D3-5B Breccia	D4-4 Vesicular basalt	D5-1D Basalt	D6-19 Vesicular basalt	D7-1 Mudstone	D8-1B Vesicular basalt	D9-1A Altered tuff	D9-9D Altered hyaloclastite	D9-33A Dolostone
SiO_2	41.9	46.1	46.4	46.7	50.6	49.8	46.3	45.4	7.79
Al_2O_3	13.9	17.8	17.2	17.3	11.3	15.9	12.4	13.6	2.00
Fe_2O_3	6.31	3.76	5.89	5.37	6.85	3.35	9.25	8.43	3.13
FeO	4.14	4.48	4.53	4.44	.11	4.76	.11	--	.72
TiO_2	2.12	2.67	2.80	2.82	.59	1.69	1.60	1.33	.10
Na_2O	3.04	3.29	3.68	3.92	3.79	3.03	2.81	2.61	.46
MgO	7.26	5.74	4.42	4.00	3.87	6.44	4.28	4.12	16.7
K_2O	1.47	1.52	1.73	1.76	2.07	.41	1.77	1.66	.29
CaO	5.77	8.07	8.63	9.65	2.46	12.7	.82	1.82	27.4
P_2O_5	.31	1.10	.86	.94	.44	.24	.11	.11	.27
MnO	.49	.13	.17	.26	.52	.14	.23	3.37	.62
LOI	12.3	4.83	3.27	2.37	15.3	1.55	19.5	17.0	40.6
Total	99.0	99.5	99.6	99.5	97.9	100.0	99.2	96.8	100.1
H_2O^+	2.79	.72	1.68	1.93	1.45	.47	5.14	5.16	1.52
H_2O^-	8.59	3.84	1.81	.79	8.69	.70	12.6	10.6	.75
CO_2	.14	.06	.02	<.01	.60	.57	.05	.08	--

	Adam	Hoss		Little Joe		Ben			
	D9-34B Dolostone	D10-4B Mn-cemented breccia	D11-1 Calcareous porcellanite	D14-2A Dolomitic mudstone	D14-3A Phosphorite (breccia)	D17-7 Hyalo-clastite	D17-8 Phosphorite (breccia)	D17-25 Basalt	D17-29 Basalt
SiO_2	9.84	41.6	69.8	68.4	2.92	46.8	8.95	50.3	46.6
Al_2O_3	2.66	11.4	4.26	8.93	.58	12.3	1.68	15.2	18.9
Fe_2O_3	2.70	9.10	.98	2.86	.31	10.4	1.58	3.36	7.59
FeO	.44	--	1.09	1.19	.21	--	.57	5.43	3.52
TiO_2	.13	1.26	.25	.51	<.02	1.25	.04	1.41	1.03
Na_2O	.53	2.56	1.30	1.68	1.44	2.86	1.50	2.74	2.52
MgO	16.5	4.92	1.08	2.58	1.00	4.17	1.25	6.77	3.02
K_2O	.43	1.44	.84	1.63	.13	2.63	.60	0.11	.25
CaO	26.0	4.11	7.29	3.07	48.3	1.85	4.6	13.7	14.1
P_2O_5	.36	.15	.26	.91	30.2	.06	26.6	0.13	.41
MnO	.14	6.93	<.02	.07	<.02	1.19	<0.02	0.16	.11
LOI	40.1	12.5	11.8	7.51	10.6	16.2	11.1	.90	2.16
Total	99.8	93.5	99.0	99.3	95.7	99.2	96.5	100.2	100.2
H_2O^+	1.90	4.83	3.38	2.52	3.22	6.16	2.49	.32	1.44
H_2O^-	.71	6.69	3.02	2.41	1.86	9.87	3.00	.34	.85
CO_2	38.9	.06	8.75	3.17	7.26	.05	7.59	.23	.16

Table 10. X-ray diffraction mineralogy of ferromanganese deposits.

[Intervals measured from the outer surface of crusts and nodules. B, bulk crust; BS, bulk side crust, usually granular texture; BU, bulk underside crust; L, crust layer; LU, layer from underside crust; BN, bulk nodule; NN, nodule nucleus; MB, manganiferous breccia. Percentages were determined by using the following weighting factors relative to quartz set at 1: δ-MnO_2 70; todorokite 10; birnessite 12 (Hein and others, 1988); plagioclase 2.8; calcite 1.65; smectite 3.0; goethite 7.0; phillipsite 17.0; illite 6.0; halite 2.0 (From Cook and others, 1975). The limit of detection for each mineral falls between 0.2 and 1.0 percent, except the manganese minerals, which are greater, perhaps as much as 10 percent for δ-MnO_2. mm, millimeters; %, percent; δ, delta.]

Sample	Type and interval (mm)	δ-MnO_2 (%)	Others (%)
D3-4A	B (0-10)	82	12-Plagioclase, 6-quartz
D3-5A	B (0-10)	87	7-Plagioclase, 6-quartz, <1-smectite
D3-7A	B (0-4)	87	7-Plagioclase, 6-quartz
D4-1A	B (0-3)	95	3-Plagioclase, 2-quartz
D4-3A	B (0-4)	92	5-Quartz, 3-plagioclase
D5-1A	B (0-25)	93	4-Plagioclase, 3-quartz
D5-1B	L (0-15)	91	6-Plagioclase, 3-quartz
D5-1C	L (15-21)	96	3-Plagioclase, 1-quartz
D5-2A	B (0-10)	88	6-Plagioclase, 6-quartz
D5-3A	B (0-16)	88	7-Plagioclase, 5-quartz
D5-3E	BS	96	3-Plagioclase, 1-quartz
D5-6	B (0-15)	86	9-Plagioclase, 5-quartz
D5-16A	BS (0-6)	94	4-Plagioclase, 1-quartz, 1-chabezite(?)
D5-17A	B (0-12)	82	10-Plagioclase, 6-quartz, 2-todorokite
D6-1A	B (0-15)	69	18-Plagioclase, 9-quartz, 3-todorokite, 1-smectite
D6-1B	B (0-10)	88	5-Plagioclase, 4-quartz, 3-todorokite
D6-2	B (0-15)	77	8-Todorokite, 6-dolomite, 5-plagioclase, 4-quartz
D6-10	B (0-30)	80	10-Todorokite, 6-plagioclase, 4-quartz
D6-34A	L (0-6)	81	8-Todorokite, 6-quartz, 5-plagioclase
D6-34B	L (6-18)	95	3-Plagioclase, 1-quartz, 1-todorokite
D6-37	B (0-15)	86	7-Plagioclase, 6-quartz, 1-smectite
D7-2C	B (0-10)	85	10-Plagioclase, 5-quartz
D7-5	B (0-15)	63	23-Todorokite, 7-quartz, 7-plagioclase
D7-8	B (0-24)	94	3-Plagioclase, 3-quartz
D8-1A	B (0-18)	81	12-Plagioclase, 6-quartz, 1-todorokite
D8-2B	L (0-12)	85	9-Plagioclase, 6-quartz
D8-2C	L (12-37)	86	5-Todorokite, 6-plagioclase, 3-quartz
D8-2D	L (37-65)	89	6-Plagioclase, 2-goethite, 3-quartz
D8-3B	L (0-5)	86	9-Plagioclase, 5-quartz
D8-3C	L (5-17)	90	4-Plagioclase, 3-quartz, 3-todorokite
D8-3D	L (17- 36)	86	9-Plagioclase, 5-quartz
D8-5	BN (0-25)	78	9-Todorokite, 7-quartz, 6-plagioclase
D8-10	NN	53	19-Plagioclase, 11-todorokite, 10-dolomite, 6-quartz, 1-smectite
D9-9A	B (0-35)	85	9-Todorokite, 3-plagioclase, 3-quartz
D9-14A	B (0-7)	90	5-Todorokite, 3-plagioclase, 2-quartz

Table 10 continued

Sample	Type and interval (mm)	δ-MnO_2 (%)	Others (%)
D9-14B	L (0-30)	91	4-Todorokite, 3-plagioclase, 2-quartz
D9-14C	L (0-20)	85	8-Todorokite, 3-plagioclase, 3-quartz, 1-smectite
D9-16A	B (0-55)	87	9-Todorokite, 2-plagioclase, 2-quartz, <1-smectite
D9-16B	L (0-10)	80	10-Todorokite, 3-quartz, 3-plagioclase, 3-birnessite
D9-16C	L (10-55)	87	7-Todorokite, 2-plagioclase, 2-birnessite, 1-quartz, 1-smectite
D9-21A	B (0-50)	88	5-Todorokite, 3-birnessite(?), 2-plagioclase, 2-quartz
D9-21B	L (0-4)	98	1-Illite(?), 1-plagioclase(?)
D9-21C	L (4-29)	97	1-Plagioclase, 1-quartz, 1-smectite
D9-21D	L (29-54)	90	5-Todorokite, 3-plagioclase, 2-quartz
D9-23	BN (0-55)	86	7-Todorokite, 3-plagioclase, 3-quartz, 1-smectite
D9-29	B (0-55)	88	7-Todorokite, 3-plagioclase, 2-quartz
D9-31	B (0-4)	90	6-Quartz, 4-plagioclase
D9-34A	B (0-12)	91	5-Quartz, 4-plagioclase
D9-41	B (0-40)	96	2-Plagioclase, 2-quartz
D10-3	B (0-40)	63	17-Todorokite, 6-phillipsite, 5-barite, 4-illite, 3-quartz, 2-smectite
D10-4A	B (0-20)	71	12-Todorokite, 6-plagioclase, 3-barite, 3-quartz, 2-illite, 2-phillipsite, 1-smectite
D10-6	B (0-40)	88	5-Plagioclase, 5-todorokite, 2-quartz
D10-7A	B (0-25)	93	4-Plagioclase, 3-quartz
D10-7B	L (0-3)	72	15-Plagioclase, 13-quartz
D10-7C	L (3-25)	97	2-Plagioclase, 1-quartz
D11-4A	L (0-8)	79	13-Plagioclase, 8-quartz
D11-4B	L (8-27)	91	4-Todorokite, 2-plagioclase, 2-goethite, 1-quartz
D11-4C	L (27-33)	92	3-Goethite, 2-plagioclase, 2-todorokite, 1-quartz
D11-6	B (0-50)	88	6-Plagioclase, 3-quartz, 3-todorokite
D11-7	B (0-45)	84	7-Quartz, 6-plagioclase, 3-todorokite
D11-11A	B (0-70)	92	3-Plagioclase, 3-quartz, 2-todorokite
D13-1A	B (0-12)	75	17-Plagioclase, 8-quartz
D13-1B	MB	17	57-Goethite, 18-plagioclase, 8-quartz
D13-1C	BU (0-4)	72	11-Todorokite, 8-phillipsite, 3-quartz , 2-plagioclase, <1-smectite
D13-2A	B (0-12)	77	8-Plagioclase, 9-birnessite, 4-todorokite, 2-quartz
D13-2C	BU (0-10)	63	11- Barite, 9-todorokite, 8-plag, 4-birnessite, 3-quartz , 2-smectite
D13-3A	B (0-27)	77	7-Plagioclase, 6-todorokite, 5-goethite, 5-quartz
D14-1A	B (0-40)	88	6-Plagioclase, 4-quartz
D14-1C	BU (0-15)	71	15-Todorokite, 5-birnessite, 3-plag, 3-goethite, 2-quartz, 1-smectite
D14-2C	B (0-6)	87	7-Plagioclase, 6-quartz
D14-2D	LU (0-5)	82	7-Todorokite, 6-plagioclase, 5-quartz
D14-2E	LU (5-11)	81	8-Plagioclase, 7-quartz, 4-todorokite
D14-3	B (0-9)	86	8-Quartz, 6-plagioclase
D14-4	B (0-40)	94	3-Quartz 3-plagioclase
D17-1	B (0-18)	91	4-Plagioclase, 3-quartz, 2-goethite
D17-3A	B (0-10)	90	5-Plagioclase, 5-quartz
D17-4	B (0-25)	91	5-Quartz, 3-plagioclase, 1-goethite
D17-6A	B (0-18)	93	3-Plagioclase, 2-quartz, 2-goethite
D17-6B	B (0-10)	95	4-Plagioclase, 1-quartz, 1-calcite
D17-22	B (0-25)	94	2-Plagioclase, 2-quartz, 2-goethite
D21-1A	B (0-15)	98	1-Plagioclase, 1-quartz
D23-2B	B (0-18)	88	5-Plagioclase, 3-quartz, 3-birnessite, 1-smectite
D23-2C	B (0-20)	85	7-Plagioclase, 5-quartz, 3-todorokite
D23-3	B (0-18)	92	3-Plagioclase, 3-quartz, 1-smectite, 1-goethite

Table 11. Chemical composition of Fe-Mn crusts and nodules.

[--, not analyzed; ICP, inductively coupled plasma; ICPMS, ICP/mass spectrometry; ICPMS/FA, ICPMS/fire assay; XRF, x-ray fluorescence spectrometry; NAA, neutron activation analysis; AA, atomic absorption; FAA, flame AA; WET, wet chemistry; LECO, induction furnace; GFAA/FA, graphite furnace AA/Fire assay; wt%, weight percent; ppb, parts per billion; ppm, parts per million. Intervals measured in millimeters from the outer surface of crusts and nodules; L, crust layer; B, bulk crust; LU, underside of crust layer; BN, bulk nodule; BS, side of bulk crust; BU, underside bulk crust; MB, manganiferous breccia. 1D13-2C was analyzed by LECO for total sulfur, which is 1.49 weight percent; gold was analyzed by GFAA/FA for samples that Pd, Pt, and Rh were analyzed and is <20 ppb for all samples.]

		Rodriguez Seamount					San Marcos Seamount		
		D3-4A B (0-10)	D3-5A B (0-10)	D3-7A B (0-4)	D4-1A B (0-3)	D4-3A B (0-4)	D5-1A B (0-25)	D5-1B L (0-15)	D5-1C L (15-21)
Fe wt%	ICP	17.6	16.9	19.3	21.4	20.0	15.1	15.0	14.6
Mn	ICP	6.30	5.70	9.90	12.3	11.8	13.8	12.9	16.0
Fe/Mn	--	2.8	3.0	1.9	1.7	1.7	1.1	1.2	.9
Si	ICP	16.1	16.3	10.7	5.00	6.92	6.03	7.48	4.39
Na	ICP	1.71	1.80	1.48	1.33	1.33	1.34	1.40	1.25
Al	ICP	2.73	3.10	1.85	.81	1.12	1.25	1.54	.96
K	FAA	.86	.93	.60	.34	.42	.51	.59	.43
Mg	ICP	.71	1.00	.67	.78	.73	.76	.74	.80
Ca	ICP	1.25	1.36	1.44	1.59	1.56	1.56	1.56	1.66
Ti	ICP	.32	.44	.29	.44	.31	.48	.39	.49
P	ICP	.42	.39	.57	.72	.70	.27	.27	.27
H_2O^+	WET	6.0	5.9	7.1	7.4	6.9	7.5	6.7	8.1
H_2O^-	WET	11.0	10.9	13.9	19.2	18.0	24.7	23.0	24.7
CO_2	WET	.20	.19	.33	.35	.40	.46	1.3	.45
As ppm	GFAA	240	220	350	470	440	210	210	220
Ba	ICP	780	660	920	970	1,000	1,100	1,000	1,200
Cd	GFAA	.70	.60	1.3	.95	1.9	1.6	1.6	1.9
Ce	ICP	1,000	970	1,300	1,500	1,500	930	810	900
Co	GFAA	1,400	1,400	2,100	4,500	3,000	1,400	1,100	1,600
Cr	GFAA	120	160	83	34	40	8.5	9.5	7.0
Cu	ICP	42	40	56	39	39	460	500	620
Mo	ICP	120	81	260	370	350	320	310	430
Ni	ICP	400	410	620	650	730	1,800	1,500	2,400
Pb	FAA	1,300	1,200	1,800	2,300	2,200	780	720	760
Sr	ICP	740	680	1,000	1,300	1,300	1,000	950	1,100
V	ICP	510	470	680	800	840	440	450	480
Y	ICP	100	93	140	170	170	160	150	190
Zn	FAA	310	290	360	350	400	420	400	460
Pd ppb	ICPMS/FA	--	--	--	--	--	3.5	3.2	4.5
Pt	ICPMS/FA	--	--	--	--	--	54	44	52
Rh	ICPMS/FA	--	--	--	--	--	5.2	4.8	5.1

Table 11 continued

		San Marcos Seamount							
		D5-2A B (0-10)	D5-3A B (0-16)	D5-3E BS	D5-6 B (0-15)	D5-16A BS (0-6)	D5-17A B (0-12)	D6-1A B (0-15)	D6-1B B (0-10)
Fe wt%	ICP	14.9	13.7	13.0	14.5	13.0	13.1	9.5	15.7
Mn	ICP	11.8	10.0	16.3	10.1	15.0	9.30	4.00	13.2
Fe/Mn	--	1.3	1.4	.8	1.4	.9	1.4	2.4	1.2
Si	ICP	9.82	13.0	4.39	11.9	5.47	13.2	23.0	8.56
Na	ICP	1.51	1.78	1.52	1.76	1.16	1.77	2.45	1.49
Al	ICP	2.05	2.40	.96	2.34	1.23	2.67	4.50	1.59
K	FAA	.69	.80	.49	.78	.52	.86	1.36	.65
Mg	ICP	.77	.72	.85	.72	.80	.91	.69	.83
Ca	ICP	1.57	1.50	1.62	1.51	1.60	1.19	1.26	1.41
Ti	ICP	.41	.35	.72	.35	.69	.42	.24	.43
P	ICP	.27	.25	.27	.27	.26	.19	.14	.30
H_2O^+	WET	4.2	7.5	6.3	6.5	8.2	5.3	4.6	7.6
H_2O^-	WET	18.8	16.9	25.6	16.5	24.5	16.5	8.0	17.3
CO_2	WET	.31	.28	.32	.26	.38	.11	.11	.26
As ppm	GFAA	200	170	190	190	190	98	90	200
Ba	ICP	1,000	1,000	900	980	920	1,700	1,100	1,500
Cd	GFAA	1.0	.90	2.0	.78	1.9	.73	.35	3.1
Ce	ICP	750	740	1,300	740	1,300	710	380	880
Co	ICP	1,100	1,100	4,100	1,100	3,600	1,200	700	2,700
Cr	GFAA	14	18	9.8	16	12	18	40	14
Cu	ICP	510	420	400	400	380	1100	210	510
Mo	ICP	270	180	220	200	220	14	42	260
Ni	ICP	1,300	1,200	3,100	1,100	2,700	1,800	780	2,800
Pb	FAA	730	650	920	720	940	650	360	1,000
Sr	ICP	960	860	980	880	960	830	520	1,100
V	ICP	440	380	400	410	390	290	200	490
Y	ICP	140	120	140	120	140	96	52	130
Zn	FAA	400	380	420	380	400	470	240	570
Pd ppb	ICPMS/FA	--	--	--	--	--	--	--	--
Pt	ICPMS/FA	--	--	--	--	--	--	--	--
Rh	ICPMS/FA	--	--	--	--	--	--	--	--

Table 11 continued

		San Marcos Seamount					Adam Seamount		
		D6-2 B (0-15)	D6-10 B (0-30)	D6-34A L (0-6)	D6-34B L (6-18)	D6-37 B (0-15)	D7-2C B (0-10)	D7-5 B (0-15)	D7-8 B (0-24)
Fe wt%	ICP	14.9	12.3	14.3	16.5	15.6	12.5	7.7	16.9
Mn	ICP	15.2	17.0	14.7	16.9	11.1	11.7	20.9	14.9
Fe/Mn	--	1.0	.7	1.0	1.0	1.4	1.1	.4	1.1
Si	ICP	8.60	9.30	7.85	5.05	11.7	13.0	10.1	8.23
Na	ICP	1.58	1.66	1.51	1.30	1.77	1.90	1.85	1.60
Al	ICP	1.65	2.16	1.52	.94	2.05	3.10	2.85	1.85
K	FAA	.91	.95	.62	.46	.71	1.12	1.09	.70
Mg	ICP	1.49	1.60	.92	.86	.70	1.08	1.45	.92
Ca	ICP	1.58	1.71	1.44	1.67	1.54	1.46	1.26	1.69
Ti	ICP	.31	.51	.41	.51	.40	.36	.26	.59
P	ICP	.23	.20	.26	.33	.30	.22	.15	.26
H_2O^+	WET	7.5	9.3	8.9	7.0	8.9	6.6	8.2	10.0
H_2O^-	WET	13.6	10.7	19.3	21.2	15.5	10.9	8.5	14.5
CO_2	WET	.65	.24	.43	.28	.29	.28	.14	.35
As ppm	GFAA	160	130	190	230	210	150	88	210
Ba	ICP	1,600	5,000	1,300	1,700	1,100	1,100	2,300	1,200
Cd	GFAA	8.3	7.4	4.2	2.8	1.0	2.0	9.1	1.8
Ce	ICP	300	580	750	940	870	680	340	1,100
Co	ICP	1,700	2,100	2,300	3,400	1,900	1,000	490	1,400
Cr	GFAA	53	45	10	8.0	18	21	27	12
Cu	ICP	850	950	620	350	240	1,200	3,500	760
Mo	ICP	250	290	240	390	260	160	270	260
Ni	ICP	6,300	5,600	4,000	2,100	1,100	2,900	6,300	2,200
Pb	FAA	400	650	970	1,400	1,100	510	380	790
Sr	ICP	650	1,000	900	1,200	980	740	560	1,000
V	ICP	440	370	420	520	450	340	320	420
Y	ICP	76	91	120	160	140	105	66	150
Zn	FAA	870	750	620	510	420	480	920	450
Pd ppb	ICPMS/FA	--	3.7	2.5	7.3	--	--	--	2.5
Pt	ICPMS/FA	--	72	72	69	--	--	--	76
Rh	ICPMS/FA	--	5.2	5.3	4.3	--	--	--	6.0

Table 11 continued

		Adam Seamount							
		D8-1A B (0-18)	D8-2A B (0-65)	D8-2B L (0-12)	D8-2C L (12-37)	D8-2D L (37-65)	D8-3A B (0-36)	D8-3B L (0-5)	D8-3C L (5-17)
Fe wt%	ICP	13.8	17.3	15.7	15.3	19.5	17.7	16.1	17.9
Mn	ICP	8.40	10.5	10.4	13.1	8.70	8.10	8.40	10.3
Fe/Mn	--	1.6	1.6	1.5	1.2	2.2	2.2	1.9	1.7
Si	ICP	11.5	8.32	12.9	7.48	8.32	9.26	10.2	6.68
Na	ICP	1.54	1.34	1.82	1.27	1.36	1.39	1.48	1.17
Al	ICP	2.31	1.79	2.59	1.53	1.96	2.10	1.95	1.35
K	FAA	.71	.58	.82	.57	.58	.73	.65	.46
Mg	ICP	.77	.86	.87	1.05	.77	1.02	.78	1.00
Ca	ICP	1.18	1.25	1.50	1.21	1.20	1.00	1.20	.92
Ti	ICP	.40	.43	.40	.49	.37	.55	0.47	.59
P	ICP	.22	.25	.28	.24	.24	.22	.26	.24
H_2O^+	WET	5.5	8.9	9.0	9.3	6.5	6.4	6.2	7.0
H_2O^-	WET	22.2	21.9	10.9	21.9	21.5	22.8	22.0	25.1
CO_2	WET	.21	.14	.23	.16	.20	.17	.22	.19
As ppm	GFAA	150	190	190	150	190	150	200	150
Ba	ICP	1,200	2,100	1,300	4,100	2,000	1,600	1,100	2,300
Cd	GFAA	.80	1.5	1.5	2.2	1.3	.95	.85	.95
Ce	ICP	790	730	860	860	530	780	1,000	980
Co	ICP	1,400	1,400	1,400	2,000	920	1,700	1,600	2,100
Cr	GFAA	16	11	15	8.5	13	20	14	10
Cu	ICP	710	1,400	970	2,100	1,400	880	640	1,400
Mo	ICP	100	190	180	170	190	48	100	50
Ni	ICP	1,600	,1600	1,600	2,700	1,200	1,900	1,200	2,200
Pb	FAA	710	750	800	740	580	760	880	900
Sr	ICP	800	950	950	1,100	910	720	840	940
V	ICP	320	430	420	400	470	340	360	380
Y	ICP	97	130	120	135	120	90	110	115
Zn	FAA	420	580	440	620	680	500	400	620
Pd ppb	ICPMS/FA	--	3.2	1.7	6.5	3.2	4.7	2.0	2.7
Pt	ICPMS/FA	--	56	46	97	64	29	49	86
Rh	ICPMS/FA	--	5.2	2.8	5.7	4.3	2.3	4.6	6.1

Table 11 continued

		Adam Seamount							
		D8-3D	D8-5	D9-9A	D9-14A	D9-14B	D9-14C	D9-16A	D9-16B
		L (17-36)	BN (0-25)	B (0-35)	B (0-7)	L (0-30)	L (0-20)	B (0-55)	L (0-10)
Fe wt%	ICP	21.0	16.2	14.0	16.9	17.2	14.6	12.1	12.2
Mn	ICP	7.70	10.5	20.6	15.6	16.1	17.7	21.2	18.7
Fe/Mn	--	2.7	1.5	.7	1.1	1.1	.8	.6	.7
Si	ICP	11.8	12.9	4.91	5.05	5.56	6.26	5.33	5.38
Na	ICP	1.64	1.78	1.51	1.28	1.37	1.40	1.43	1.47
Al	ICP	3.00	2.62	.98	.85	.89	.86	1.03	1.13
K	FAA	.78	.87	.63	.50	.54	.74	.71	.61
Mg	ICP	1.34	1.35	1.18	.97	.96	1.09	1.20	1.07
Ca	ICP	1.70	1.10	1.53	1.35	1.41	1.16	1.42	1.41
Ti	ICP	.55	.50	.33	.38	.38	.12	.27	.33
P	ICP	.24	.20	.28	.32	.31	.23	.24	.26
H_2O^+	WET	10.3	11.0	8.7	8.4	9.8	8.8	9.4	7.5
H_2O^-	WET	8.0	9.0	15.5	20.7	18.2	19.6	17.1	21.4
CO_2	WET	.21	.18	.30	.28	.30	.23	.24	.24
As ppm	GFAA	170	120	200	220	230	170	170	180
Ba	ICP	2,100	2,100	2,000	2,400	2,200	2,000	4,000	2,000
Cd	GFAA	.90	1.3	8.1	5.1	5.8	12	11	7.8
Ce	ICP	600	830	640	770	770	260	540	640
Co	ICP	1,200	2,300	2,700	2,800	2,800	2,000	2,300	2,500
Cr	GFAA	40	22	14	9.0	8.5	12	12	10
Cu	ICP	1,100	1,900	810	600	520	510	1,000	780
Mo	ICP	52	< 5	400	350	330	290	400	330
Ni	ICP	1,800	3,900	6,900	3,300	3,300	4,500	7,100	6,100
Pb	FAA	650	910	890	1,100	1,100	300	660	840
Sr	ICP	780	860	1,000	1,100	1,100	760	1,000	940
V	ICP	420	340	510	560	550	470	470	440
Y	ICP	98	79	120	120	120	82	100	100
Zn	FAA	660	640	850	700	740	920	910	770
Pd ppb	ICPMS/FA	3.2	3.7	--	3.0	3.2	4.7	4.2	3.5
Pt	ICPMS/FA	99	79	--	64	64	29	89	62
Rh	ICPMS/FA	6.0	5.3	--	3.1	4.3	2.3	5.1	4.9

Table 11 continued

		Adam Seamount							
		D9-16C L (10-55)	D9-21A B (0-50)	D9-21B L (0-4)	D9-21C L (4-29)	D9-21D L (29-54)	D9-23 BN (0-55)	D9-29 B (0-55)	D9-31 B (0-4)
Fe wt%	ICP	11.8	15.0	15.9	15.6	13.8	13.7	13.7	19.1
Mn	ICP	19.5	17.7	19.0	17.7	17.8	15.6	18.3	11.6
Fe/Mn	--	.6	.8	.8	.9	.8	.9	.7	1.6
Si	ICP	3.93	3.83	2.85	2.81	5.05	6.31	5.98	7.62
Na	ICP	1.28	1.26	1.18	1.19	1.41	1.36	1.43	1.41
Al	ICP	.88	.51	.29	.32	.84	1.26	.93	1.14
K	FAA	.61	.48	.35	.37	.61	.63	.71	.47
Mg	ICP	1.16	.85	.79	.77	.98	1.15	1.22	.70
Ca	ICP	1.37	1.58	1.92	1.80	1.35	1.15	1.43	1.51
Ti	ICP	.32	.32	.45	.43	.19	.35	.32	.41
P	ICP	.23	.31	.37	.36	.25	.24	.26	.41
H_2O^+	WET	7.0	8.5	9.2	10.5	7.4	10.6	9.1	9.1
H_2O^-	WET	22.7	23.4	21.4	24.9	22.7	18.1	16.9	18.5
CO_2	WET	.22	.32	.37	.33	.20	.21	.30	.39
As ppm	GFAA	170	240	270	260	200	160	190	280
Ba	ICP	5,100	1,700	1,600	1,500	1,700	3,000	4,600	1,200
Cd	GFAA	9.0	5.8	2.2	2.4	9.7	4.5	5.9	0.80
Ce	ICP	560	640	920	850	330	660	570	990
Co	ICP	2,300	2,600	3,400	2,900	2,100	2,500	2,300	2,000
Cr	GFAA	11	5.5	5.5	2.8	8.0	16	16	18
Cu	ICP	1,200	390	440	270	550	750	930	160
Mo	ICP	390	510	720	620	350	220	410	260
Ni	ICP	7,000	3,500	2,500	2,400	5,400	5,100	6,300	850
Pb	FAA	810	950	1,400	1,300	430	890	810	1,400
Sr	ICP	1,100	1,100	1,400	1,300	780	920	1,100	1,100
V	ICP	450	610	700	650	490	390	490	600
Y	ICP	110	150	200	190	95	84	120	160
Zn	FAA	800	670	600	510	920	660	760	490
Pd ppb	ICPMS/FA	5.3	3.7	3.5	3.2	3.8	--	--	--
Pt	ICPMS/FA	72	44	51	21	31	--	--	--
Rh	ICPMS/FA	5.4	3.0	5.1	4.0	3.5	--	--	--

Table 11 continued

		Adam Seamount		Hoss Seamount					
		D9-34A	D9-41	D10-3	D10-4A	D10-6	D10-7A	D10-7B	D10-7C
		B (0-12)	B (0-40)	B (0-40)	B (0-20)	B (0-40)	B (0-25)	L (0-3)	L (3-25)
Fe wt%	ICP	18.3	16.0	14.0	13.1	18.9	15.8	11.0	16.5
Mn	ICP	15.2	16.4	13.7	10.7	8.30	11.8	5.50	13.1
Fe/Mn	--	1.2	1.0	1.0	1.2	2.3	1.3	2.0	1.3
Si	ICP	7.06	3.97	11.4	12.3	9.30	8.93	19.8	4.58
Na	ICP	1.54	1.25	1.48	1.53	1.35	1.46	2.30	1.22
Al	ICP	1.19	.49	1.90	2.43	1.50	1.08	3.90	.68
K	FAA	.61	.37	1.10	1.08	.58	.47	1.12	.38
Mg	ICP	.95	.72	1.81	1.43	.83	.70	.60	.77
Ca	ICP	1.53	1.77	.91	1.65	.95	1.34	1.52	1.34
Ti	ICP	.39	.42	.19	.38	.50	.42	.26	.53
P	ICP	.36	.37	.16	.35	.27	.28	.21	.31
H_2O^+	WET	9.9	8.4	8.6	7.5	8.2	7.8	6.4	8.5
H_2O^-	WET	13.0	24.3	8.8	13.3	19.8	24.2	9.8	25.8
CO_2	WET	.36	.51	.17	.36	.20	.29	.36	.29
As ppm	GFAA	260	270	84	84	170	190	130	220
Ba	ICP	2,000	1,300	2,2100	8,200	2,100	1,900	940	2,500
Cd	GFAA	3.0	1.3	3.4	1.4	.50	1.2	.38	1.2
Ce	ICP	810	900	270	480	930	850	550	1,000
Co	ICP	2,600	2,800	2,200	2,200	2,600	2,600	900	3,500
Cr	GFAA	18	8.3	24	49	44	24	32	7.5
Cu	ICP	420	220	1,300	1,100	530	470	160	630
Mo	ICP	350	560	75	47	< 5	270	54	330
Ni	ICP	2,700	1,900	4,600	3,100	1,700	1,300	460	1,700
Pb	FAA	1,200	1,400	420	600	1,200	1,200	600	1,400
Sr	ICP	1,200	1,300	1,700	1,000	940	1,100	680	1,300
V	ICP	600	620	300	310	460	470	290	520
Y	ICP	150	190	49	73	110	130	77	150
Zn	FAA	630	470	760	580	530	490	270	550
Pd ppb	ICPMS/FA	--	--	--	--	--	--	--	--
Pt	ICPMS/FA	--	--	--	--	--	--	--	--
Rh	ICPMS/FA	--	--	--	--	--	--	--	--

Table 11 continued

		Hoss Seamount			Little Joe Seamount				
		D11-4A	D11-4B	D11-4C	D11-4D	D11-6	D11-7	D11-11A	D13-1A
		L (0-8)	L (8-27)	L (27-33)	B (0-36)	B (0-50)	B (0-45)	B (0-70)	B (0-12)
Fe wt%	ICP	13.0	15.9	20.5	16.5	14.2	13.7	15.4	13.3
Mn	ICP	7.30	15.3	13.5	13.9	12.4	11.1	14.2	4.00
Fe/Mn	--	1.8	1.0	1.5	1.2	1.1	1.2	1.1	3.3
Si	ICP	16.4	4.49	4.35	6.26	7.48	9.21	5.19	17.9
Na	ICP	2.12	1.28	1.19	1.31	1.40	1.52	1.32	1.91
Al	ICP	3.10	.67	.82	.99	1.52	1.83	.98	3.40
K	FAA	.98	.42	.37	.46	.58	.65	.46	.94
Mg	ICP	.63	.73	.80	.73	.75	.70	.72	.62
Ca	ICP	1.41	1.64	1.46	1.57	1.45	1.51	1.62	1.23
Ti	ICP	.37	.48	.52	.47	.41	.42	.50	.36
P	ICP	.23	.33	.33	.30	.27	.27	.31	.21
H_2O^+	WET	7.4	9.6	10.3	8.6	7.2	8.3	8.0	5.4
H_2O^-	WET	14.4	24.0	19.6	23.1	23.3	22.7	24.2	15.1
CO_2	WET	.23	.45	.33	.25	.27	.29	.31	.19
As ppm	GFAA	170	250	250	240	180	180	240	150
Ba	ICP	960	1,700	2,000	1,700	5,200	1,900	1,300	990
Cd	GFAA	.35	1.6	1.1	1.4	1.3	1.2	1.3	.25
Ce	ICP	720	940	810	840	730	790	940	640
Co	ICP	1,400	2,700	1,900	2,200	1,700	1,900	2,700	730
Cr	GFAA	24	8.0	13	8.0	16	17	7.0	36
Cu	ICP	200	420	650	410	1,100	600	280	220
Mo	ICP	130	530	510	450	350	330	420	16
Ni	ICP	650	2,200	2,300	1,900	2,500	1,600	1,900	570
Pb	FAA	780	1,300	1,300	1,100	880	960	1,100	980
Sr	ICP	770	1,300	1,300	1,200	1,200	1,000	1,100	590
V	ICP	330	600	690	570	480	450	520	310
Y	ICP	100	185	170	160	150	150	170	69
Zn	FAA	310	510	740	540	570	440	450	310
Pd ppb	ICPMS/FA	--	--	--	2.2	--	--	2.5	--
Pt	ICPMS/FA	--	--	--	33	--	--	35	--
Rh	ICPMS/FA	--	--	--	5.4	--	--	5.5	--

Table 11 continued

		Little Joe Seamount							
		D13-1B	D13-1C	D13-2A	D13-2C	D13-3A	D14-1A	D14-1C	D14-2C
		MB	BU (0-4)	B (0-12)	BU(0-10)	B (0-27)	B (0-40)	BU(0-15)	B (0-6)
Fe wt%	ICP	21.1	15.2	27.7	11.8	25.6	16.9	16.4	16.4
Mn	ICP	2.47	10.9	2.59	5.00	5.60	14.9	19.5	12.4
Fe/Mn	--	8.5	1.4	11	2.4	4.6	1.1	.8	1.3
Si	ICP	8.09	8.27	8.74	13.5	9.68	6.55	5.80	8.74
Na	ICP	1.12	1.43	1.27	1.45	1.61	1.46	1.48	1.57
Al	ICP	1.56	1.92	1.75	2.53	1.96	1.07	.80	1.48
K	FAA	.49	.77	.44	1.37	.54	.47	.76	.55
Mg	ICP	.85	1.21	.77	1.75	.97	.77	1.27	.74
Ca	ICP	.61	1.04	.62	.59	.95	1.76	1.29	1.62
Ti	ICP	.71	.52	.67	.41	.66	.45	.19	.48
P	ICP	.27	.24	.34	.12	.38	.38	.23	.36
H_2O^+	WET	5.7	8.1	9.9	6.4	7.3	7.0	5.9	7.4
H_2O^-	WET	31.6	20.9	17.7	14.7	12.8	18.2	15.2	17.8
CO_2	WET	.10	.28	.11	.10	.20	.42	.26	.40
As ppm	GFAA	190	170	220	55	280	250	180	220
Ba	ICP	1,100	1,800	990	56,000	1,100	1,300	3,200	1,100
Cd	GFAA	< .10	2.0	< .10	.28	1.6	1.2	11	1.3
Ce	ICP	860	810	790	290	960	980	300	960
Co	ICP	500	3,000	440	1,500	740	2,500	2,200	2,700
Cr	GFAA	39	42	30	47	68	10	21	18
Cu	ICP	410	830	490	1,000	550	230	770	210
Mo	ICP	< 5	110	< 5	< 5	69	490	390	270
Ni	ICP	1,200	4,200	940	3,000	2,100	1,700	5,700	1,500
Pb	FAA	1,200	920	1,700	420	1,400	1,300	440	1,100
Sr	ICP	370	700	430	3,600	540	1,200	910	1,100
V	ICP	390	380	480	180	540	550	510	440
Y	ICP	89	87	91	78	78	190	94	140
Zn	FAA	490	600	580	560	610	470	880	420
Pd ppb	ICPMS/FA	--	--	--	--	--	--	--	--
Pt	ICPMS/FA	--	--	--	--	--	--	--	--
Rh	ICPMS/FA	--	--	--	--	--	--	--	--

Table 11 continued

		Little Joe Seamount				Ben Seamount			
		D14-2D LU (0-5)	D14-2E LU (5-11)	D14-3B B (0-9)	D14-4 B (0-40)	D17-1 B (0-18)	D17-3A B (0-10)	D17-4 B (0-25)	D17-6A B (0-18)
Fe wt%	ICP	15.5	16.4	16.4	15.9	17.3	16.7	15.9	16.2
Mn	ICP	16.2	13.9	11.3	13.5	14.9	14.3	14.0	14.8
Fe/Mn	--	1.0	1.2	1.5	1.2	1.2	1.2	1.1	1.1
Si	ICP	6.64	8.79	9.23	6.31	5.00	5.89	5.38	4.44
Na	ICP	1.51	1.57	1.63	1.34	1.28	1.34	1.26	1.19
Al	ICP	1.21	1.45	1.71	.99	.76	1.08	.92	.65
K	FAA	.56	.57	.61	.46	.41	.46	.46	.38
Mg	ICP	.87	.78	.70	.71	.78	.77	.76	.72
Ca	ICP	1.61	1.70	1.59	1.61	1.66	1.67	1.54	1.63
Ti	ICP	.44	.38	.39	.48	.53	.48	.59	.41
P	ICP	.32	.37	.36	.34	.35	.36	.29	.34
H_2O^+	WET	6.1	6.4	6.4	9.1	7.0	7.2	9.4	8.8
H_2O^-	WET	17.6	16.3	15.6	23.4	22.3	21.6	24.5	25.2
CO_2	WET	.39	.46	.40	.31	.52	.44	.31	.33
As ppm	GFAA	210	240	230	240	230	230	230	250
Ba	ICP	1,400	1,300	1,100	1,200	1,300	1,300	1,200	1,300
Cd	GFAA	4.1	1.8	1.3	1.5	1.6	1.5	1.4	1.4
Ce	ICP	870	860	900	970	1100	970	1100	930
Co	ICP	2,700	2,200	1,900	2,700	2,700	2,400	2,900	2,100
Cr	GFAA	17	24	19	7.5	11	8.5	8.5	4.3
Cu	ICP	410	330	200	210	350	470	390	410
Mo	ICP	350	440	260	350	440	400	310	450
Ni	ICP	3,900	1,700	1,100	1,600	1,800	1,800	1,900	1,800
Pb	FAA	1,000	1,100	1,100	1,100	1,100	1,100	1,000	1,100
Sr	ICP	1,100	1,200	1,000	1,100	1,200	1,200	1,100	1,200
V	ICP	480	550	450	510	500	510	470	590
Y	ICP	140	150	140	160	190	160	170	190
Zn	FAA	620	480	430	430	460	460	430	470
Pd ppb	ICPMS/FA	--	--	--	2.8	--	--	3.3	1.5
Pt	ICPMS/FA	--	--	--	32	--	--	35	28
Rh	ICPMS/FA	--	--	--	4.8	--	--	5.1	4.4

Table 11 continued

		Ben Seamount		Flint Seamount			
		D17-6B	D17-22	D21-1A	D23-2B	D23-2C	D23-3
		B (0-10)	B (0-25)	B (0-15)	B (0-18)	B (0-20)	B (0-18)
Fe wt%	ICP	16.1	15.5	14.4	16.1	16.1	15.7
Mn	ICP	16.7	15.4	22.2	13.9	12.8	15.1
Fe/Mn	--	1.0	1.0	.6	1.2	1.3	1.0
Si	ICP	4.72	4.21	2.29	6.22	8.65	5.61
Na	ICP	1.34	1.32	1.60	1.05	1.54	1.35
Al	ICP	1.02	.69	.44	1.52	1.84	.97
K	FAA	.50	.41	.46	.61	.64	.44
Mg	ICP	.88	.78	.96	.92	.85	.82
Ca	ICP	1.85	1.63	2.04	1.60	1.73	1.59
Ti	ICP	.84	.58	.78	.81	.61	.59
P	ICP	.32	.31	.41	.27	.34	.31
H_2O^+	WET	7.1	7.1	14.3	7.1	6.2	5.8
H_2O^-	WET	19.2	25.6	14.9	22.4	19.2	22.1
CO_2	WET	.54	.61	.34	.40	.38	.40
As ppm	GFAA	210	220	290	160	190	210
Ba	ICP	1,200	1,200	1,200	1,400	1,300	1,400
Cd	GFAA	1.9	1.5	4.2	2.0	1.8	2.0
Ce	ICP	1,600	1,100	1,700	1,400	1,100	1,100
Co	ICP	5,100	3,500	8,900	4,300	2,700	3,300
Cr	GFAA	8.5	9.0	11	13	14	6.5
Cu	ICP	350	360	280	480	440	560
Mo	ICP	290	410	540	210	270	360
Ni	ICP	2,500	2,400	3,800	2,200	1,900	2,500
Pb	FAA	1,300	1,100	1,800	1,100	1,000	1,200
Sr	ICP	1,100	1,200	1,400	980	990	1,100
V	ICP	430	460	570	330	390	450
Y	ICP	170	180	160	160	180	175
Zn	FAA	450	440	420	460	440	500
Pd ppb	ICPMS/FA	--	--	2.5	--	--	--
Pt	ICPMS/FA	--	--	120	--	--	--
Rh	ICPMS/FA	--	--	6.6	--	--	--

Table 12. Hygroscopic water-free chemical composition (data in Table 11 normalized to 0% H_2O^-).

[Thickness of intervals measured in millimeters; L, crust layer; B, bulk crust; LU, underside crust layer; BN, bulk nodule; BS, side bulk crust; B, underside bulk crust; MB, manganiferous breccia. --, no data; wt%, weight percent; ppm, parts per million; ppb, parts per billion. D13-2C was analyzed by Leco induction furnace for total sulfur, which is 1.75 weight percent.]

	Rodriguez Seamount					San Marcos Seamount					
	D3-4A B(0-10)	D3-5A B(0-10)	D3-7A B(0-4)	D4-1A B(0-3)	D4-3A B(0-4)	D5-1A B(0-25)	D5-1B L(0-15)	D5-1C L(15-21)	D5-2A B(0-10)	D5-3A B(0-16)	D5-3E BS
Fe wt%	19.8	19.0	22.4	26.5	24.4	20.1	19.5	19.4	18.3	16.5	17.5
Mn	7.08	6.40	11.5	15.2	14.4	18.3	16.8	21.2	14.5	12.0	21.9
Fe/Mn	2.8	3.0	2.0	1.7	1.7	1.1	1.2	.9	1.3	1.4	.8
Si	18.1	18.3	12.4	6.19	8.41	7.97	9.74	5.84	12.1	15.6	5.91
Na	1.92	2.02	1.72	1.65	1.62	1.78	1.82	1.66	1.86	2.14	2.04
Al	3.07	3.48	2.15	1.00	1.37	1.66	2.00	1.27	2.52	2.89	1.29
K	.97	1.04	.20	.42	.51	.68	.77	.57	.85	.96	.66
Mg	.80	1.12	.78	.97	.89	1.01	.96	1.06	.95	.87	1.14
Ca	1.40	1.53	1.67	1.97	1.90	2.07	2.03	2.20	1.93	1.81	2.18
Ti	.36	.49	.34	.55	.38	.64	.51	.65	.51	.42	.97
P	.47	.44	.66	.89	.85	.36	.35	.36	.33	.30	.36
H_2O^+	6.74	6.62	8.25	9.16	8.41	9.96	8.70	10.8	5.17	9.03	8.47
H_2O^-	11.0	10.9	13.9	19.2	18.0	24.7	23.0	24.7	18.8	16.9	25.6
CO_2	.23	.21	.38	.43	.49	.61	1.69	.60	.38	.34	.43
As ppm	270	247	407	582	537	279	273	292	246	205	255
Ba	876	741	1,069	1,200	1,220	1,461	1,299	1,594	1,232	1,203	1,210
Cd	.79	.67	1.5	1.2	2.3	2.1	2.0	2.5	1.3	1.1	2.7
Ce	1,124	1,089	1,510	1,856	1,829	1,235	1,052	1,195	924	890	1,747
Co	1,573	1,571	2,439	5,569	3,659	1,859	1,429	2,125	1,355	1,324	5,511
Cr	135	180	96	42	49	11	12	9.3	17	22	13
Cu	47	45	65	48	48	611	649	823	628	505	538
Mo	135	91	302	458	427	425	403	571	333	217	296
Ni	449	460	720	804	890	2,390	1,948	3,187	1,601	1,444	4,167
Pb	1,461	1,347	2,091	2,847	2,683	1,036	935	1,009	899	782	1,237
Sr	831	763	1,161	1,609	1,585	1,328	1,234	1,461	1,182	1,035	1,317
V	573	527	790	990	1024	584	584	637	542	457	538
Y	112	104	163	210	207	212	195	252	172	144	188
Zn	348	325	418	433	488	558	519	611	493	457	565
Pd ppb	--	--	--	--	--	4.6	4.2	6.0	--	--	--
Pt	--	--	--	--	--	72	57	69	--	--	--
Rh	--	--	--	--	--	6.9	6.2	6.8	--	--	--

Table 12 continued

	San Marcos Seamount										Adam Seamount
	D5-6 B(0-15)	D5-16A BS (0-6)	D5-17A B(0-12)	D6-1A B(0-15)	D6-1B B(0-10)	D6-2 B(0-15)	D6-10 B(0-30)	D6-34A L(0-6)	D6-34B L(6-18)	D6-37 B(0-15)	D7-2C B(0-10)
Fe wt%	17.4	17.2	15.7	10.3	19.0	17.2	13.8	17.7	20.9	18.5	14.0
Mn	12.1	19.9	11.1	4.35	16.0	17.6	19.0	18.2	21.4	13.1	13.1
Fe/Mn	1.4	.9	1.4	2.4	1.2	1.0	.7	1.0	1.0	1.4	1.1
Si	14.3	7.28	15.8	25.0	10.4	9.95	10.4	9.79	6.35	13.8	14.6
Na	2.11	1.54	2.12	2.66	1.80	1.83	1.86	1.87	1.65	2.09	2.13
Al	2.80	1.63	3.20	4.89	1.92	1.91	2.42	1.88	1.19	2.43	3.48
K	.93	.69	1.03	1.48	.79	1.05	1.06	.77	.58	.84	1.26
Mg	.86	1.06	1.09	.75	1.00	1.72	1.79	1.14	1.09	.83	1.21
Ca	1.81	2.12	1.43	1.37	1.70	1.83	1.91	1.78	2.12	1.82	1.64
Ti	.42	.91	.50	.26	.52	.36	.57	.51	.65	.47	.40
P	.32	.34	.23	.15	.36	.27	.22	.32	.42	.36	.25
H_2O^+	7.78	10.9	6.35	5.00	9.19	8.68	10.4	11.0	8.88	10.5	7.41
H_2O^-	16.5	24.5	16.5	8.00	17.3	13.6	10.7	19.3	21.2	15.5	10.9
CO_2	.31	.50	.13	.12	.31	.75	.27	.53	.36	.34	.31
As ppm	228	252	117	98	242	185	146	235	292	249	168
Ba	1,174	1,219	2,036	1,196	1,814	1,852	5,599	1,611	2,157	1,302	1,235
Cd	.93	2.5	.87	.38	3.8	9.6	8.3	5.2	3.6	1.2	2.3
Ce	886	1,722	850	413	1,064	347	649	929	1,193	1,030	763
Co	1,317	4,768	1,437	761	3,265	1,968	2,352	2,850	4,315	2,249	1,122
Cr	19	16	22	44	17	61	50	12	10	21	24
Cu	479	503	1317	228	617	984	1,064	768	444	284	1,347
Mo	240	291	17	46	314	289	325	297	495	308	180
Ni	1,317	3,576	2,156	848	3,386	7,292	6,271	4,957	2,665	1,302	3,255
Pb	862	1,245	778	391	1,209	463	728	1,202	1,777	1,302	572
Sr	1,054	1,272	994	565	1,330	752	1,120	1,115	1,523	1,160	831
V	491	517	347	217	593	509	414	520	660	533	382
Y	144	185	115	56.5	157	88	102	149	203	166	118
Zn	455	530	563	261	689	1007	840	768	647	497	539
Pd ppb	--	--	--	--	--	--	4.1	3.1	9.3	--	--
Pt	--	--	--	--	--	--	81	89	88	--	--
Rh	--	--	--	--	--	--	5.8	6.6	5.5	--	--

Table 12 continued

	Adam Seamount										
	D7-5 B(0-15)	D7-8 B(0-24)	D8-1A B(0-18)	D8-2A B(0-65)	D8-2B L(0-12)	D8-2C L(12-37)	D8-2D L(37-65)	D8-3A B(0-36)	D8-3B L(0-5)	D8-3C L(5-17)	D8-3D L(17-36)
Fe wt%	8.4	19.8	17.7	22.2	17.6	19.6	24.8	22.9	20.6	23.9	22.8
Mn	22.8	17.4	10.8	13.4	11.7	16.8	11.1	10.5	10.8	13.8	8.37
Fe/Mn	.4	1.1	1.6	1.7	1.5	1.2	2.2	2.2	1.9	1.7	2.7
Si	11.0	9.59	14.8	10.6	14.5	9.60	10.6	12.0	13.1	8.95	12.8
Na	2.02	1.87	1.98	1.72	2.04	1.63	1.73	1.80	1.90	1.56	1.78
Al	3.11	2.16	2.97	2.29	2.91	1.96	2.50	2.72	2.50	1.80	3.26
K	1.19	.82	.91	.74	.92	.73	.74	.95	.83	.61	.85
Mg	1.58	1.08	.99	1.10	.98	1.34	.98	1.32	1.00	1.34	1.46
Ca	1.38	1.98	1.52	1.60	1.68	1.55	1.53	1.30	1.54	1.23	1.85
Ti	.28	.69	.51	.55	.45	.63	.47	.71	.60	.79	.60
P	.16	.30	.28	.32	.31	.31	.31	.29	.33	.32	.26
H_2O^+	8.96	11.7	7.07	11.4	10.1	11.9	8.28	8.29	7.95	9.35	11.2
H_2O^-	8.50	14.5	22.2	21.9	10.9	21.9	21.5	22.8	22.0	25.1	8.00
CO_2	.15	.41	.27	.18	.26	.21	.26	.22	.28	.25	.23
As ppm	96	246	193	243	213	192	242	194	256	200	185
Ba	2,514	1,404	1,542	2,689	1,459	5,250	2,548	2,073	1,410	3,071	2,283
Cd	10	2.1	1.0	1.9	1.6	2.8	1.7	1.2	1.1	1.3	.98
Ce	372	1,287	1,015	935	965	1,101	675	1,010	1,282	1,308	652
Co	536	1,637	1,799	1,793	1,571	2,561	1,172	2,202	2,051	2,804	1,304
Cr	30	14	21	14	17	11	17	26	18	13	44
Cu	3,825	889	913	1,793	1,089	2,689	1,783	1,140	821	1,869	1,196
Mo	295	304	129	243	202	218	242	62	128	67	57
Ni	6,885	2,573	2,057	2,049	1,796	3,457	1,529	2,461	1,538	2,937	1,957
Pb	415	924	913	960	898	948	739	984	1,128	1,202	707
Sr	612	1,170	1,028	1,216	1,066	1,408	1,159	933	1,077	1,255	848
V	350	491	411	551	471	512	599	440	462	507	457
Y	72.1	175	125	166	135	173	153	117	141	154	107
Zn	1,005	526	540	743	494	794	866	648	513	828	717
Pd ppb	--	2.9	--	4.1	1.9	8.3	4.1	6.1	2.6	3.6	3.5
Pt	--	89	--	72	52	124	82	38	63	115	108
Rh	--	7.0	--	6.7	3.1	7.3	5.5	3.0	5.9	8.1	6.5

Table 12 continued

	Adam Seamount										
	D8-5 BN(0-25)	D9-9A B(0-35)	D9-14A B(0-7)	D9-14B L(0-30)	D9-14C L(0-20)	D9-16A B(0-55)	D9-16B L(0-10)	D9-16C L(10-55)	D9-21A B(0-50)	D9-21B L(0-4)	D9-21C L(4-29)
Fe wt%	17.8	16.6	21.3	21.0	18.2	14.6	15.5	15.3	19.6	20.2	20.8
Mn	11.5	24.4	19.7	19.7	22.0	25.6	23.8	25.2	23.1	24.2	23.6
Fe/Mn	1.5	.7	1.1	1.1	.8	.6	.7	.6	.8	.8	.9
Si	14.2	5.80	6.31	6.85	7.84	6.39	6.87	5.05	4.96	3.69	3.73
Na	1.96	1.79	1.61	1.67	1.74	1.72	1.87	1.66	1.64	1.50	1.58
Al	2.88	1.16	1.07	1.09	1.07	1.24	1.44	1.14	.67	.37	.43
K	.96	.75	.63	.66	.92	.86	.78	.79	.63	.45	.49
Mg	1.48	1.40	1.22	1.17	1.36	1.45	1.36	1.50	1.11	1.01	1.03
Ca	1.21	1.81	1.70	1.72	1.44	1.71	1.79	1.77	2.06	2.44	2.40
Ti	.55	.39	.48	.47	.15	.33	.42	.41	.42	.57	.57
P	.22	.33	.40	.38	.29	.29	.33	.30	.41	.47	.48
H_2O^+	12.1	10.3	10.6	12.0	10.9	11.3	9.54	9.06	11.1	11.7	14.0
H_2O^-	9.00	15.5	20.7	18.2	19.6	17.1	21.4	22.7	23.4	21.4	24.9
CO_2	.20	.36	.35	.37	.29	.29	.31	.29	.42	.47	.44
As ppm	132	237	277	281	211	205	229	220	313	344	346
Ba	2,308	2,367	3,026	2,689	2,488	4,825	2,545	6,598	2,219	2,036	1,997
Cd	1.4	9.6	6.4	7.1	15	13	9.9	12	7.6	2.7	3.2
Ce	912	757	971	941	323	651	814	724	836	1,170	1,132
Co	2,527	3,195	3,531	3,423	2,488	2,774	3,181	2,975	3,394	4,326	3,862
Cr	24	17	11	10	15	15	13	14	7.2	7.0	3.7
Cu	2,088	959	757	636	634	1,206	992	1,552	509	560	360
Mo	5	473	441	403	361	483	420	505	666	916	826
Ni	4,286	8,166	4,161	4,034	5,597	8,565	7,761	9,056	4,569	3,181	3,196
Pb	1,000	1,053	1,387	1,345	373	796	1,069	1,048	1,240	1,781	1,731
Sr	945	1,183	1,387	1,345	945	1,206	1,196	1,423	1,436	1,781	1,731
V	374	604	706	672	585	567	560	582	796	891	866
Y	86.8	142	151	147	102	121	127	142	196	254	253
Zn	703	1,006	883	905	1,144	1,098	980	1,035	875	763	679
Pd ppb	4.1	--	3.8	3.9	5.8	5.1	4.5	6.9	4.8	4.5	4.3
Pt	87	--	81	78	36	107	79	93	57	65	28
Rh	5.8	--	3.9	5.3	2.9	6.2	6.2	7.0	3.9	6.5	5.3

Table 12 continued

	Adam Seamount						Hoss Seamount				
	D9-21D	D9-23	D9-29	D9-31	D9-34A	D9-41	D10-3	D10-4A	D10-6	D10-7A	D10-7B
	L(29-54)	BN(0-55)	B(0-55)	B(0-4)	B(0-40)	B(0-40)	B(0-40)	B(0-20)	B(0-40)	B(0-25)	L(0-3)
Fe wt%	17.9	16.7	16.5	23.4	21.0	21.1	15.4	15.1	23.6	20.8	12.2
Mn	23.0	19.0	22.0	14.2	17.5	21.7	15.0	12.3	10.3	15.6	6.10
Fe/Mn	.8	.9	.7	1.7	1.2	1.0	1.0	1.2	2.3	1.3	2.0
Si	6.47	7.69	7.22	9.33	8.16	5.28	12.5	14.2	11.6	11.7	22.0
Na	1.82	1.66	1.72	1.73	1.77	1.65	1.62	1.76	1.68	1.93	2.55
Al	1.09	1.54	1.12	1.40	1.37	.65	2.08	2.80	1.87	1.42	4.32
K	.79	.77	.85	.58	.70	.49	1.21	1.25	.72	.62	1.24
Mg	1.27	1.40	1.47	.86	1.09	.95	1.98	1.65	1.03	.92	.67
Ca	1.75	1.40	1.72	1.85	1.76	2.34	1.00	1.90	1.18	1.77	1.69
Ti	.25	.43	.39	.50	.45	.56	.21	.44	.62	.55	.29
P	.32	.29	.31	.50	.41	.49	.18	.40	.34	.37	.23
H_2O^+	9.57	12.9	11.0	11.2	11.4	11.1	9.43	8.65	10.2	10.3	7.10
H_2O^-	22.7	18.1	16.9	18.5	13.0	24.3	8.80	13.3	19.8	24.2	9.80
CO_2	.26	.26	.36	.48	.41	.67	.19	.42	.25	.38	.40
As ppm	259	195	229	344	299	357	92	97	212	251	144
Ba	2,199	3,663	5,535	1,472	2,299	1,717	24,232	9,458	2,618	2,507	1,042
Cd	13	5.5	7.1	0.98	3.5	1.7	3.7	1.6	.62	1.6	.42
Ce	427	806	686	1,215	931	1,189	296	554	1,160	1,121	610
Co	2,717	3,053	2,768	2,454	2,989	3,699	2,412	2,537	3,242	3,430	998
Cr	10	20	19	22	21	11	26	57	55	32	36
Cu	712	916	1,119	196	483	291	1,425	1,269	661	620	177
Mo	453	269	493	319	402	740	82	54	6.2	356	60
Ni	6,986	6,227	7,581	1,043	3,103	2,510	5,044	3,576	2,120	1,715	510
Pb	556	1,087	975	1,718	1,379	1,849	461	692	1,496	1,583	665
Sr	1,009	1,123	1,324	1,350	1,379	1,717	1,864	1,153	1,172	1,451	754
V	634	476	590	736	690	819	329	358	574	620	322
Y	123	103	144	196	172	251	54	84	137	172	85
Zn	1,190	806	915	601	724	621	833	669	661	646	299
Pd ppb	4.9	--	--	--	--	--	--	--	--	--	--
Pt	40	--	--	--	--	--	--	--	--	--	--
Rh	4.5	--	--	--	--	--	--	--	--	--	--

Table 12 continued

	Hoss Seamount								Little Joe Seamount		
	D10-7C	D11-4A	D11-4B	D11-4C	D11-4D	D11-6	D11-7	D11-11A	D13-1A	D13-1B	D13-1C
	L(3-25)	L(0-8)	L(8-27)	L(27-33)	B(0-36)	B(0-50)	B(0-45)	B(0-70)	B(0-12)	MB	BU(0-4)
Fe wt%	22.2	15.2	20.9	25.5	21.5	18.5	17.7	20.3	15.7	30.8	19.2
Mn	17.7	8.53	20.1	16.8	18.1	16.2	14.4	18.7	4.71	3.61	13.8
Fe/Mn	1.3	1.8	1.0	1.5	1.2	1.2	1.2	1.1	3.3	8.5	1.4
Si	6.20	19.2	5.92	5.35	8.19	9.78	11.9	6.86	21.1	11.8	10.5
Na	1.64	2.48	1.68	1.48	1.70	1.83	1.97	1.74	2.25	1.64	1.81
Al	.92	3.62	.88	1.02	1.29	1.98	2.37	1.29	4.00	2.28	2.43
K	.51	1.14	.55	.46	.60	.76	.84	.61	1.11	.72	.97
Mg	1.04	.74	.96	1.00	.95	.98	.91	.95	.73	1.24	1.53
Ca	1.81	1.65	2.16	1.82	2.04	1.89	1.95	2.14	1.45	.89	1.31
Ti	.71	.43	.63	.65	.61	.54	.54	.66	.42	1.04	.66
P	.42	.27	.43	.41	.39	.35	.35	.41	.25	.40	.30
H_2O^+	11.5	8.64	12.6	12.8	11.2	9.39	10.7	10.6	6.36	8.33	10.2
H_2O^-	25.8	14.4	24.0	19.6	23.1	23.3	22.7	24.2	15.1	31.6	20.9
CO_2	.39	.27	.59	.41	.33	.35	.38	.41	.22	.15	.35
As ppm	296	199	329	311	312	235	233	317	177	278	215
Ba	3,369	1,121	2,237	2,488	2,211	6,780	2,458	1,715	1,166	1,608	2,276
Cd	1.6	.41	2.0	1.3	1.8	1.7	1.6	1.7	.29	.15	2.5
Ce	1,348	841	1,237	1,007	1,092	952	1,022	1,240	754	1,257	1,024
Co	4,717	1,636	3,553	2,363	2,861	2,216	2,458	3,562	860	731	3,793
Cr	10	28	11	16	10	21	22	9.2	42	57	53
Cu	849	234	553	808	533	1,434	776	369	259	599	1,049
Mo	445	152	697	634	585	456	427	554	19	7.3	139
Ni	2,291	759	2,895	2,861	2,471	3,259	2,070	2,507	671	1,754	5,310
Pb	1,887	911	1,711	1,617	1,430	1,147	1,242	1,451	1,154	1,754	1,163
Sr	1,752	900	1,711	1,617	1,560	1,565	1,294	1,451	695	541	885
V	701	386	789	858	741	626	582	686	365	570	480
Y	202	117	243	211	208	196	194	224	81	130	110
Zn	741	362	671	920	702	743	569	594	365	716	759
Pd ppb	--	--	--	--	2.9	--	--	3.3	--	--	--
Pt	--	--	--	--	43	--	--	46	--	--	--
Rh	--	--	--	--	7.0	--	--	7.3	--	--	--

Table 12 continued

	Little Joe Seamount										Ben
	D13-2A B(0-12)	D13-2C BU(0-10)	D13-3A B(0-27)	D14-1A B(0-40)	D14-1C BU(0-15)	D14-2C B(0-6)	D14-2D LU(0-5)	D14-2E LU(5-11)	D14-3B B(0-9)	D14-4 B(0-40)	D17-1 B(0-18)
Fe wt%	33.7	13.8	29.4	20.7	19.3	20.0	18.8	19.6	19.4	20.8	22.3
Mn	3.15	5.86	6.42	18.2	23.0	15.1	19.7	16.6	13.4	17.6	19.2
Fe/Mn	11	2.4	4.6	1.1	.8	1.3	1.0	1.2	1.5	1.2	1.2
Si	10.6	15.8	11.1	7.95	6.84	10.6	8.01	10.5	11.7	8.22	6.44
Na	1.54	1.70	1.85	1.78	1.75	1.91	1.83	1.88	1.93	1.75	1.65
Al	2.13	2.97	2.25	1.31	.94	1.80	1.47	1.73	2.03	1.29	.98
K	.54	1.61	.62	.58	.90	.67	.68	.68	.72	.60	.53
Mg	.94	2.05	1.11	.94	1.50	.90	1.06	.93	.83	.93	1.00
Ca	.75	.69	1.09	2.15	1.52	1.97	1.95	2.03	1.88	2.10	2.14
Ti	.81	.48	.76	.55	.22	.58	.53	.45	.46	.63	.68
P	.41	.14	.44	.47	.27	.44	.39	.44	.43	.44	.45
H_2O^+	12.0	7.50	8.37	8.56	6.96	9.00	7.40	7.65	7.58	11.9	9.01
H_2O^-	17.7	14.7	12.8	18.2	15.2	17.8	17.6	16.3	15.6	23.4	22.3
CO_2	.13	.12	.23	.51	.31	.49	.47	.55	.47	.41	.67
As ppm	267	64	321	306	212	268	255	287	273	313	296
Ba	1,203	65,651	1,261	1,589	3,774	1,338	1,699	1,553	1,303	1,567	1,673
Cd	.12	.33	1.8	1.4	13	1.6	5.0	2.1	1.6	2.0	2.1
Ce	960	340	1,101	1,198	354	1,168	1,056	1,027	1,066	1,266	1,416
Co	535	1,758	849	3,056	2,594	3,285	3,277	2,628	2,251	3,525	3,475
Cr	37	55	78	12	25	22	21	29	23	9.8	14
Cu	595	1,172	631	281	908	255	498	394	237	274	450
Mo	6.1	5.9	79	599	460	328	425	526	308	457	566
Ni	1,142	3,517	2,408	2,078	6,722	1,825	4,733	2,031	1,303	2,089	2,317
Pb	2,066	492	1,606	1,589	519	1,338	1,214	1,314	1,303	1,436	1,416
Sr	522	4,220	619	1,467	1,073	1,338	1,335	1,434	1,185	1,436	1,544
V	583	211	619	672	601	535	583	657	533	666	644
Y	111	91	89	232	111	170	170	179	166	209	245
Zn	705	657	700	575	1,038	511	752	573	509	561	592
Pd ppb	--	--	--	--	--	--	--	--	--	3.7	--
Pt	--	--	--	--	--	--	--	--	--	42	--
Rh	--	--	--	--	--	--	--	--	--	6.3	--

Table 12 continued

	Ben Seamount					Flint Seamount			
	D17-3A B(0-10)	D17-4 B(0-25)	D17-6A B(0-18)	D17-6B B(0-10)	D17-22 B(0-25)	D21-1A B(0-15)	D23-2B B(0-18)	D23-2C B(0-20)	D23-3 B(0-18)
Fe wt%	21.3	21.1	21.7	19.9	20.8	16.9	20.7	19.9	20.2
Mn	18.2	18.5	19.8	20.7	20.7	26.1	17.9	15.8	19.4
Fe/Mn	1.2	1.1	1.1	1.0	1.0	0.6	1.2	1.3	1.0
Si	7.53	7.15	5.88	5.82	5.65	2.70	7.99	10.6	7.19
Na	1.71	1.67	1.59	1.66	1.77	1.88	1.35	1.91	1.73
Al	1.38	1.22	.87	1.26	.93	.52	1.96	2.28	1.25
K	.59	.61	.51	.62	.55	.54	.79	.79	.57
Mg	.98	1.01	.96	1.09	1.05	1.13	1.19	1.05	1.05
Ca	2.13	2.04	2.18	2.29	2.19	2.40	2.06	2.14	2.04
Ti	.61	.78	.55	1.04	.78	.92	1.04	.76	.76
P	.46	.38	.46	.40	.42	.48	.35	.42	.40
H_2O^+	9.18	12.5	11.8	8.79	9.54	16.8	9.15	7.67	7.45
H_2O^-	21.6	24.5	25.2	19.2	25.6	14.9	22.4	19.2	22.1
CO_2	.56	.41	.44	.67	.82	.40	.52	.47	.51
As ppm	293	305	334	260	296	341	206	235	270
Ba	1,658	1,589	1,738	1,485	1,613	1,410	1,804	1,609	1,797
Cd	1.9	1.9	1.9	2.3	2.0	4.9	2.6	2.2	2.6
Ce	1,237	1,457	1,243	1,980	1,478	1,998	1,804	1,361	1,412
Co	3,061	3,841	2,807	6,312	4,704	10,458	5,541	3,342	4,236
Cr	11	11	5.8	11	12	13	17	17	8.3
Cu	599	517	548	433	484	329	619	545	719
Mo	510	411	602	359	551	635	271	334	462
Ni	2,296	2,517	2,406	3,094	3,226	4,465	2,835	2,351	3,209
Pb	1,403	1,325	1,471	1,609	1,478	2,115	1,418	1,238	1,540
Sr	1,531	1,457	1,604	1,361	1,613	1,645	1,263	1,225	1,412
V	651	623	789	532	618	670	425	483	578
Y	204	225	254	210	242	188	206	223	225
Zn	587	570	628	557	591	494	593	545	642
Pd ppb	--	4.4	2.0	--	--	2.9	--	--	--
Pt	--	46	37	--	--	141	--	--	--
Rh	--	6.8	5.9	--	--	7.8	--	--	--

Table 13. Rare-earth element concentrations (in ppm) of Fe-Mn crust and nodule samples from six seamounts, normalized to 0% H_2O^-.

[Rare earth element concentrations determined by inductively couple plasma mass spectrometry (ICPMS); -- means not analyzed. Ce anomaly calculated from chondrite-normalized values: Ce* =2Ce/(La+Pr). Thickness of crust intervals measured in millimeters; L, crust layer; B, bulk crust; BN, bulk nodule; ∑REE, sum of the rare-earth elements.]

	San Marcos Seamount				Adam Seamount			
	D5-1A B(0-25)	D5-1B L(0-15)	D5-1C L(15-21)	D6-10 B(0-30)	D7-8 B(0-24)	D8-2A BN(0-65)	D8-3A B(0-36)	D8-3B L(0-5)
La	393	366	465	168	340	379	352	344
Ce	1,199	1,136	1,250	686	1,228	1,046	1,083	1,385
Pr	105	99.9	127	36.5	92.0	91.7	86.1	88.1
Nd	409	397	513	150	361	366	338	351
Sm	96.1	94.7	119	33.8	87.0	82.1	76.0	80.6
Eu	23.2	22.7	28.7	8.42	20.8	19.5	17.9	18.7
Gd	85.4	86.1	111	33.9	79.5	79.6	67.6	73.3
Tb	13.8	14.2	18.1	5.49	13.1	13.1	10.6	11.6
Dy	80.3	82.2	105	34.2	74.9	74.8	57.9	64.6
Ho	13.7	14.4	18.6	6.65	13.2	13.8	9.65	10.9
Er	36.5	38.4	50.2	18.5	35.1	36.9	25.5	28.6
Tm	5.50	5.73	7.40	2.91	5.26	5.44	3.76	4.15
Yb	34.0	34.8	45.6	18.6	33.3	34.7	23.2	26.5
Lu	4.40	4.51	5.72	2.61	4.30	4.53	3.16	3.50
∑REE	2,499	2,398	2,863	1,206	2,388	2,247	2,155	2,490
Ce*	1.40	1.41	1.22	2.03	1.64	1.32	1.46	1.88

	Adam Seamount						
	D8-3C L(5-17)	D8-3D L(17-36)	D8-5 BN (0-25)	D9-16A B(0-55)	D9-16B L(0-10)	D9-16C L(10-55)	D9-21A B(0-50)
La	497	260	237	197	235	250	286
Ce	1,455	564	813	729	926	819	880
Pr	118	62.4	56.3	39.7	49.0	47.0	55.2
Nd	467	249	218	164	200	191	227
Sm	105	55.5	48.6	36.1	44.0	41.8	47.8
Eu	24.2	13.0	10.8	8.69	10.4	9.91	11.6
Gd	97.1	50.5	41.4	36.8	44.1	42.7	50.1
Tb	15.4	7.89	6.29	6.02	6.95	6.78	8.15
Dy	82.9	43.5	32.7	36.8	42.1	41.8	50.3
Ho	13.6	7.48	5.60	7.64	8.12	8.46	10.4
Er	34.4	19.2	14.4	21.6	21.6	24.5	29.4
Tm	5.05	2.85	2.04	3.32	3.27	3.69	4.48
Yb	31.4	18.5	13.5	21.7	21.1	23.9	27.9
Lu	4.22	2.49	1.85	3.03	3.00	3.34	3.92
∑REE	2,951	1,356	1,502	1,311	1,615	1,514	1,692
Ce*	1.41	1.04	1.65	1.89	1.99	1.71	1.59

Table 13 continued

	Hoss Seamount		Little Joe	Ben Seamount		Flint
	D11-4D	D11-11A	D14-4	D17-4	D17-6A	D21-1A
	B(0-36)	B(0-70)	B(0-40)	B(0-25)	B(0-18)	B(0-15)
La	378	409	389	437	472	259
Ce	1,143	1,240	1,358	1,536	1,337	1,622
Pr	79.2	--	84.2	102	109	47.2
Nd	321	369	341	404	440	186
Sm	68.5	--	73.6	89.7	97.7	38.7
Eu	16.1	20.0	17.8	21.6	23.4	9.14
Gd	68.7	--	72.3	85.2	93.7	39.5
Tb	11.1	--	11.7	13.6	15.1	6.43
Dy	66.7	--	68.1	77.9	87.3	40.2
Ho	13.0	16.0	13.3	14.6	17.0	8.54
Er	35.0	--	36.3	39.1	44.7	24.3
Tm	5.33	--	5.30	5.77	6.60	3.78
Yb	32.9	44.0	34.2	36.8	42.2	24.6
Lu	4.56	--	4.71	4.94	5.71	3.47
∑REE	2,244	2,098	2,509	2,868	2,791	2,312
Ce*	1.52	--	1.74	1.70	1.37	3.31

Table 14. Statistics for all crust and nodule data from Tables 12 and 13.

[Std. Dev., Standard deviation; wt%, weight percent ppb, parts per billion; ppm, parts per million]

	Count	Mean	Std. Dev.	Median	Minimum	Maximum
Fe wt%	86	19.5	3.90	19.6	8.42	33.7
Mn	86	16.0	5.57	16.8	3.15	26.1
Fe/Mn	86	1.6	1.4	1.2	.4	11
Si	86	10.0	4.28	9.60	2.70	25.0
Na	86	1.81	.22	1.77	1.35	2.66
Al	86	1.90	.92	1.80	.37	4.89
K	86	.78	.23	.74	.42	1.61
Mg	86	1.12	.27	1.05	.67	2.05
Ca	86	1.78	.37	1.81	.69	2.44
Ti	86	.55	.19	.54	.15	1.04
P	86	.37	.12	.36	.14	.89
H_2O^+	86	9.65	2.02	9.41	5.00	16.8
H_2O^-	86	18.8	5.09	19.2	8.00	31.6
CO_2	86	.39	.20	.36	.12	1.69
As ppm	86	252	81.7	250	64.5	582
Ba	86	3,199	7,356	1,728	741	65,651
Cd	86	3.2	3.4	1.9	.12	15
Ce	86	1,056	379	1,060	296	1,998
Co	86	2,797	1,474	2,673	535	10,458
Cr	86	26	27	17	3.7	180
Cu	86	769	589	619	45	3,825
Mo	86	339	207	330	5.5	916
Ni	86	3,148	2,024	2,513	449	9,056
Pb	86	1,225	475	1,225	373	2,847
Sr	86	1,269	447	1,259	522	4,220
V	86	575	153	580	211	1,024
Y	86	161	52.1	164	54	254
Zn	86	666	196	644	261	1,190
Pd ppb	32	4.4	1.6	4.1	1.9	9.3
Pt	32	72	28	72	28	141
Rh	32	5.9	1.4	6.2	2.9	8.1
La ppm	21	339	94.0	352	168	497
Ce	21	1,116	291	1,143	564	1,622
Pr	20	78.8	27.6	85.2	36.5	127
Nd	21	317	107	341	150	513
Sm	20	70.8	25.9	74.8	33.8	119
Eu	21	17.0	6.08	17.9	8.42	28.7
Gd	20	66.9	23.0	70.5	33.9	111
Tb	20	10.8	3.77	11.3	5.49	18.1
Dy	20	62.2	21.0	65.7	32.7	105
Ho	21	11.6	3.64	13.0	5.60	18.6
Er	20	30.7	9.42	31.9	14.4	50.2
Tm	20	4.58	1.38	4.76	2.04	7.40
Yb	21	29.7	8.79	31.4	13.5	45.6
Lu	20	3.90	1.04	4.07	1.85	5.72

Table 15. Statistics for 60 bulk crusts and nodules from Tables 12 and 13.

[Std. Dev., Standard deviation; wt%, weight percent ppb, parts per billion; ppm, parts per million]

	Count	Mean	Std. Dev.	Median	Minimum	Maximum
Fe wt.%	60	19.4	3.96	19.7	8.42	33.7
Mn	60	15.9	5.39	16.6	3.15	26.1
Fe/Mn	60	1.5	1.4	1.2	.4	11
Si	60	10.2	4.20	9.75	2.70	25.0
Na	60	1.82	.20	1.78	1.35	2.66
Al	60	1.94	.89	1.89	.52	4.89
K	60	.79	.25	.73	.42	1.61
Mg	60	1.12	.29	1.04	.73	2.05
Ca	60	1.79	.37	1.87	.69	2.40
Ti	60	.56	.19	.54	.21	1.04
P	60	.38	.13	.37	.14	.89
H_2O^+	60	9.38	2.01	9.19	5.00	16.8
H_2O^-	60	18.3	4.80	18.4	8.00	25.6
CO_2	60	.38	.15	.38	.12	.82
As ppm	60	254	91	250	65	582
Ba	60	3,549	8,768	1,666	741	65,651
Cd	60	3.0	3.0	1.9	.12	13
Ce	60	1,091	408	1,085	296	1,998
Co	60	2,891	1,623	2,771	535	10,458
Cr	60	30	30	21	5.8	180
Cu	60	702	570	574	45	3,825
Mo	60	331	188	329	5.9	740
Ni	60	3,017	1,949	2,489	449	8,565
Pb	60	1,254	500	1,268	391	2,847
Sr	60	1,281	491	1,283	522	4,220
V	60	571	156	580	211	1,024
Y	60	162	53	169	54	254
Zn	60	634	178	593	261	1,098
Pd ppb	15	4.1	1.3	4.1	2.0	7.2
Pt	15	69	30	72	37	141
Rh	15	6.0	1.4	6.3	3.0	7.8
La ppm	13	343	91.1	378	168	472
Ce	13	1,161	281	1,199	686	1,622
Pr	12	77.3	26.0	85.2	36.5	109
Nd	13	314	98.2	341	150	440
Sm	12	68.9	23.8	74.8	33.8	97.7
Eu	13	16.8	5.52	17.9	8.42	23.4
Gd	12	66.0	20.8	70.5	33.9	93.7
Tb	12	10.7	3.36	11.4	5.49	15.1
Dy	12	62.4	18.2	67.4	34.2	87.3
Ho	13	12.1	3.23	13.2	6.65	17.0
Er	12	31.9	7.92	35.0	18.5	44.7
Tm	12	4.79	1.12	5.28	2.91	6.60
Yb	13	31.4	7.75	33.3	18.6	44.0
Lu	12	4.11	.89	4.35	2.61	5.71

Table 16. Statistics for crust layer data from Tables 12 and 13.

[Std. Dev., Standard deviation; wt%, weight percent; ppb, parts per billion; ppm, parts per million]

	Count	Mean	Std. Dev.	Median	Minimum	Maximum
Fe wt%	22	19.6	3.28	19.6	12.2	25.5
Mn	22	17.1	5.69	17.2	6.10	25.2
Fe/Mn	22	1.3	.6	1.2	.6	2.7
Si	22	9.28	4.72	8.48	3.69	22.0
Na	22	1.80	.27	1.76	1.48	2.55
Al	22	1.80	1.03	1.60	.37	4.32
K	22	.72	.20	.73	.45	1.24
Mg	22	1.09	.21	1.03	.67	1.50
Ca	22	1.85	.29	1.80	1.23	2.44
Ti	22	.54	.13	.55	.25	.79
P	22	.35	.07	.33	.23	.48
H_2O^+	22	9.99	1.91	9.56	7.10	14.0
H_2O^-	22	19.9	5.08	21.5	8.00	25.8
CO_2	22	.43	.31	.37	.21	1.69
As ppm	22	255	54	256	144	346
Ba	22	2,344	1,320	2,096	1,042	6,598
Cd	22	3.4	3.5	2.1	.41	13
Ce	22	1,012	272	1,042	427	1,455
Co	22	2,655	1,072	2,673	998	4,717
Cr	22	16	9.6	13	3.7	44
Cu	22	901	607	788	177	2,689
Mo	22	397	244	422	57	916
Ni	22	3,283	2,197	2,878	510	9,056
Pb	22	1,184	403	1,098	556	1,887
Sr	22	1,309	303	1,295	754	1,781
V	22	602	151	583	322	891
Y	22	171	50.1	162	85	254
Zn	22	715	213	729	299	1,190
Pd ppb	15	4.8	2.1	4.3	1.9	9.3
Pt	15	77	27	79	28	124
Rh	15	6.1	1.2	6.2	3.1	8.1
La ppm	7	345	105	344	235	497
Ce	7	1,076	322	1,136	564	1,455
Pr	7	84.5	32.5	88.1	47.0	127
Nd	7	338	129	351	191	513
Sm	7	77.3	30.8	80.6	41.8	119
Eu	7	18.2	7.33	18.7	9.91	28.7
Gd	7	72.1	27.2	73.3	42.7	111
Tb	7	11.5	4.49	11.6	6.78	18.1
Dy	7	66.1	25.1	64.6	41.8	105
Ho	7	11.7	4.09	10.9	7.48	18.6
Er	7	31.0	10.9	28.6	19.2	50.2
Tm	7	4.59	1.59	4.15	2.85	7.40
Yb	7	28.8	9.29	26.5	18.5	45.6
Lu	7	3.83	1.08	3.50	2.49	5.72

Table 17. Statistics for nodule data from Adam Seamount from Table 12.

[Std. Dev., Standard deviation; wt%, weight percent; ppb, parts per billion; ppm, parts per million]

	Count	Mean	Std. Dev.	Median	Minimum	Maximum
Fe wt%	7	19.4	2.79	18.2	16.7	24.8
Mn	7	16.0	4.52	16.8	11.1	22.0
Fe/Mn	7	1.3	.5	1.2	.8	2.2
Si	7	10.2	3.10	9.60	6.85	14.5
Na	7	1.78	.16	1.73	1.63	2.04
Al	7	1.99	.79	1.96	1.07	2.91
K	7	.81	.12	.77	.66	.96
Mg	7	1.25	.21	1.34	.98	1.48
Ca	7	1.51	.18	1.53	1.21	1.72
Ti	7	.45	.15	.47	.15	.63
P	7	.30	.05	.31	.22	.38
H_2O^+	7	11.2	1.57	11.9	8.28	12.9
H_2O^-	7	17.0	5.08	18.2	9.00	21.9
CO_2	7	.26	.06	.26	.20	.37
As ppm	7	210	46	211	132	281
Ba	7	2,915	1,216	2,548	1,459	5,250
Cd	7	5.0	4.9	2.8	1.4	15
Ce	7	804	252	813	323	1,101
Co	7	2,399	787	2,527	1,172	3,423
Cr	7	16	4.8	17	10	24
Cu	7	1,405	794	1,089	634	2,689
Mo	7	243	128	242	5.0	403
Ni	7	3,847	1,765	4,034	1,529	6,227
Pb	7	913	302	948	373	1,345
Sr	7	1,142	181	1,123	945	1,408
V	7	527	99	512	374	672
Y	7	128	32	135	87	173
Zn	7	816	198	806	494	1,144
Pd ppb	6	4.7	2.2	4.1	1.9	8.3
Pt	6	76	31	80	36	124
Rh	6	5.0	1.7	5.4	2.9	7.3

Table 18. Statistics for Fe-Mn crust data from Rodriguez Seamount from Table 12.

[Std. Dev., Standard deviation; wt%, weight percent; ppb, parts per billion; ppm, parts per million]

	Count	Mean	Std. Dev.	Median	Minimum	Maximum
Fe wt%	5	22.4	3.14	22.4	19.0	26.5
Mn	5	10.9	4.07	11.5	6.40	15.2
Fe/Mn	5	2.6	.6	2.2	2.1	3.4
Si	5	12.7	5.50	12.43	6.19	18.3
Na	5	1.79	.18	1.72	1.62	2.02
Al	5	2.21	1.06	2.15	1.00	3.48
K	5	.73	.27	.70	.42	1.04
Mg	5	.91	.14	.89	.78	1.12
Ca	5	1.69	.24	1.67	1.40	1.97
Ti	5	.42	.09	.38	.34	.55
P	5	.66	.21	.66	.44	.89
H_2O^+	5	17.3	5.36	16.1	12.2	23.8
H_2O^-	5	7.84	1.11	8.25	6.62	9.16
CO_2	5	.35	.12	.38	.21	.49
As ppm	5	408	151	407	247	582
Ba	5	1,021	208	1,069	741	1,220
Cd	5	1.3	.63	1.2	.67	2.3
Ce	5	1,482	369	1,510	1,089	1,856
Co	5	2,962	1,690	2,439	1,571	5,569
Cr	5	100	58	96	42	180
Cu	5	51	8.2	48	45	65
Mo	5	282	166	302	91	458
Ni	5	665	201	720	449	890
Pb	5	2,086	684	2,091	1,347	2,847
Sr	5	1,190	401	1,161	763	1,609
V	5	781	229	790	527	1,024
Y	5	159	50	163	104	210
Zn	5	403	66	418	325	488

Table 19. Statistics for Fe-Mn crust data from San Marcos Seamount, from Tables 12 and 13.

[Std. Dev., Standard deviation; wt%, weight percent; ppb, parts per billion; ppm, parts per million]

	Count	Mean	Std. Dev.	Median	Minimum	Maximum
Fe wt%	13	17.0	2.63	17.4	10.3	20.1
Mn	13	15.4	4.85	16.0	4.35	21.9
Fe/Mn	13	1.5	.4	1.5	.8	2.6
Si	13	12.0	5.09	10.4	5.91	25.0
Na	13	1.97	.28	1.86	1.54	2.66
Al	13	2.38	.96	2.42	1.29	4.89
K	13	.90	.23	.85	.65	1.48
Mg	13	1.09	.32	1.01	.75	1.79
Ca	13	1.85	.24	1.83	1.37	2.18
Ti	13	.55	.20	.51	.26	.97
P	13	.31	.07	.33	.15	.39
H_2O^+	13	21.9	7.85	20.3	8.70	34.4
H_2O^-	13	8.54	1.96	9.03	5.00	10.9
CO_2	13	.38	.17	.34	.12	.75
As ppm	13	213	60	242	98	279
Ba	13	1,790	1,191	1,302	1,174	5,599
Cd	13	3.0	2.9	2.1	.38	9.6
Ce	13	992	416	924	347	1747
Co	13	2,461	1,459	1,968	761	5,511
Cr	13	25	16	19	11	61
Cu	13	639	308	552	228	1,317
Mo	13	271	122	296	17	429
Ni	13	3,014	1,978	2,390	848	7,292
Pb	13	963	346	899	391	1,585
Sr	13	1,115	241	1,160	565	1,387
V	13	489	110	517	217	613
Y	13	147	45	157	57	212
Zn	13	585	188	558	261	1,007
Pd ppb	3	5.3	1.6	4.6	4.1	7.2
Pt	3	80	8.2	81	72	88
Rh	3	6.2	.62	5.8	5.8	6.9
La ppm	2	281	159	281	168	393
Ce	2	943	363	943	686	1,199
Pr	2	70.8	48.5	71	36.5	105
Nd	2	280	183	280	150	409
Sm	2	65.0	44.1	65.0	33.8	96.0
Eu	2	15.8	10.48	15.8	8.42	23.2
Gd	2	59.7	36.4	59.7	33.9	85.0
Tb	2	9.6	5.89	9.6	5.49	13.8
Dy	2	57.2	32.7	57.2	34.2	80.0
Ho	2	10.2	4.97	10.2	6.65	13.7
Er	2	27.5	12.8	27.5	18.5	36.5
Tm	2	4.20	1.83	4.20	2.91	5.50
Yb	2	26.3	10.9	26.3	18.6	34.0
Lu	2	3.50	1.26	3.50	2.61	4.40

Table 20. Statistics for Fe-Mn crust data from Adam Seamount, from Tables 12 and 13.

[Std. Dev., Standard deviation; wt%, weight percent; ppb, parts per billion; ppm, parts per million]

	Count	Mean	Std. Dev.	Median	Minimum	Maximum
Fe wt%	14	18.5	4.18	19.7	8.42	23.4
Mn	14	18.3	5.16	18.6	10.5	25.6
Fe/Mn	14	1.1	.5	1.1	.4	2.2
Si	14	9.01	3.28	8.74	4.96	14.80
Na	14	1.80	0.15	1.75	1.60	2.13
Al	14	1.82	0.95	1.38	0.60	3.48
K	14	.81	.22	.78	.49	1.26
Mg	14	1.20	.22	1.16	.86	1.58
Ca	14	1.74	.27	1.72	1.30	2.34
Ti	14	.48	.12	.46	.28	.71
P	14	.34	.09	.32	.16	.50
H_2O^+	14	10.2	1.58	11.0	7.07	11.7
H_2O^-	14	17.9	4.95	17.8	8.50	24.3
CO_2	14	.35	.13	.35	.15	.67
As ppm	14	243	71	240	96	357
Ba	14	2,494	1,260	2,259	1,235	5,535
Cd	14	4.9	4.0	2.9	.98	13
Ce	14	919	241	951	372	1,228
Co	14	2,421	947	2,611	536	3,699
Cr	14	18	6.3	18	7.2	30
Cu	14	1,102	894	936	196	3,825
Mo	14	374	193	361	62	740
Ni	14	4,213	2,532	3,179	1,043	8,565
Pb	14	1,083	400	980	415	1,849
Sr	14	1,198	279	1,211	612	1,717
V	14	581	153	578	350	819
Y	14	153	44	148	72	251
Zn	14	766	196	733	526	1,098
Pd ppb	6	4.5	1.1	4.5	2.9	6.1
Pt	6	74	24	76	38	107
Rh	6	5.1	1.7	5.0	3.0	7.0
La ppm	5	311	72.3	340	197	379
Ce	5	993	193	1,046	729	1,228
Pr	5	73.0	24.0	86.1	39.7	92.0
Nd	5	291	90.9	338	164	366
Sm	5	65.8	22.5	76.0	36.1	87.0
Eu	5	15.7	5.27	17.9	8.69	20.8
Gd	5	62.7	18.9	67.6	36.8	79.6
Tb	5	10.2	3.10	10.6	6.02	13.1
Dy	5	58.9	16.4	57.9	36.8	74.9
Ho	5	10.9	2.57	10.4	7.64	13.8
Er	5	29.7	6.40	29.4	21.6	36.9
Tm	5	4.45	.92	4.48	3.32	5.44
Yb	5	28.2	5.83	27.9	21.7	34.7
Lu	5	3.79	.67	3.92	3.03	4.53

Table 21. Statistics for Fe-Mn crust data from Hoss Seamount, from Tables 12 and 13.

[Std. Dev., Standard deviation; wt%, weight percent; ppb, parts per billion; ppm, parts per million; --, no data]

	Count	Mean	Std. Dev.	Median	Minimum	Maximum
Fe wt%	8	19.1	2.98	19.4	15.1	23.6
Mn	8	15.1	2.78	15.3	10.3	18.7
Fe/Mn	8	1.3	.4	1.2	1.0	2.3
Si	8	10.8	2.40	11.7	6.86	14.2
Na	8	1.78	.12	1.75	1.62	1.97
Al	8	1.89	.54	1.93	1.29	2.80
K	8	.83	.26	.74	.60	1.25
Mg	8	1.17	.41	.96	.91	1.98
Ca	8	1.73	.42	1.90	1.00	2.14
Ti	8	.52	.14	.55	.21	.66
P	8	.35	.08	.36	.18	.41
H_2O^+	8	10.1	.84	10.3	8.65	11.2
H_2O^-	8	19.9	5.77	22.9	8.80	24.2
CO_2	8	.34	.08	.36	.19	.42
As ppm	8	218	85	234	92	317
Ba	8	6,497	7,671	2,563	1,715	24,232
Cd	8	1.8	.87	1.6	.62	3.7
Ce	8	936	334	1,072	296	1,240
Co	8	2,840	513	2,699	2,216	3,562
Cr	8	29	18	24	9.2	57
Cu	8	886	425	719	369	1,434
Mo	8	315	234	392	6.2	585
Ni	8	2,845	1,082	2,489	1,715	5,044
Pb	8	1,188	407	1,336	461	1,583
Sr	8	1,439	235	1451	1,153	1,864
V	8	564	147	601	329	741
Y	8	159	62	183	54	224
Zn	8	677	84	665	569	833
Pd ppb	2	3.1	.31	3.1	2.9	3.3
Pt	2	45	2.3	45	43	46
Rh	2	7.1	.17	7.1	7.0	7.3
La ppm	2	394	21.6	394	378	409
Ce	2	1,192	68.6	1,192	1,143	1,240
Pr	1	79.2	--	79.2	79.2	79.2
Nd	2	345	33.8	345	321	369
Sm	1	68.5	--	68.5	68.5	68.5
Eu	2	18.1	2.74	18.1	16.1	20.0
Gd	1	68.7	--	68.7	68.7	68.7
Tb	1	11.1	--	11.1	11.1	11.1
Dy	1	66.7	--	66.7	66.7	66.7
Ho	2	14.5	2.13	14.5	13.0	16.0
Er	1	35.0	--	35.0	35.0	35.0
Tm	1	5.33	--	5.33	5.33	5.33
Yb	2	38.4	7.85	38.4	32.9	44.0
Lu	1	4.56	--	4.56	4.56	4.56

Table 22. Statistics for Fe-Mn crust data from Little Joe Seamount, from Table 12.

[Std. Dev., Standard deviation; wt%, weight percent; ppb, parts per billion; ppm, parts per million]

	N	Mean	Std. Dev.	Median	Minimum	Maximum
Fe wt%	10	21.1	5.97	19.4	13.8	33.7
Mn	10	12.3	6.84	13.6	3.15	23.0
Fe/Mn	10	2.8	3.0	1.4	.8	11
Si	10	11.4	4.22	10.5	6.84	21.1
Na	10	1.82	.18	1.80	1.54	2.25
Al	10	2.10	.90	2.08	.94	4.00
K	10	.83	.33	.70	.54	1.61
Mg	10	1.15	.41	.95	.73	2.05
Ca	10	1.49	.54	1.48	.69	2.15
Ti	10	.55	.17	.54	.22	.81
P	10	.36	.11	.42	.14	.47
H_2O^+	10	8.75	1.98	8.21	6.36	12.0
H_2O^-	10	17.1	3.16	16.4	12.8	23.4
CO_2	10	.33	.15	.33	.12	.51
As ppm	10	242	78	268	65	321
Ba	10	8,131	20,225	1,546	1,166	65,651
Cd	10	2.6	3.8	1.7	.10	13
Ce	10	924	341	1,045	340	1,358
Co	10	2,229	1,180	2,423	535	3,793
Cr	10	36	22	31	9.8	78
Cu	10	579	354	487	237	1,172
Mo	10	250	225	224	5.9	599
Ni	10	2,807	1,912	2,249	671	6,722
Pb	10	1,262	480	1,297	492	2,066
Sr	10	1,347	1,066	1,129	522	4,220
V	10	532	145	587	211	672
Y	10	137	54	111	81	232
Zn	10	648	178	633	365	1,038

Table 23. Statistics for 6 Fe-Mn bulk crusts, Ben Seamount, from Tables 12 and 13.

[Std. Dev., Standard deviation; wt%, weight percent; ppb, parts per billion; ppm, parts per million]

	Count	Mean	Std. Dev.	Median	Minimum	Maximum
Fe wt%	6	21.2	.79	21.2	19.9	22.3
Mn	6	19.5	1.05	19.5	18.2	20.7
Fe/Mn	6	1.1	.1	1.1	1.0	1.2
Si	6	6.41	.78	6.16	5.65	7.53
Na	6	1.67	.06	1.66	1.59	1.77
Al	6	1.11	.21	1.10	.87	1.38
K	6	.57	.05	.57	.51	.62
Mg	6	1.02	.05	1.01	.96	1.09
Ca	6	2.16	.08	2.16	2.04	2.29
Ti	6	.74	.17	.73	.55	1.04
P	6	.43	.03	.43	.38	.46
H_2O^+	6	10.1	1.57	9.36	8.79	12.5
H_2O^-	6	23.1	2.48	23.4	19.2	25.6
CO_2	6	.60	.16	.62	.41	.82
As ppm	6	297	24	296	260	334
Ba	6	1,626	86	1,636	1,485	1,738
Cd	6	2.0	.17	2.0	1.9	2.3
Ce	6	1,497	259	1,447	1,237	1,980
Co	6	4,033	1,299	3,658	2,807	6,312
Cr	6	11	2.8	11	5.8	14
Cu	6	505	63	500	433	599
Mo	6	500	95	531	359	602
Ni	6	2,643	410	2,461	2,296	3,226
Pb	6	1,450	96	1,443	1,325	1,609
Sr	6	1,518	96	1,538	1,361	1,613
V	6	643	83	633	532	789
Y	6	230	20	234	204	254
Zn	6	587	24	589	557	628
Pd ppb	2	3.2	1.7	3.2	2.0	4.4
Pt	2	42	6.3	42	37	46
Rh	2	6.3	.62	6.3	5.9	6.8
La ppm	2	455	24.6	455	437	472
Ce	2	1,437	141	1,437	1,337	1,536
Pr	2	106	5.31	106	102	109
Nd	2	422	25.4	422	404	440
Sm	2	93.7	5.70	93.7	89.7	97.7
Eu	2	22.5	1.28	22.5	21.6	23.4
Gd	2	89.4	6.05	89.4	85.2	93.7
Tb	2	14.4	1.04	14.4	13.6	15.1
Dy	2	82.6	6.66	82.6	77.9	87.3
Ho	2	15.8	1.70	15.8	14.6	17.0
Er	2	41.9	3.95	41.9	39.1	44.7
Tm	2	6.19	.59	6.19	5.77	6.60
Yb	2	39.5	3.84	39.5	36.8	42.2
Lu	2	5.32	.54	5.32	4.94	5.71

Table 24. Statistics for Fe-Mn crust data from Flint Seamount, from Table 12.

[Std. Dev., Standard deviation; wt%, weight percent; ppb, parts per billion; ppm, parts per million]

	Count	Mean	Std. Dev.	Median	Minimum	Maximum
Fe wt%	4	19.4	1.71	20.0	16.9	20.7
Mn	4	19.8	4.43	18.6	15.8	26.1
Fe/Mn	4	1.0	.3	1.1	.6	1.3
Si	4	7.13	3.30	7.59	2.70	10.6
Na	4	1.72	.26	1.81	1.35	1.91
Al	4	1.50	.78	1.60	.52	2.28
K	4	.67	.14	.68	.54	.79
Mg	4	1.10	.07	1.09	1.05	1.19
Ca	4	2.16	.16	2.10	2.00	2.40
Ti	4	.87	.14	.84	.76	1.04
P	4	.41	.06	.41	.35	.48
H_2O^+	4	10.3	4.42	8.41	7.45	16.8
H_2O^-	4	19.7	3.48	20.7	14.9	22.4
CO_2	4	.48	.05	.49	.40	.52
As ppm	4	263	58	252	206	341
Ba	4	1,655	187	1,703	1,410	1,804
Cd	4	3.1	1.3	2.6	2.2	4.9
Ce	4	1,644	308	1,608	1,361	1,998
Co	4	5,894	3,174	4,889	3,342	10,458
Cr	4	14	4.2	15	8.3	17
Cu	4	553	165	582	329	719
Mo	4	425	161	398	271	635
Ni	4	3,215	904	3,022	2,351	4,465
Pb	4	1,578	379	1,479	1,238	2,115
Sr	4	1,386	190	1,337	1,225	1,645
V	4	539	108	530	425	670
Y	4	210	17	214	188	225
Zn	4	568	64	569	494	642

Table 25. Correlation matrix for bulk crusts; data from Tables 12 and 13.

[n=60, zero correlation at 99 and 95 percent confidence levels for major, minor elements, volatiles, and Ce1 are |0.329| and |0.254|; n=13 (|0.672|, |0.553|) for La, Ce2, Nd, Eu, Ho, Yb; n=12 (|0.696|, |0.575|) for Pr, Sm, Gd, Tb, Dy, Er, Tm, Lu, and n=15 (|0.631|, |0.512|) for PGEs]

	Thick	Depth	Latitude	Longitude	Fe	Mn	Fe/Mn	Si	Na	Al
Depth	0.158									
Latitude	-.246	-.239								
Long	.095	.092	-.180							
Fe	-.036	-.244	-.022	-.220						
Mn	.298	.075	-.278	.276	-.176					
Fe/Mn	-.173	-.130	.059	-.333	.559	-.671				
Si	-.259	.029	.310	-.121	-.345	-.836	.317			
Na	-.139	.129	.231	.000	-.528	-.397	-.009	.714		
Al	-.252	.181	.260	-.050	-.426	-.761	.283	.946	.711	
K	-.118	.190	.102	-.028	-.715	-.442	-.013	.744	.535	.800
Mg	.122	.112	-.193	.000	-.401	.206	-.193	-.096	-.228	.009
Ca	.115	.000	-.113	.338	-.003	.677	-.580	-.587	-.175	-.569
Ti	.003	.251	-.326	.236	.392	.166	.120	-.428	-.345	-.320
P	-.204	-.616	.260	-.032	.631	.082	.079	-.383	-.385	-.476
H2O+	.340	-.072	-.335	.146	.245	.498	-.065	-.636	-.465	-.619
H2O-	.313	.247	-.174	.071	.400	.348	-.151	-.549	-.442	-.564
CO_2	-.069	-.010	-.151	.103	.201	.529	-.381	-.592	-.364	-.605
As	-.090	-.528	.214	-.068	.670	.211	.033	-.515	-.393	-.600
Ba	.011	.017	-.103	-.162	-.261	-.198	.021	.172	-.137	.139
Cd	.203	-.085	-.146	.068	-.338	.646	-.356	-.403	-.160	-.325
Ce1	-.137	-.166	.002	.223	.492	.234	-.059	-.483	-.359	-.471
Co	-.002	-.243	-.287	.372	.121	.590	-.359	-.664	-.402	-.653
Cr	-.285	-.522	.451	-.174	.044	-.570	.348	.532	.192	.462
Cu	.225	.497	-.203	.067	-.465	.171	-.170	.030	.044	.223
Mo	.296	-.183	-.216	.129	.110	.807	-.491	-.778	-.376	-.804
Ni	.300	.106	-.275	.091	-.426	.639	-.384	-.418	-.200	-.299
Pb	-.167	-.563	.084	-.005	.726	.045	.252	-.413	-.417	-.503
Sr	.082	-.079	-.161	-.039	-.048	.172	-.250	-.268	-.388	-.344
V	.066	-.519	.149	-.069	.630	.365	-.050	-.629	-.495	-.733
Y	.154	-.010	-.179	.179	.405	.497	-.294	-.663	-.438	-.696
Zn	.375	.113	-.324	-.043	-.117	.527	-.186	-.458	-.386	-.385
Pd	.059	-.023	.439	-.019	-.050	-.134	.206	.281	-.001	.300
Pt	-.252	-.443	-.236	.731	-.653	.618	-.567	-.400	.466	-.176
Rh	.102	-.019	-.166	.262	-.228	.269	-.393	-.226	.351	-.182
La	-.060	.521	.023	-.454	.874	-.461	.498	.052	-.510	-.114
Ce2	-.461	-.005	-.509	.109	.455	.008	.104	-.385	.007	-.407
Pr	-.234	.761	.228	-.482	.838	-.585	.577	.264	-.353	.135
Nd	-.085	.723	.212	-.487	.841	-.573	.556	.233	-.388	.098
Sm	-.233	.805	.277	-.489	.804	-.590	.561	.299	-.319	.180
Eu	-.098	.776	.285	-.480	.788	-.575	.531	.270	-.321	.156
Gd	-.198	.755	.220	-.521	.824	-.555	.530	.246	-.403	.105
Tb	-.184	.758	.221	-.516	.815	-.544	.513	.242	-.396	.103
Dy	-.196	.723	.220	-.503	.797	-.489	.453	.186	-.423	.041
Ho	.057	.500	.069	-.450	.736	-.326	.294	-.021	-.521	-.173
Er	-.169	.523	.058	-.506	.752	-.298	.287	-.031	-.568	-.203
Tm	-.189	.508	.061	-.471	.733	-.263	.249	-.062	-.566	-.231
Yb	.132	.378	.003	-.379	.647	-.209	.177	-.130	-.505	-.268
Lu	-.195	.377	-.053	-.479	.692	-.172	.176	-.161	-.619	-.342

Table 25 continued

	K	Mg	Ca	Ti	P	H_2O^+	H_2O^-	CO_2	As	Ba	Cd
Mg	0.517										
Ca	-.582	-.350									
Ti	-.477	-.183	.378								
P	-.693	-.466	.396	.151							
$H2O^+$	-.491	.044	.312	.326	.175						
$H2O^-$	-.647	-.334	.500	.554	.253	.323					
CO_2	-.549	-.172	.763	.365	.404	.178	.475				
As	-.816	-.534	.463	.207	.933	.306	.386	.441			
Ba	.512	.602	-.455	-.166	-.320	-.092	-.190	-.283	-.391		
Cd	.069	.548	.050	-.319	-.235	.193	-.211	.031	-.162	-.033	
Ce1	-.725	-.517	.589	.739	.676	.310	.541	.492	.703	-.375	-.365
Co	-.514	-.016	.588	.587	.398	.497	.393	.486	.420	-.107	.094
Cr	.343	.071	-.448	-.254	.137	-.365	-.516	-.319	-.032	.087	-.150
Cu	.442	.596	-.334	-.227	-.564	.005	-.229	-.350	-.581	.228	.426
Mo	-.664	-.189	.781	.115	.404	.477	.479	.625	.557	-.264	.332
Ni	.180	.746	-.006	-.160	-.409	.254	-.138	.041	-.348	.159	.887
Pb	-.779	-.529	.319	.383	.901	.323	.352	.327	.891	-.309	-.328
Sr	-.006	.298	.068	.078	.071	.178	.249	.139	.070	.795	-.106
V	-.839	-.423	.471	.080	.856	.408	.431	.442	.937	-.375	.030
Y	-.800	-.497	.796	.502	.555	.372	.751	.695	.662	-.290	-.221
Zn	.020	.665	-.148	-.230	-.320	.297	-.021	-.026	-.249	.152	.827
Pd	.328	.311	-.492	-.191	-.346	-.551	.033	-.166	-.439	.184	.237
Pt	.109	.371	.177	.101	-.046	.528	-.722	-.011	-.149	.253	.546
Rh	-.298	-.336	.637	.413	.214	.571	-.151	.304	.330	-.218	-.210
La	-.623	-.836	.150	.279	.501	-.109	.818	.356	.597	-.760	-.845
Ce2	-.713	-.706	.540	.798	.740	.590	.329	.443	.736	-.826	-.656
Pr	-.397	-.712	-.019	.261	.252	-.231	.699	.355	.367	-.695	-.843
Nd	-.432	-.730	.020	.244	.289	-.250	.725	.358	.404	-.694	-.842
Sm	-.343	-.675	-.038	.231	.192	-.264	.654	.362	.313	-.663	-.819
Eu	-.361	-.680	.007	.233	.213	-.283	.663	.390	.336	-.663	-.816
Gd	-.421	-.726	.013	.199	.262	-.214	.691	.348	.386	-.671	-.818
Tb	-.425	-.732	.024	.187	.261	-.199	.675	.349	.389	-.668	-.811
Dy	-.478	-.761	.093	.172	.307	-.162	.682	.394	.441	-.675	-.798
Ho	-.639	-.828	.280	.143	.484	-.069	.721	.414	.609	-.671	-.742
Er	-.667	-.845	.273	.113	.503	.017	.714	.424	.625	-.683	-.717
Tm	-.686	-.851	.311	.114	.516	.038	.702	.451	.645	-.684	-.705
Yb	-.687	-.828	.375	.141	.543	.010	.682	.434	.662	-.649	-.675
Lu	-.755	-.857	.382	.104	.607	.130	.698	.434	.712	-.666	-.654

Table 25 continued

	Ce1	Co	Cr	Cu	Mo	Ni	Pb	Sr	V	Y	Zn	Pd	Pt
Co	0.705												
Cr	-.137	-.293											
Cu	-.517	-.298	-.154										
Mo	.361	.506	-.497	-.193									
Ni	-.392	.155	-.230	.554	.233								
Pb	.771	.506	.061	-.589	.361	-.446							
Sr	.084	.305	-.216	-.066	.257	.042	.086						
V	.549	.388	-.100	-.462	.685	-.161	.804	.101					
Y	.729	.531	-.485	-.423	.764	-.252	.579	.306	.662				
Zn	-.464	-.031	-.268	.595	.228	.869	-.340	.046	.008	-.204			
Pd	-.382	-.175	.188	.238	-.425	.214	-.245	-.504	-.385	-.441	.303		
Pt	.156	.564	.134	.128	.132	.580	.163	.021	-.217	-.384	.162	.071	
Rh	.506	.286	-.181	-.208	.325	-.132	.260	.440	.047	.433	-.449	-.467	.297
La	.431	-.200	-.623	-.294	.028	-.872	.310	.363	.421	.793	-.617	-.334	-.674
Ce2	.965	.555	-.527	-.580	.225	-.618	.781	.599	.358	.688	-.861	-.477	-.027
Pr	.326	-.380	-.481	-.088	-.226	-.860	.053	.110	.152	.640	-.615	-.211	-.602
Nd	.315	-.377	-.506	-.134	-.164	-.862	.087	.152	.205	.668	-.607	-.250	-.638
Sm	.281	-.430	-.449	-.049	-.258	-.835	-.014	.059	.100	.605	-.596	-.207	-.579
Eu	.276	-.424	-.457	-.100	-.210	-.832	.010	.083	.126	.624	-.604	-.228	-.594
Gd	.292	-.408	-.506	-.079	-.178	-.847	.040	.146	.197	.670	-.577	-.272	-.609
Tb	.288	-.412	-.514	-.068	-.169	-.843	.035	.151	.199	.672	-.572	-.293	-.588
Dy	.299	-.390	-.547	-.114	-.093	-.836	.071	.219	.261	.722	-.569	-.342	-.577
Ho	.338	-.254	-.646	-.287	.161	-.782	.255	.424	.472	.840	-.536	-.493	-.593
Er	.363	-.251	-.676	-.248	.152	-.778	.241	.447	.493	.856	-.516	-.482	-.554
Tm	.369	-.235	-.685	-.268	.192	-.766	.258	.479	.518	.873	-.514	-.509	-.531
Yb	.362	-.160	-.668	-.354	.270	-.713	.327	.500	.530	.863	-.514	-.542	-.525
Lu	.411	-.143	-.713	-.340	.291	-.716	.352	.576	.607	.907	-.487	-.566	-.521

	Rh	La	Ce2	Pr	Nd	Sm	Eu	Gd	Tb	Dy	Ho	Er	Tm	Yb
La	.140													
Ce2	.457	.626												
Pr	.093	.950	.525											
Nd	.124	.960	.522	.999										
Sm	.100	.921	.481	.996	.993									
Eu	.139	.920	.481	.994	.992	.999								
Gd	.125	.952	.498	.993	.996	.992	.991							
Tb	.149	.944	.492	.989	.992	.989	.988	.999						
Dy	.192	.946	.500	.978	.983	.977	.977	.994	.996					
Ho	.308	.943	.533	.918	.917	.906	.896	.950	.955	.972				
Er	.260	.941	.553	.896	.911	.882	.883	.931	.937	.958	.998			
Tm	.289	.929	.553	.882	.897	.869	.870	.919	.926	.951	.995	.998		
Yb	.386	.888	.539	.865	.840	.851	.818	.905	.913	.938	.983	.996	.997	
Lu	.299	.909	.585	.819	.839	.797	.798	.862	.868	.898	.975	.985	.986	.992

Table 26. Correlation matrix for crust layers; original data in Tables 12 and 13.

[n=22, zero correlation at 99 and 95 percent confidence levels for major, minor elements, volatiles, and Ce1 are |0.531| and |0.422|; n=7 (|0.859|, |0.753|) for REEs; and n=15 (|0.631|, |0.512|) for PGEs]

	Thick	**Depth**	**Latitude**	**Longitude**	**Fe**	**Mn**	**Fe/Mn**	**Si**	**Na**	**Al**
Depth	-0.004									
Latitude	-.122	.341								
Long	.157	.216	.336							
Fe	.078	.295	-.020	.004						
Mn	.285	-.583	.190	-.064	-.015					
Fe/Mn	-.134	.597	-.231	.094	.300	-.912				
Si	-.325	.353	-.158	.026	-.442	-.883	.662			
Na	-.322	.039	-.121	-.003	-.716	-.623	.342	.899		
Al	-.233	.456	-.100	.065	-.363	-.903	.744	.971	.823	
K	-.093	.187	-.120	.064	-.688	-.660	.435	.905	.923	.898
Mg	.532	-.017	-.035	-.013	.159	.402	-.191	-.468	-.535	-.315
Ca	-.110	-.418	.307	-.064	-.001	.573	-.494	-.502	-.295	-.552
Ti	-.099	.307	.132	.128	.713	.064	.092	-.401	-.634	-.366
P	-.113	-.424	.010	-.232	.414	.615	-.516	-.712	-.606	-.810
H2O+	.210	-.085	-.004	.399	.398	.370	-.210	-.546	-.575	-.532
H2O-	.316	-.086	.280	.189	.338	.656	-.567	-.740	-.658	-.766
CO_2	-.151	.161	.707	.052	-.010	.137	-.225	-.107	-.042	-.126
As	-.042	-.351	.174	-.037	.441	.631	-.498	-.748	-.617	-.821
Ba	.765	-.048	-.212	.069	.063	.360	-.251	-.395	-.456	-.313
Cd	.456	-.536	-.030	-.083	-.381	.673	-.645	-.433	-.158	-.402
Ce1	-.252	.173	.215	.013	.362	.221	-.244	-.362	-.442	-.434
Co	.102	-.605	-.159	-.061	.164	.737	-.655	-.726	-.562	-.813
Cr	-.232	.190	-.287	-.269	-.197	-.741	.717	.740	.612	.786
Cu	.504	.478	-.089	.081	.305	-.052	.156	-.120	-.387	.017
Mo	.076	-.547	.118	-.059	.163	.802	-.694	-.782	-.563	-.850
Ni	.443	-.513	-.032	-.088	-.280	.739	-.681	-.555	-.321	-.505
Pb	-.114	-.423	-.102	.022	.389	.475	-.393	-.596	-.542	-.693
Sr	.152	-.303	.037	-.040	.434	.682	-.563	-.812	-.752	-.868
V	.116	-.407	.016	-.020	.501	.688	-.494	-.838	-.744	-.877
Y	-.033	-.119	.333	.052	.453	.584	-.475	-.722	-.676	-.770
Zn	.518	-.328	-.174	-.035	.267	.606	-.389	-.679	-.618	-.589
Pd	.341	-.259	.160	.288	-.115	.492	-.428	-.511	-.523	-.429
Pt	.103	.237	-.156	-.039	.225	-.300	.317	.225	-.251	.346
Rh	.005	.115	.137	.084	.183	.079	.004	-.244	-.587	-.141
La	-.483	.689	.446	.415	.585	-.189	.066	-.044	-.574	-.173
Ce2	-.559	.439	.240	.219	.311	-.089	-.115	.021	-.195	-.266
Pr	-.583	.803	.598	.564	.582	-.246	.104	.048	-.413	-.079
Nd	-.583	.796	.609	.575	.566	-.228	.088	.030	-.413	-.095
Sm	-.585	.807	.648	.616	.546	-.222	.075	.036	-.378	-.091
Eu	-.578	.801	.685	.654	.515	-.193	.047	.011	-.368	-.110
Gd	-.566	.767	.654	.624	.505	-.162	.019	-.029	-.411	-.154
Tb	-.556	.763	.686	.658	.479	-.139	-.006	-.046	-.400	-.169
Dy	-.529	.723	.748	.724	.389	-.053	-.092	-.118	-.380	-.236
Ho	-.464	.640	.805	.788	.258	.081	-.217	-.239	-.382	-.344
Er	-.396	.584	.832	.820	.169	.160	-.289	-.307	-.379	-.404
Tm	-.380	.566	.845	.834	.146	.185	-.313	-.330	-.380	-.423
Yb	-.374	.552	.832	.822	.134	.197	-.321	-.343	-.388	-.436
Lu	-.346	.502	.812	.805	.099	.249	-.375	-.395	-.419	-.496

Table 26 continued

	K	Mg	Ca	Ti	P	H_2O^+	H_2O^-	CO_2	As	Ba	Cd	Ce1
Mg	-0.248											
Ca	-.493	-.197										
Ti	-.659	.174	.062									
P	-.834	-.156	.723	.416								
H2O+	-.597	.214	.402	.456	.452							
H2O-	-.678	.228	.163	.418	.502	.313						
CO_2	-.125	-.276	.395	.016	.233	-.056	.204					
As	-.823	-.172	.752	.352	.935	.496	.582	.311				
Ba	-.213	.687	-.238	.156	-.095	.215	.350	-.306	-.138			
Cd	-.033	.583	.033	-.487	-.060	-.068	.279	-.133	.000	.431		
Ce1	-.568	-.079	.155	.794	.552	.224	.571	.224	.463	.016	-.372	
Co	-.703	.203	.473	.396	.749	.410	.575	-.097	.638	.266	.276	.494
Cr	.655	-.149	-.295	-.293	-.556	-.449	-.856	-.170	-.619	-.252	-.322	-.507
Cu	-.086	.634	-.570	.278	-.351	.128	.204	-.310	-.382	.712	.090	.041
Mo	-.736	-.057	.837	.129	.857	.521	.501	.250	.894	.057	.241	.259
Ni	-.185	.697	.041	-.267	.008	.077	.355	-.142	.038	.558	.947	-.199
Pb	-.754	-.130	.539	.609	.863	.503	.462	.074	.766	.051	-.186	.673
Sr	-.891	.042	.592	.560	.882	.583	.661	.149	.833	.300	-.006	.618
V	-.883	.009	.687	.343	.892	.633	.558	.172	.925	.096	.095	.327
Y	-.848	-.132	.726	.569	.860	.594	.616	.350	.886	.000	-.179	.625
Zn	-.448	.734	-.093	-.027	.107	.262	.453	-.268	.166	.584	.742	-.213
Pd	-.356	.282	.212	.137	.181	.043	.359	-.074	.105	.546	.259	.061
Pt	.121	.613	-.516	.476	-.518	-.122	-.149	-.291	-.682	.552	-.153	.078
Rh	-.319	.483	-.164	.573	-.119	.059	.381	.072	-.201	.443	-.082	.372
La	-.839	-.480	-.169	.837	.531	.015	.541	.193	.351	-.363	-.610	.806
Ce2	-.579	-.643	-.374	.586	.724	-.507	.772	.148	.475	-.365	-.411	1.000
Pr	-.773	-.641	.014	.785	.601	.044	.470	.333	.499	-.535	-.705	.770
Nd	-.783	-.643	.033	.777	.611	.055	.475	.330	.513	-.533	-.693	.767
Sm	-.762	-.680	.074	.745	.634	.039	.476	.382	.552	-.555	-.696	.759
Eu	-.765	-.691	.126	.715	.651	.057	.476	.407	.583	-.558	-.679	.739
Gd	-.800	-.660	.083	.730	.655	.047	.515	.366	.564	-.519	-.648	.764
Tb	-.797	-.675	.120	.701	.672	.046	.521	.401	.590	-.520	-.635	.752
Dy	-.804	-.696	.208	.625	.719	.052	.553	.444	.660	-.504	-.573	.726
Ho	-.818	-.686	.311	.519	.761	.067	.595	.472	.727	-.442	-.462	.679
Er	-.804	-.677	.375	.440	.771	.063	.614	.485	.767	-.384	-.387	.639
Tm	-.804	-.669	.394	.416	.774	.068	.618	.501	.771	-.372	-.365	.623
Yb	-.810	-.660	.391	.416	.772	.071	.624	.473	.773	-.356	-.351	.625
Lu	-.833	-.635	.355	.401	.789	.037	.678	.465	.761	-.309	-.300	.646

Table 26 continued

	Co	Cr	Cu	Mo	Ni	Pb	Sr	V	Y	Zn	Pd	Pt
Cr	-0.618											
Cu	-.150	-.141										
Mo	.661	-.607	-.349									
Ni	.363	-.380	.208	.295								
Pb	.829	-.496	-.281	.682	-.049							
Sr	.783	-.675	-.025	.833	.142	.869						
V	.660	-.611	-.185	.925	.173	.749	.882					
Y	.587	-.658	-.155	.828	-.060	.755	.900	.851				
Zn	.349	-.406	.433	.287	.789	.018	.250	.388	.043			
Pd	.451	-.304	.208	.288	.271	.254	.487	.229	.305	.241		
Pt	-.097	.398	.736	-.543	.025	-.137	-.162	-.506	-.324	.150	.347	
Rh	.135	.041	.426	-.099	.146	.125	.212	-.076	.125	.160	.278	.698
La	-.083	-.418	.126	-.092	-.530	.427	.378	.199	.673	-.441	-.102	.003
Ce2	.164	-.659	-.023	-.081	-.380	.780	.382	.089	.494	-.421	-.268	-.294
Pr	-.272	-.371	-.107	-.045	-.653	.284	.310	.224	.756	-.625	-.150	-.178
Nd	-.265	-.380	-.116	-.023	-.641	.283	.325	.244	.770	-.620	-.131	-.187
Sm	-.298	-.387	-.166	.003	-.653	.260	.326	.263	.790	-.652	-.129	-.237
Eu	-.309	-.397	-.199	.047	-.640	.236	.346	.304	.818	-.657	-.095	-.266
Gd	-.244	-.431	-.146	.051	-.601	.292	.383	.313	.814	-.608	-.074	-.232
Tb	-.256	-.444	-.174	.085	-.592	.277	.399	.345	.835	-.615	-.051	-.261
Dy	-.243	-.494	-.231	.190	-.538	.264	.464	.436	.889	-.604	.030	-.328
Ho	-.195	-.560	-.270	.334	-.433	.257	.564	.560	.946	-.549	.162	-.385
Er	-.173	-.590	-.292	.423	-.364	.246	.625	.629	.973	-.518	.252	-.424
Tm	-.166	-.600	-.296	.447	-.343	.238	.639	.653	.978	-.502	.274	-.429
Yb	-.147	-.605	-.288	.456	-.327	.251	.652	.656	.980	-.490	.290	-.425
Lu	-.077	-.659	-.244	.478	-.272	.310	.699	.683	.974	-.434	.319	-.409

	Rh	La	Ce2	Pr	Nd	Sm	Eu	Gd	Tb	Dy	Ho	Er	Tm	Yb
La	0.554													
Ce2	.260	.806												
Pr	.355	.969	.770											
Nd	.349	.967	.767	1.000										
Sm	.305	.953	.759	.998	.998									
Eu	.280	.940	.739	.993	.995	.999								
Gd	.330	.959	.764	.995	.997	.998	.997							
Tb	.310	.948	.752	.991	.993	.996	.998	.999						
Dy	.262	.917	.726	.971	.975	.982	.989	.989	.994					
Ho	.227	.867	.679	.925	.933	.943	.957	.957	.967	.989				
Er	.195	.821	.639	.883	.893	.906	.924	.923	.936	.968	.994			
Tm	.193	.808	.623	.870	.880	.894	.913	.913	.927	.962	.991	.999		
Yb	.195	.805	.625	.865	.876	.888	.908	.909	.922	.958	.989	.999	.999	
Lu	.236	.810	.646	.854	.865	.876	.894	.899	.913	.949	.984	.994	.996	.997

Table 27. Correlation matrix for 7 nodules from Adam Seamount, original data in Table 12.

[zero correlation at 99 and 95 percent confidence levels are |0.859| and |0.753|, respectively; n=6 for PGEs (|0.903|, |0.813|)]

	Thick	Fe	Mn	Fe/Mn	Si	Na	Al	K	Mg	Ca	Ti	P
Fe	-0.118											
Mn	.336	-.283										
Fe/Mn	.000	.687	-.876									
Si	-.539	-.152	-.866	.572								
Na	-.579	-.315	-.646	.354	.890							
Al	-.377	.044	-.965	.737	.951	.743						
K	-.455	-.567	-.270	.003	.655	.780	.452					
Mg	.399	-.584	.426	-.600	-.205	-.240	-.289	.227				
Ca	-.277	.340	.124	.006	-.235	-.130	-.221	-.526	-.739			
Ti	.085	.181	-.553	.385	.365	.012	.519	-.344	-.011	.019		
P	.019	.382	.362	-.150	-.544	-.416	-.498	-.740	-.556	.925	-.026	
H_2O^+	.505	-.697	.526	-.786	-.311	-.256	-.400	-.051	.801	-.295	.144	-.103
CO_2	.064	.228	.529	-.293	-.606	-.269	-.661	-.445	-.343	.636	-.443	.796
As	-.008	.574	.312	.024	-.559	-.396	-.497	-.677	-.654	.839	-.227	.931
Ba	.424	.008	.349	-.324	-.454	-.757	-.325	-.535	.444	-.065	.420	.076
Cd	.025	-.208	.862	-.679	-.664	-.359	-.826	.082	.288	.016	-.867	.167
Ce	.033	-.031	-.330	.096	.250	.034	.334	-.394	-.130	.362	.876	.289
Co	.497	-.423	.725	-.804	-.605	-.465	-.689	-.307	.656	-.067	-.015	.213
Cr	.183	-.369	-.484	.257	.579	.572	.566	.664	.324	-.792	.019	-.836
Cu	-.148	.210	-.535	.441	.431	-.012	.556	-.027	.172	-.316	.755	-.422
Mo	.147	.228	.745	-.440	-.830	-.595	-.840	-.549	-.270	.647	-.537	.807
Ni	.589	-.608	.763	-.829	-.560	-.393	-.658	.083	.825	-.472	-.413	-.215
Pb	.403	-.029	-.069	-.075	-.073	-.107	.002	-.525	.030	.250	.652	.382
Sr	.171	.403	.170	-.053	-.425	-.624	-.277	-.880	-.198	.608	.562	.701
V	-.019	.622	.479	-.065	-.709	-.571	-.662	-.662	-.445	.671	-.343	.819
Y	-.220	.618	-.114	-.235	-.152	-.378	-.005	-.690	-.564	.727	.461	.659
Zn	.179	.237	.727	-.370	-.771	-.656	-.795	-.220	.298	-.115	-.627	.127
Pd	.424	.193	.390	-.235	-.487	-.781	-.374	-.357	.470	-.209	.140	-.080
Pt	.574	.349	-.266	.263	-.001	-.439	.203	-.548	.194	-.081	.875	-.010
Rh	.088	.371	-.731	.659	.456	.077	.661	-.351	-.415	.213	.869	.075

Table 27 continued

	H_2O^+	CO_2	As	Ba	Cd	Ce	Co	Cr	Cu	Mo	Ni	Pb
CO_2	-0.012											
As	-.345	.858										
Ba	.439	-.302	-.115									
Cd	.187	.516	.267	-.035								
Ce	.275	-.170	-.009	.368	-.715							
Co	.897	.377	.039	.379	.407	.146						
Cr	.070	-.536	-.735	-.398	-.307	-.224	-.206					
Cu	-.067	-.802	-.519	.525	-.645	.460	-.289	.104				
Mo	-.036	.836	.847	.084	.681	-.259	.314	-.751	-.667			
Ni	.783	.113	-.261	.284	.634	-.358	.772	.158	-.367	.210		
Pb	.494	.245	.172	.171	-.465	.767	.526	-.092	.029	-.046	.003	
Sr	.131	.232	.507	.660	-.231	.678	.278	-.770	.282	.375	-.222	.552
V	-.305	.814	.931	.025	.476	-.212	.121	-.783	-.445	.887	-.102	-.015
Y	-.361	.126	.558	.427	-.310	.539	-.226	-.779	.363	.315	-.623	.195
Zn	.032	.398	.305	.207	.828	-.707	.321	-.338	-.319	.608	.511	-.432
Pd	.207	-.326	-.132	.910	.205	-.026	.199	-.391	.550	.115	.317	-.252
Pt	.218	-.437	-.169	.781	-.599	.671	.114	-.175	.851	-.329	-.244	.481
Rh	-.269	-.436	-.053	.296	-.924	.774	-.432	.017	.690	-.430	-.825	.447

	Sr	V	Y	Zn	Pd	Pt
V	0.472					
Y	.853	.507				
Zn	-.023	.606	-.103			
Pd	.431	.144	.370	.515		
Pt	.689	-.138	.577	-.206	.580	
Rh	.508	-.257	.642	-.707	.032	.716

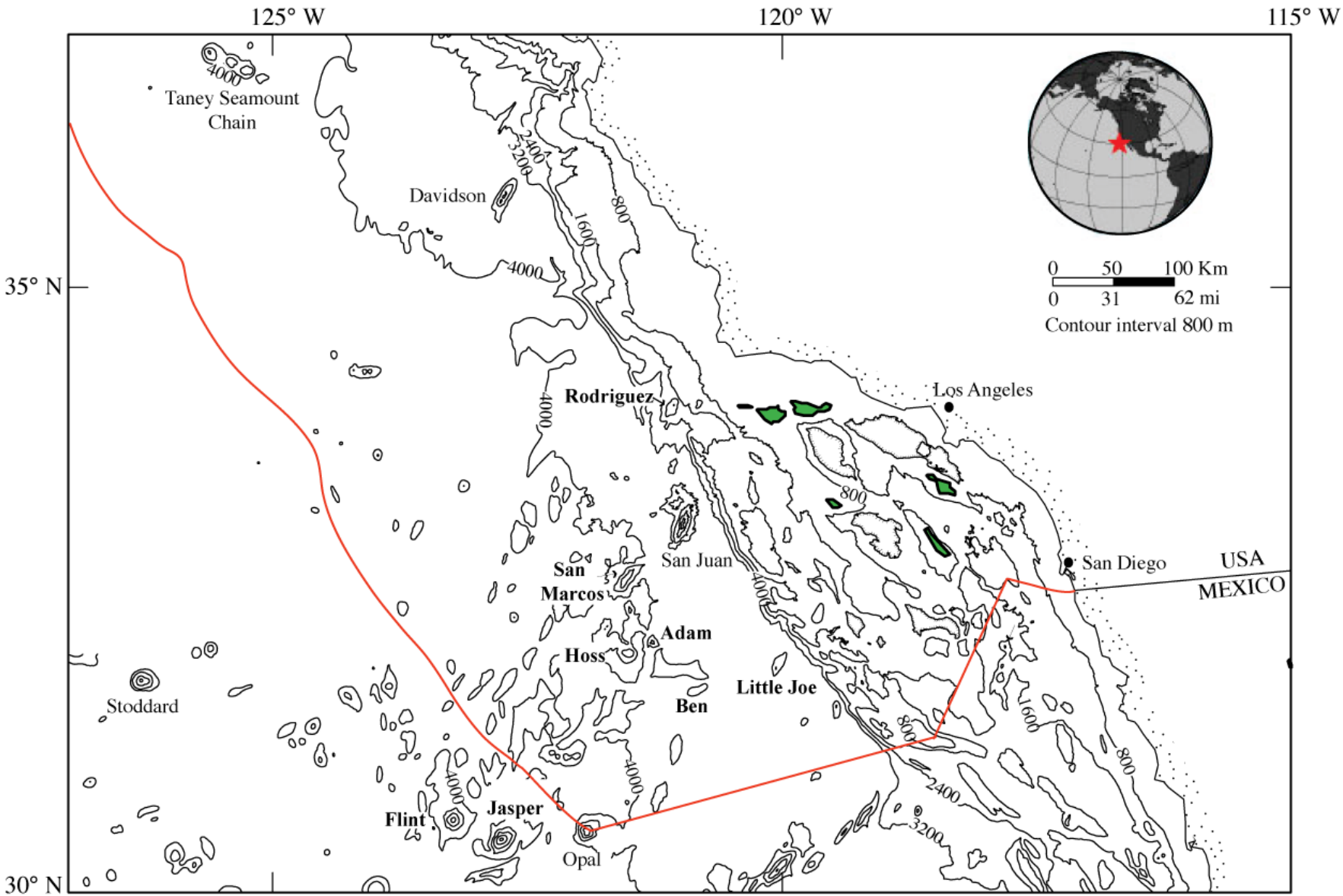

Figure 1. Map showing islands (green) and seamounts within the Southern California Borderland. Seamounts pertaining to this study are in bold type; the 200 nmi U.S. Exclusive Economic Zone (EEZ) boundary is shown in red.

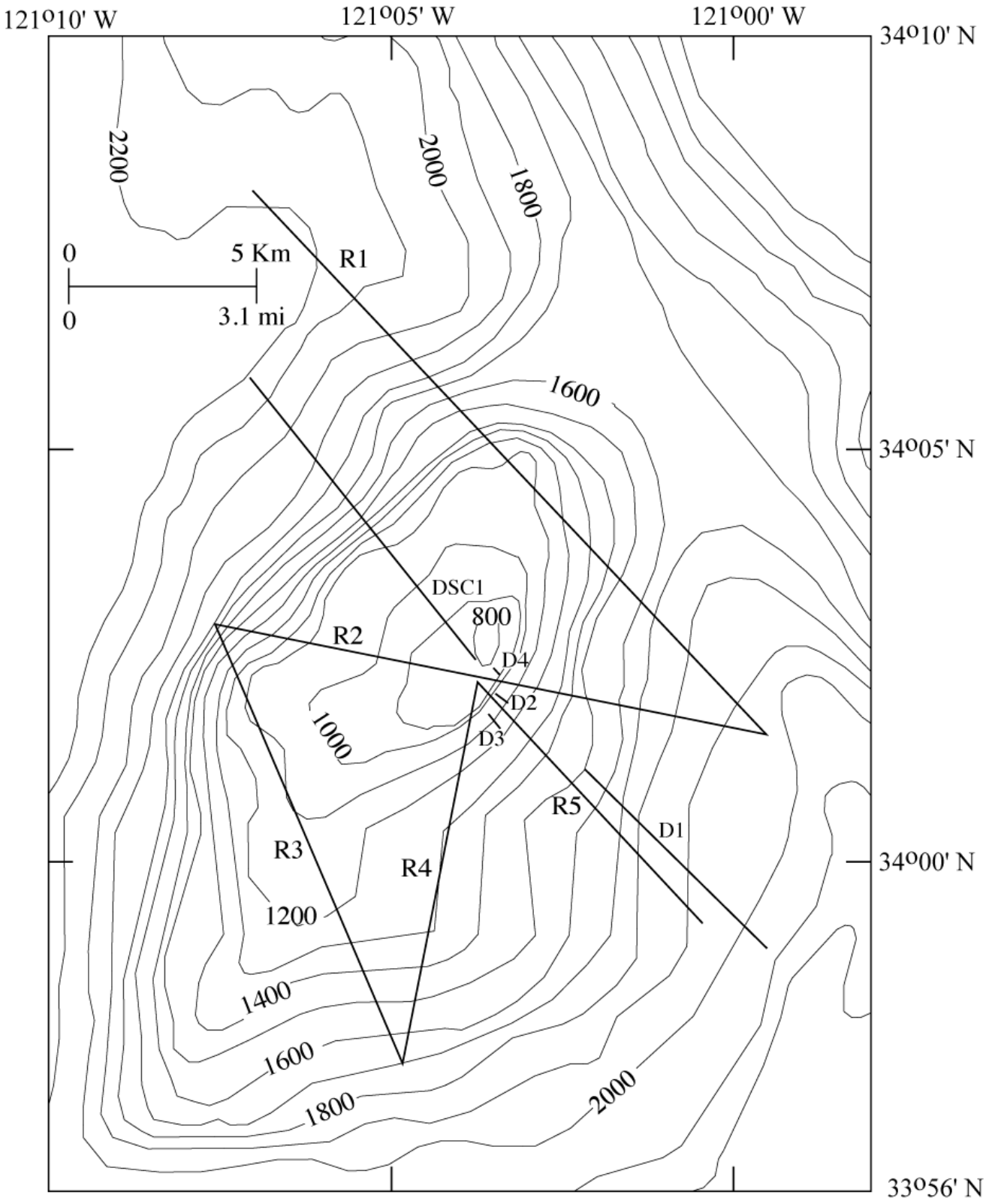

Figure 2. Map showing Rodriguez Seamount bathymetry. D, dredge; DSC, deep-sea camera; and R, geophysical line locations; contour interval is 100 m.

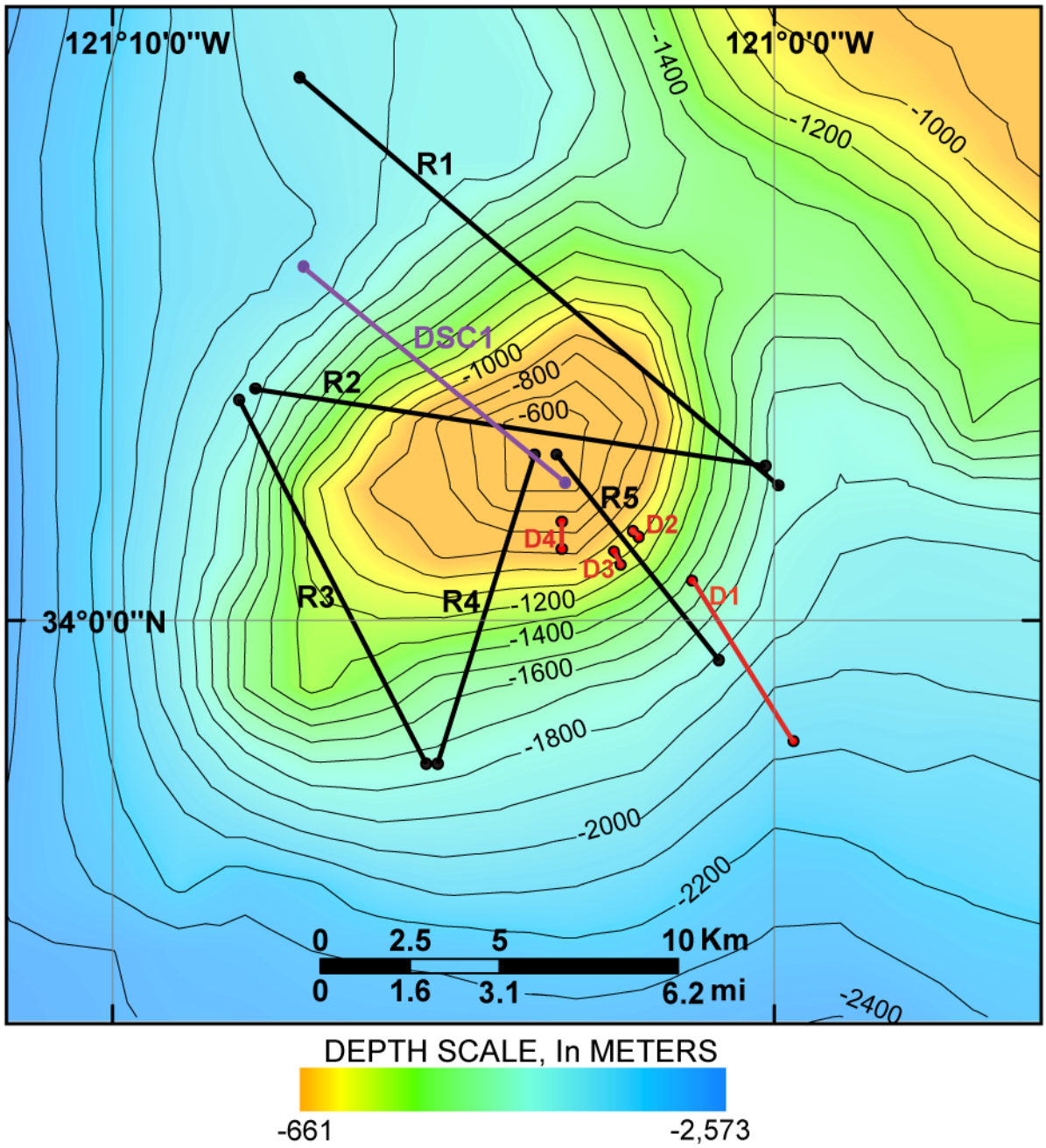

Figure 3. Map showing Rodriguez Seamount ETOPO bathymetry. D, dredges in red; DSC, deep-sea camera in purple; and R, geophysical lines in black; contour interval is 100 m.

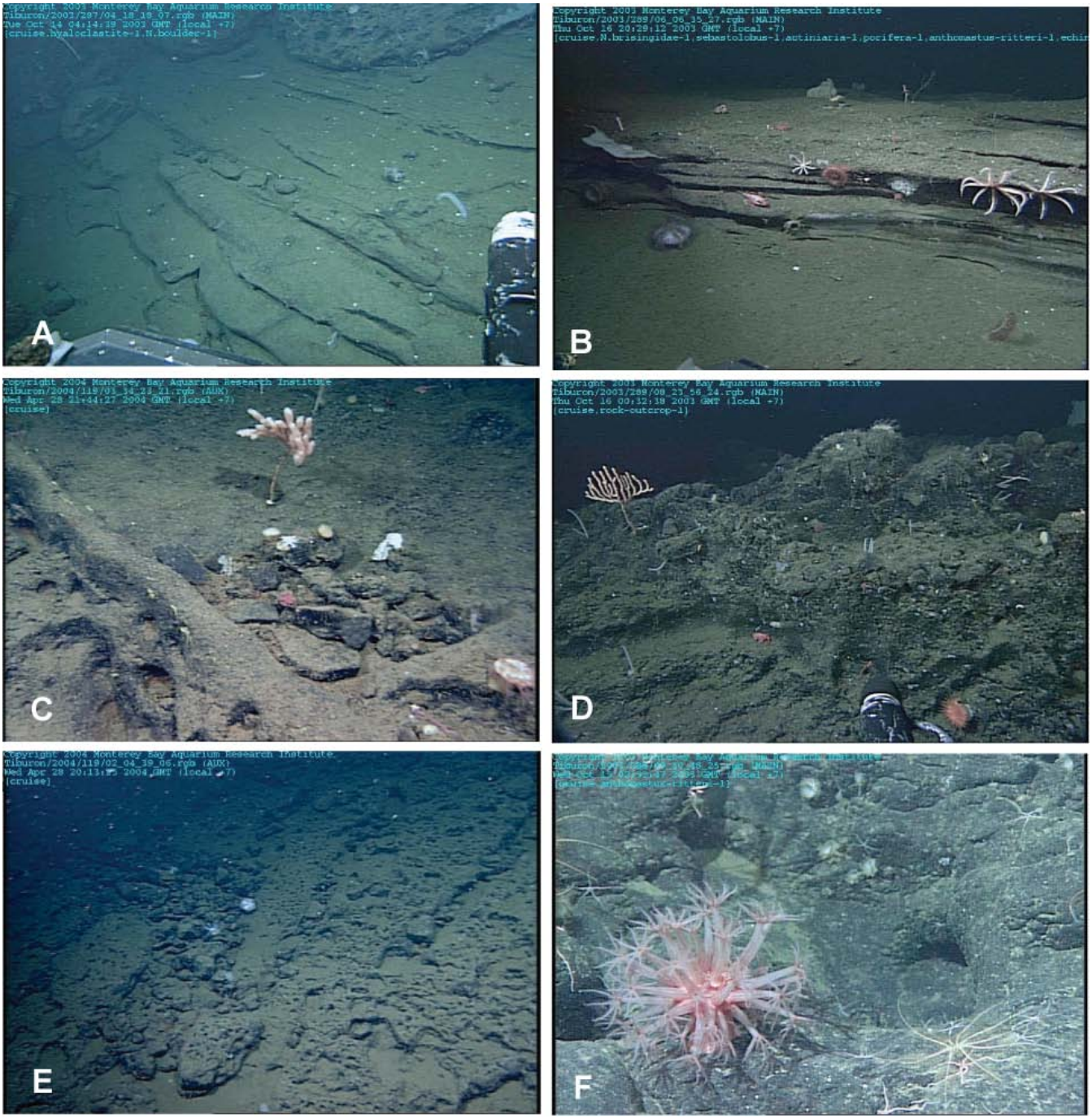

Figure 4. Seabed photos of Rodriguez Seamount courtesy of MBARI, collected during the 2004 and 2003 cruises aboard the RV Western Flyer. A, Bedded volcaniclastic sandstone at 664 m water depth, dive T628. B, Cross section of bedded volcaniclastic sandstone at 681 m showing evidence of beach deposition, dive T631 (Paduan and others, 2009). C, An eroded volcaniclastic ridge approximately 0.25 m high at 838 m that has trapped basalt talus, dive T661. D, Outcrop and perhaps a vent at the summit of a volcanic cone at 755 m, dive T630. E, Pitted and eroded pavement typical of volcaniclastic material at 999 m, dive T661. F, Ferromanganese crusts on lava flow at 1,694 m, with a pink mushroom coral (Anthomastus ritteri), dive T629.

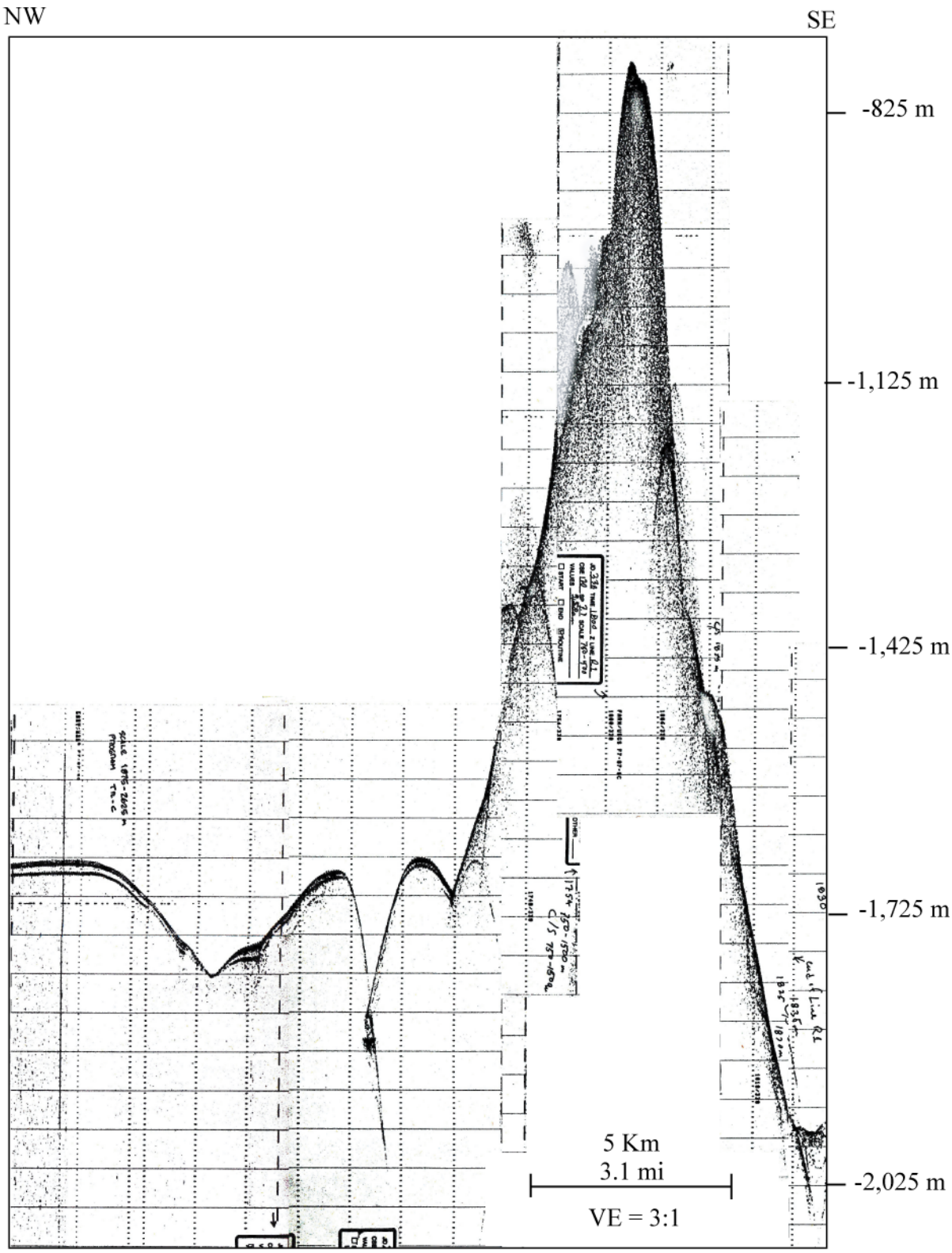

Figure 5. Rodriguez Seamount 3.5 kHz bathymetry line R1; VE, vertical exaggeration.

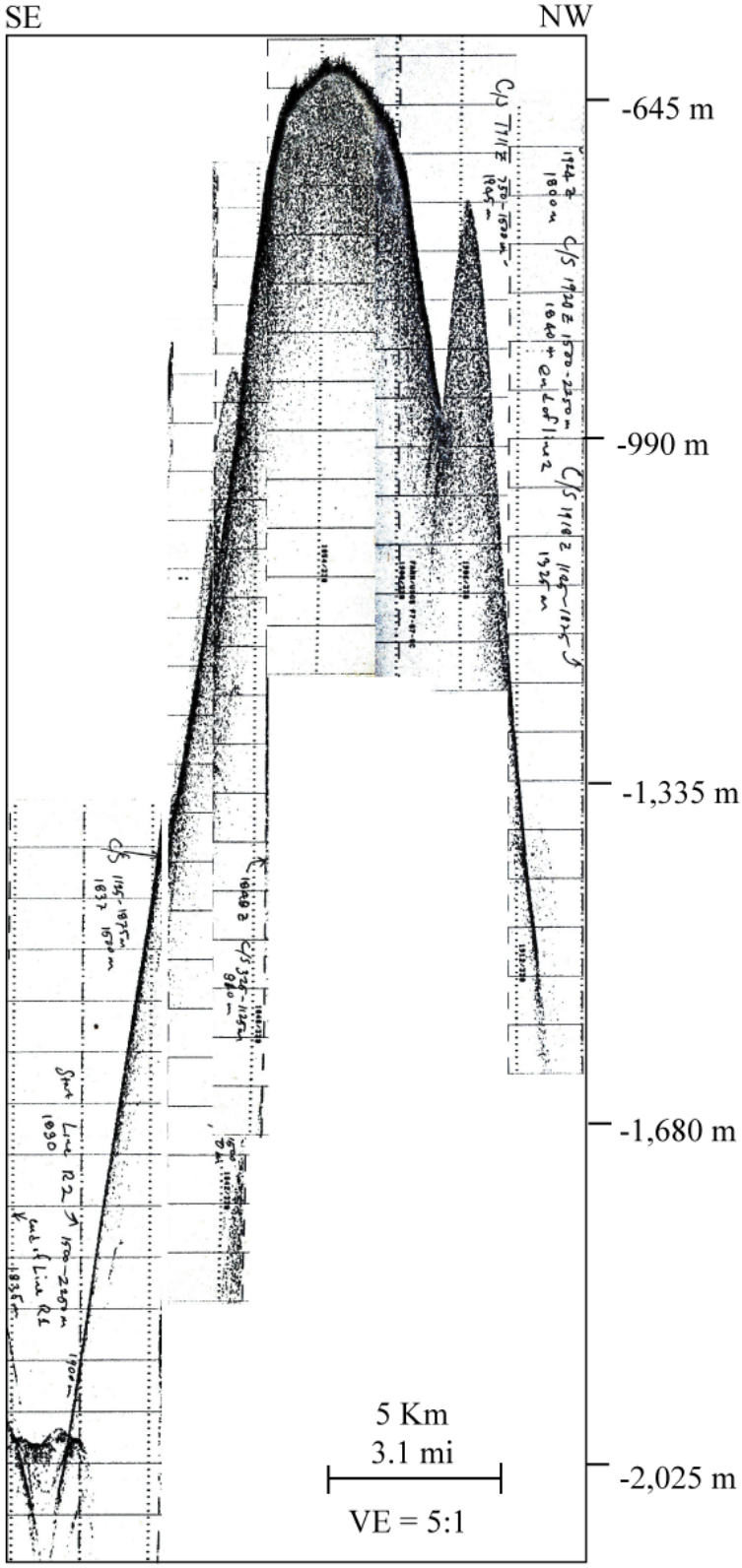

Figure 6. Rodriguez Seamount 3.5 kHz bathymetry line R2; VE, vertical exaggeration.

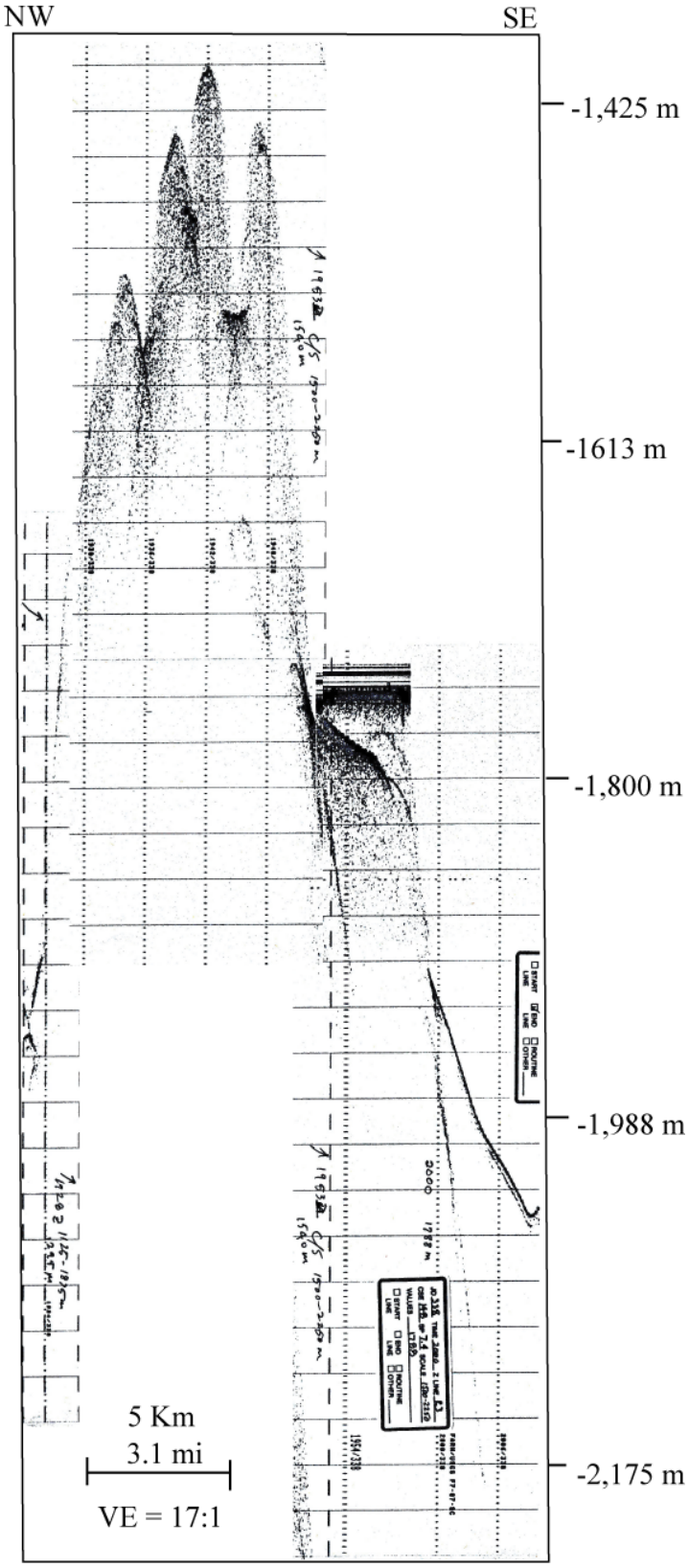

Figure 7. Rodriguez Seamount 3.5 kHz bathymetry line R3; VE, vertical exaggeration.

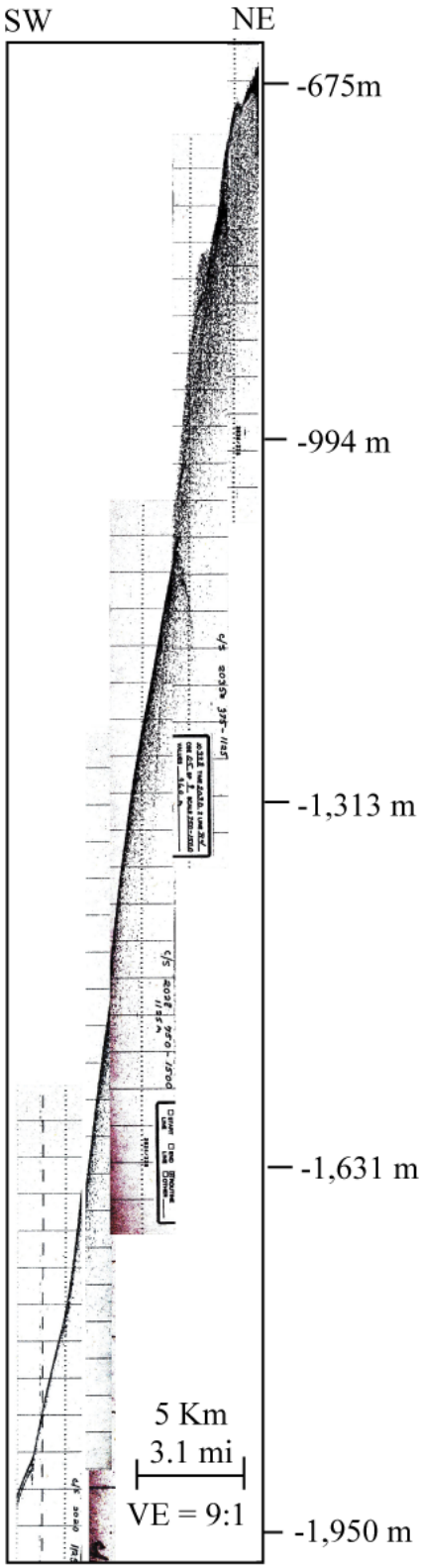

Figure 8. Rodriguez Seamount 3.5 kHz bathymetry line R4; VE, vertical exaggeration.

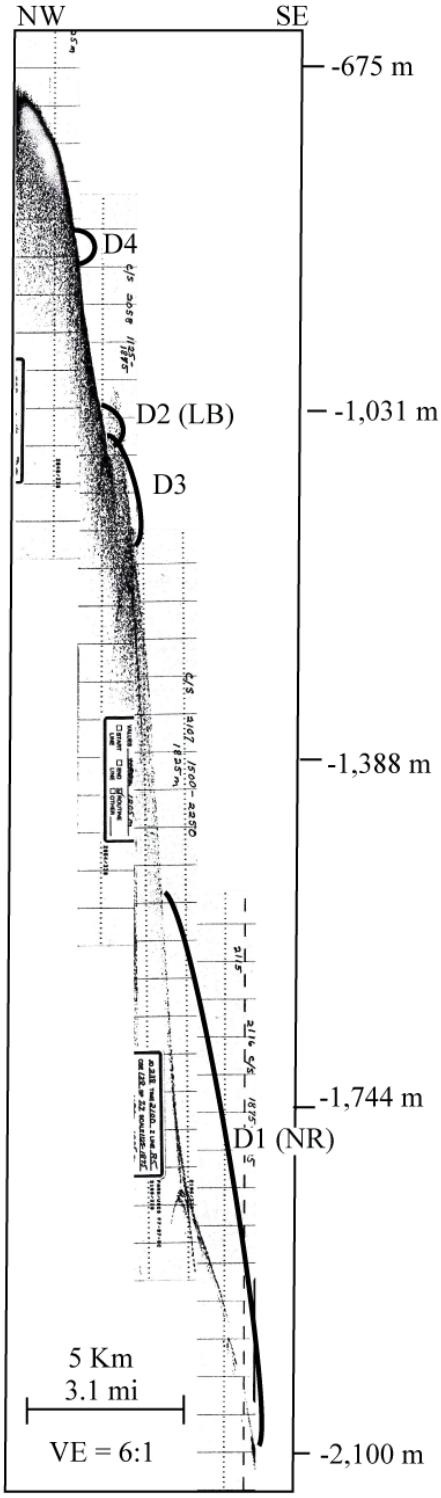

Figure 9. Rodriguez Seamount 3.5 kHz bathymetry line R5 with D, dredges 1-4; NR, No Recovery; LB, Lost Bag; VE, vertical exaggeration.

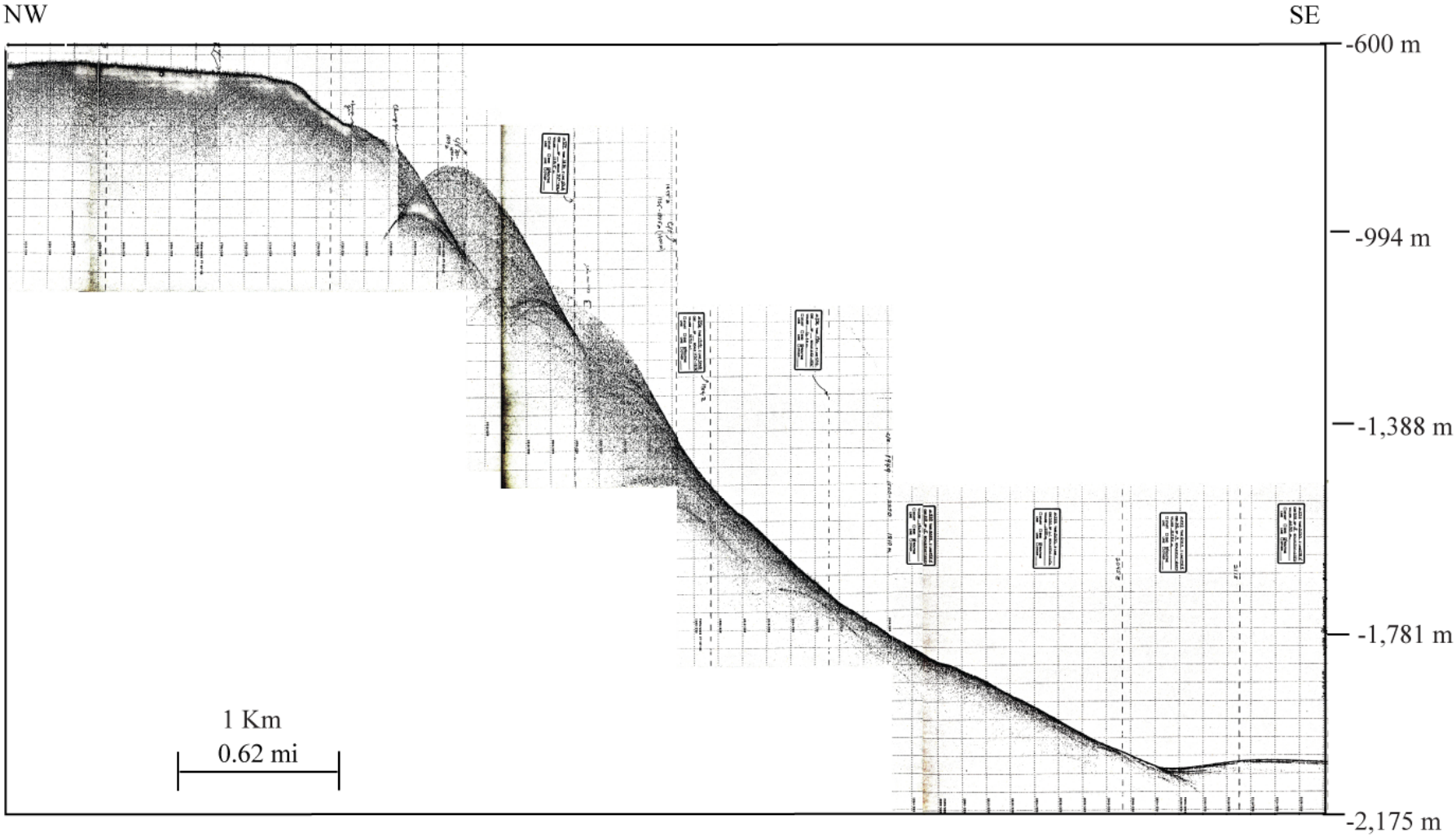

Figure 10. Rodriguez Seamount 3.5 kHz bathymetry. DSC1, deep-sea camera line 1.

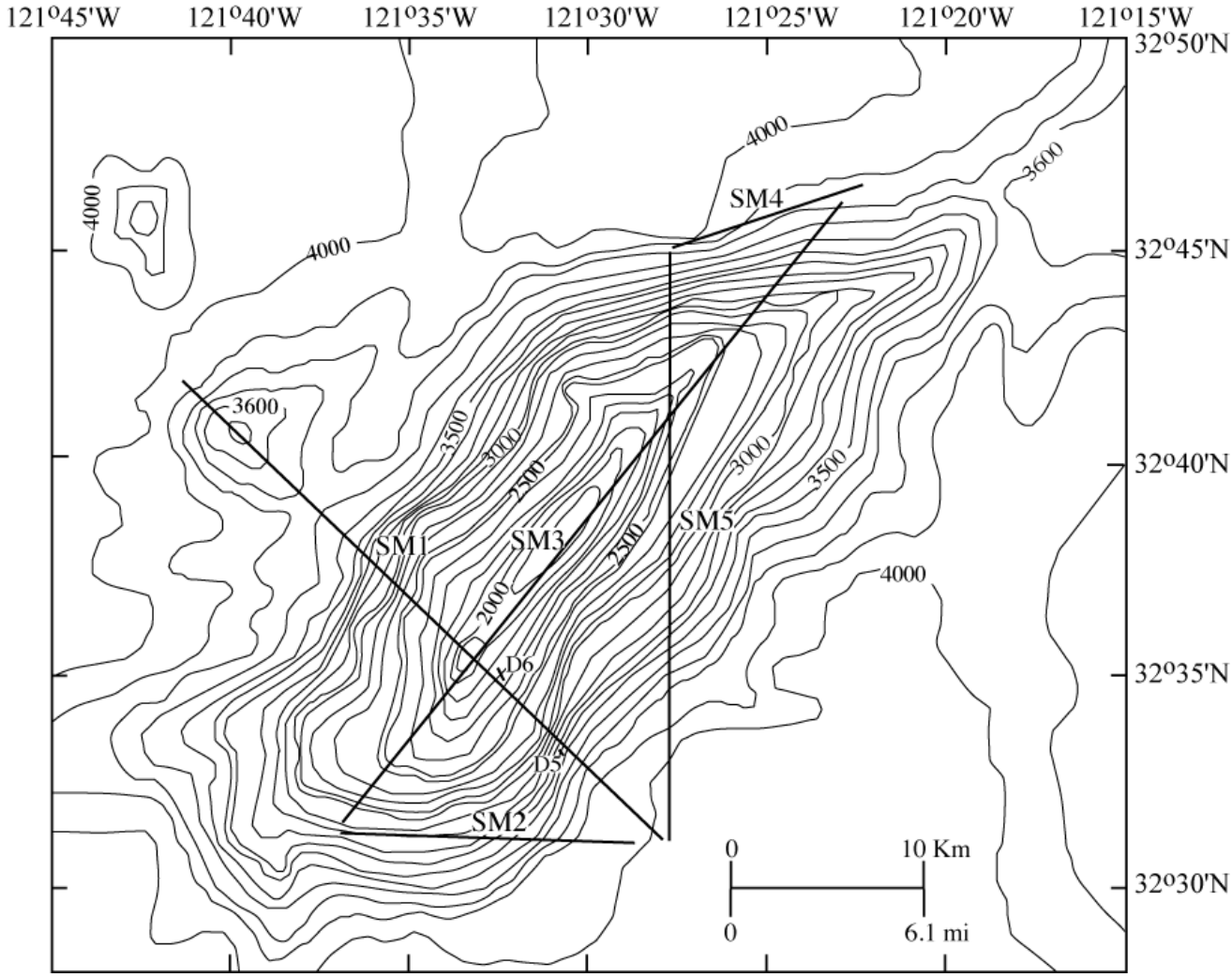

Figure 11. Map showing San Marcos Seamount bathymetry. D, dredge; and SM, geophysical line locations for San Marcos Seamount; contour interval is 100 m.

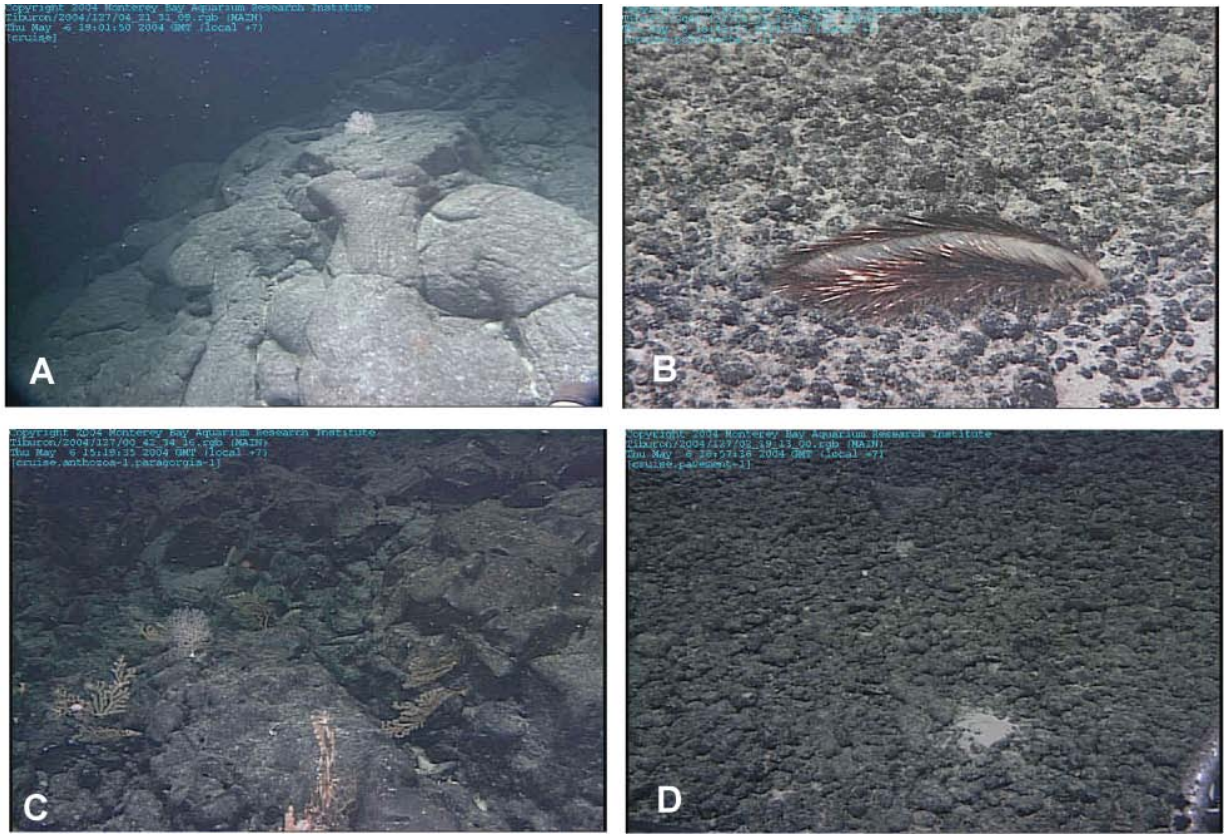

Figure 12. Seabed photos of San Marcos Seamount courtesy of MBARI, collected during a 2004 cruise aboard the RV *Western Flyer*; all photos from dive T669. *A*, pillow lava at 2,334 m. *B*, volcaniclastic deposit of coarse-grained spatter at 2,347 m, with a sea worm, Aphroditidae. *C*, outcrop at 2,029 m thought to be welded volcaniclastic spatter. *D*, light colored probably pelagic sediment pockets with ferromanganese encrusted volcaniclastic spatter at 2,343 m.

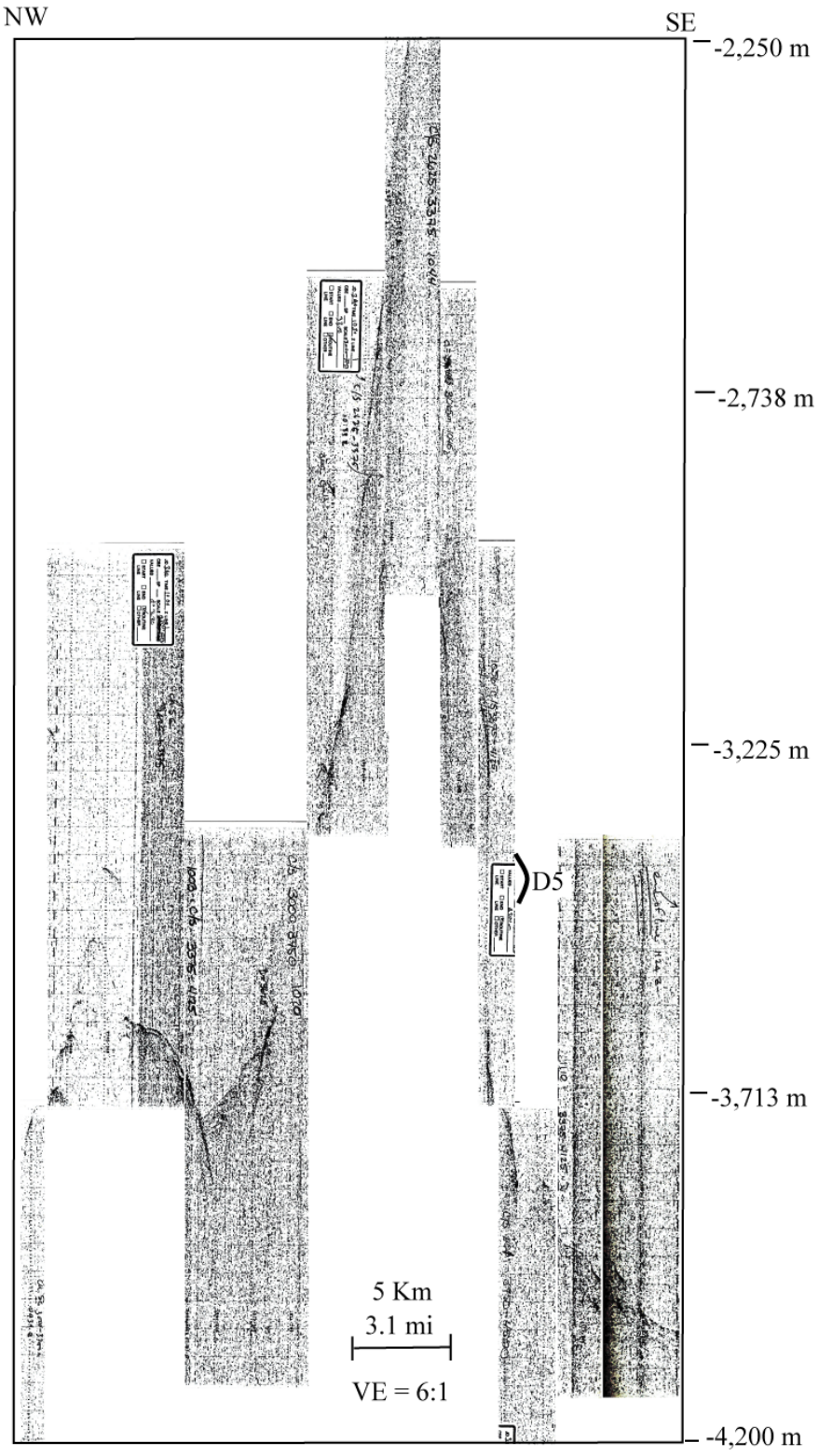

Figure 13. San Marcos Seamount 3.5 kHz bathymetry line SM1 with D, dredge; VE, vertical exaggeration.

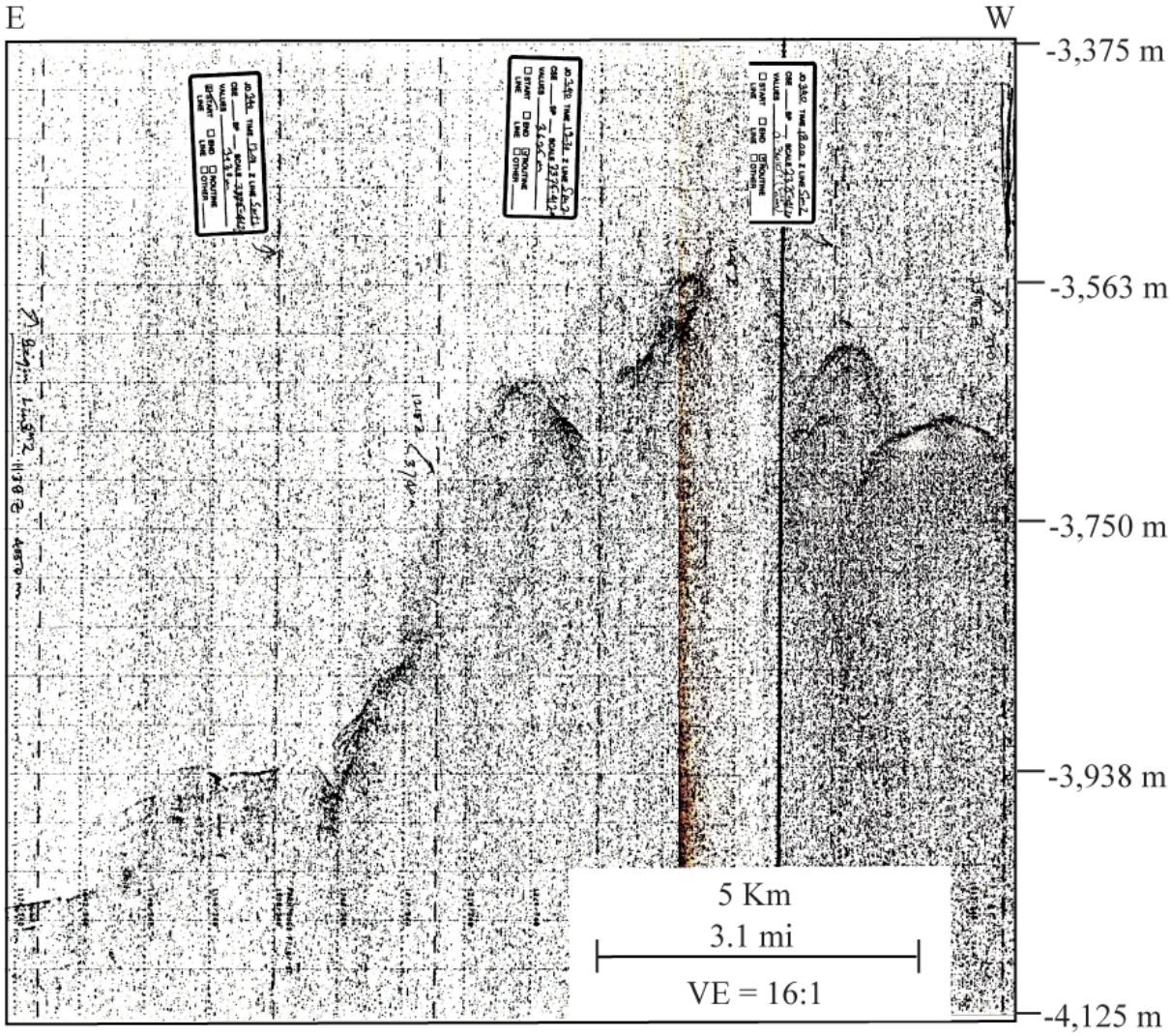

Figure 14. San Marcos Seamount 3.5 kHz bathymetry line SM2; VE, vertical exaggeration.

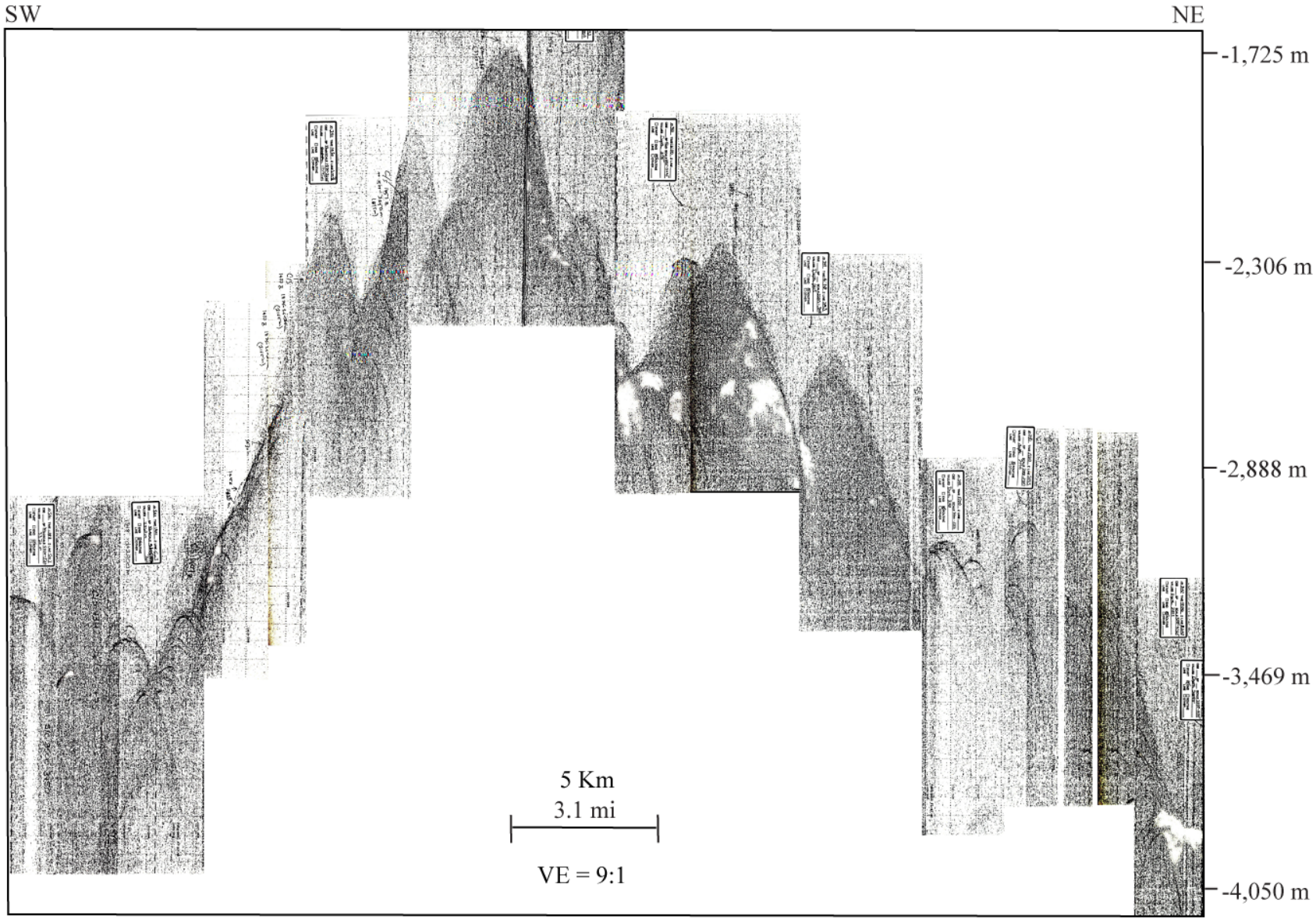

Figure 15. San Marcos Seamount 3.5 kHz bathymetry line SM3; VE, vertical exaggeration.

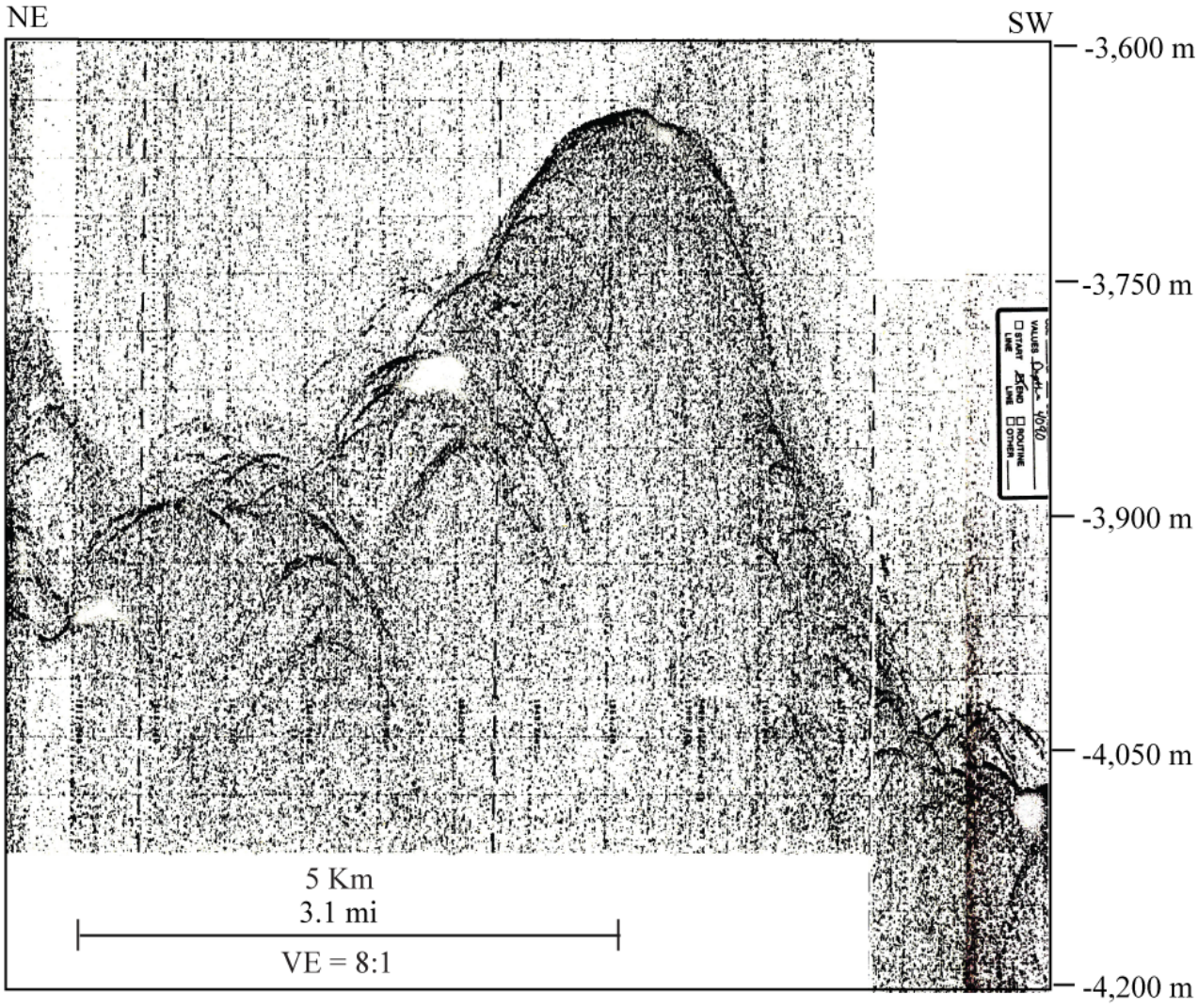

Figure 16. San Marcos Seamount 3.5 kHz bathymetry line SM4; VE, vertical exaggeration.

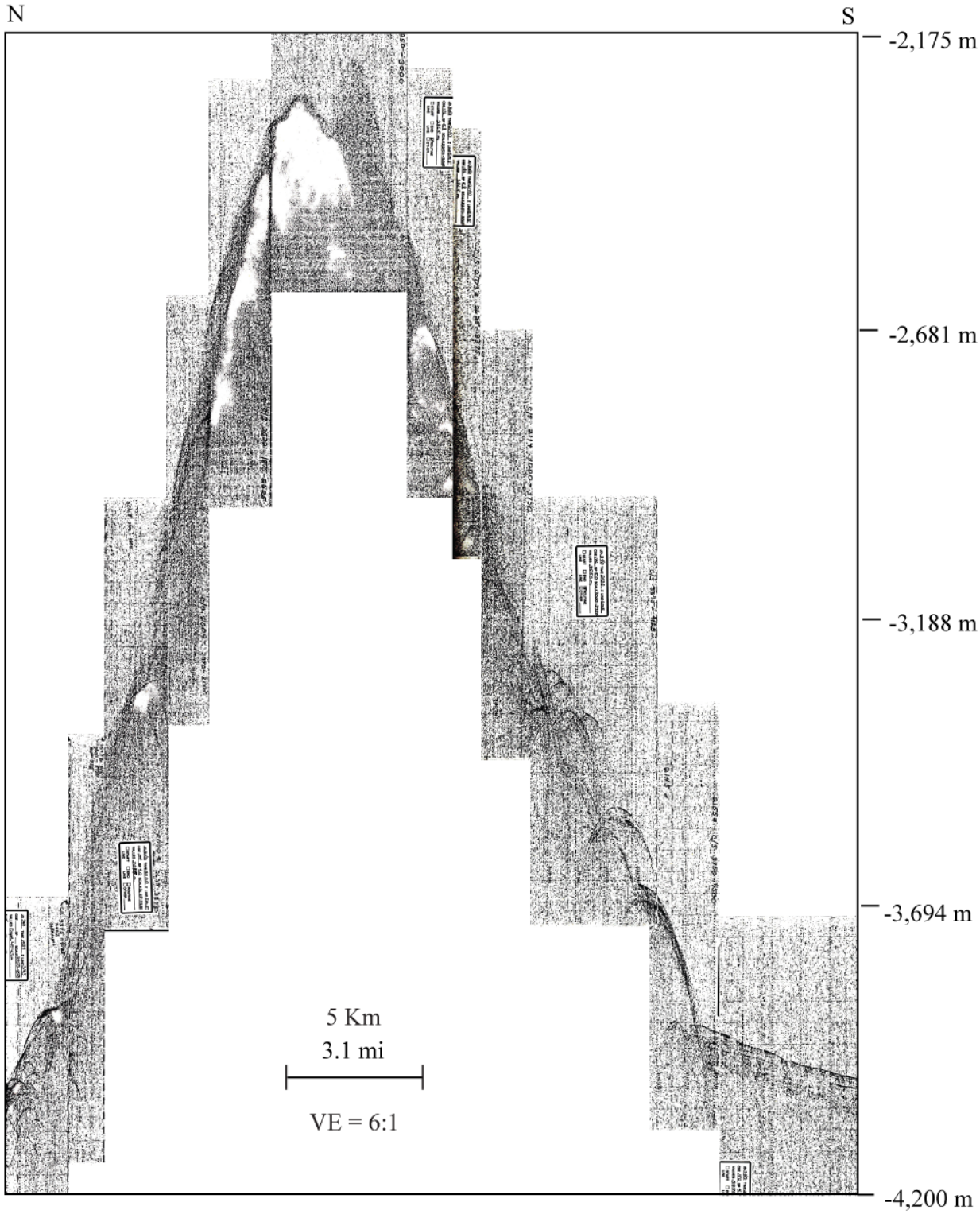

Figure 17. San Marcos Seamount 3.5 kHz bathymetry line SM5; VE, vertical exaggeration.

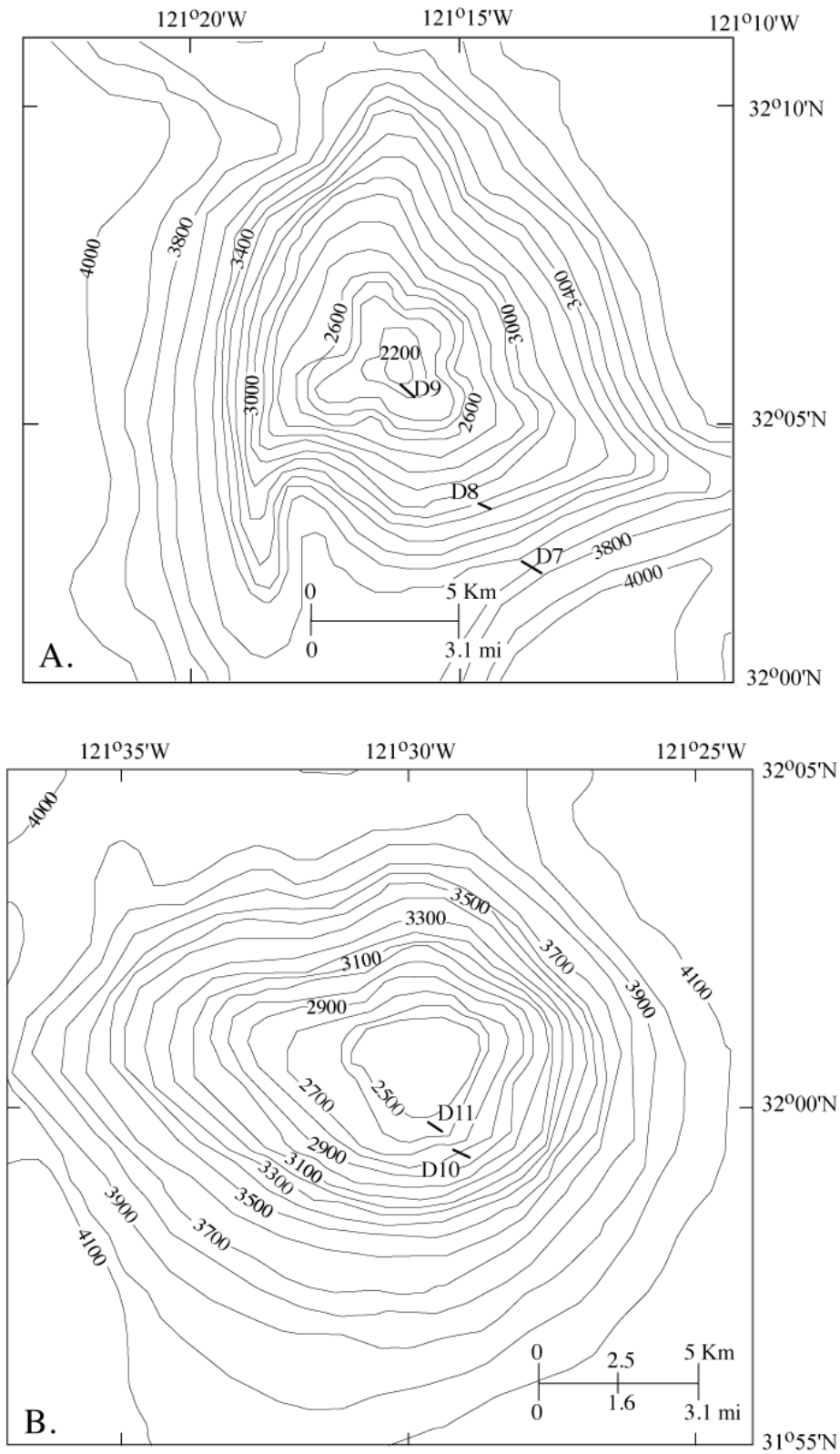

Figure 18. Maps showing *A*, Adam Seamount; and *B*, Hoss Seamount; bathymetry and D, dredge locations; contour interval for both seamounts is 100 m.

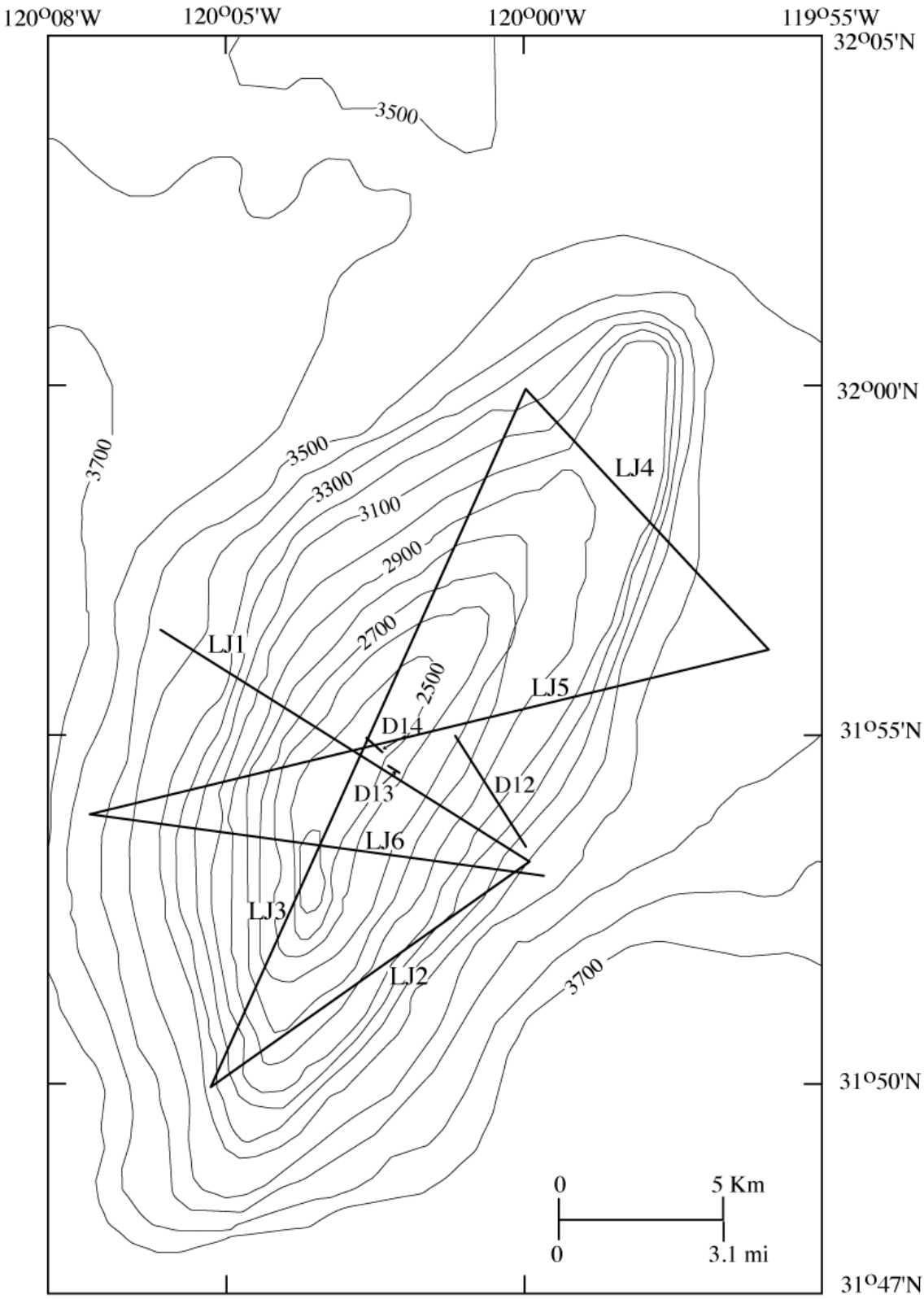

Figure 19. Map showing Little Joe Seamount bathymetry, D, dredge; and LJ, geophysical line locations; contour interval is 100 m.

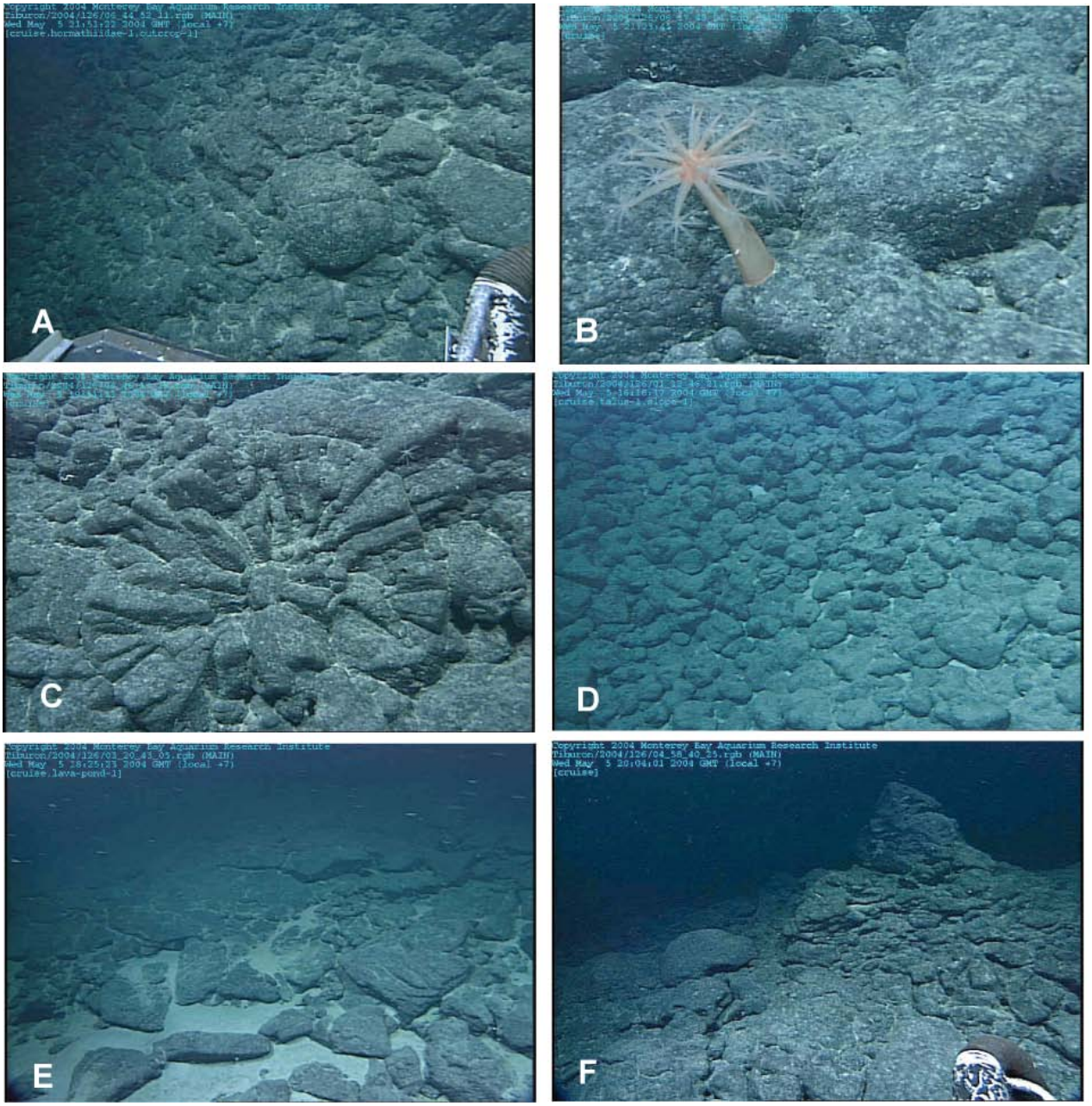

Figure 20. Seabed photos of Little Joe Seamount courtesy of MBARI, collected during a 2004 cruise aboard the RV *Western Flyer*; all photos from dive T668. *A*, Pillow basalt at 2,161 m. *B*, A stalked mushroom coral (*Anthomastus ritteri*) on pillow basalt at 2,247 m. *C*, Truncated pillow lava showing cross section of radial jointing due to contraction of the lava during cooling at 2,353 m. *D*, Talus of pillow lava fragments at 2,597 m. *E*, Slabs of volcaniclastic rock and pockets of pelagic sediment at 2,385 m. *F*, Small mound vent or hornito at 2,335 m.

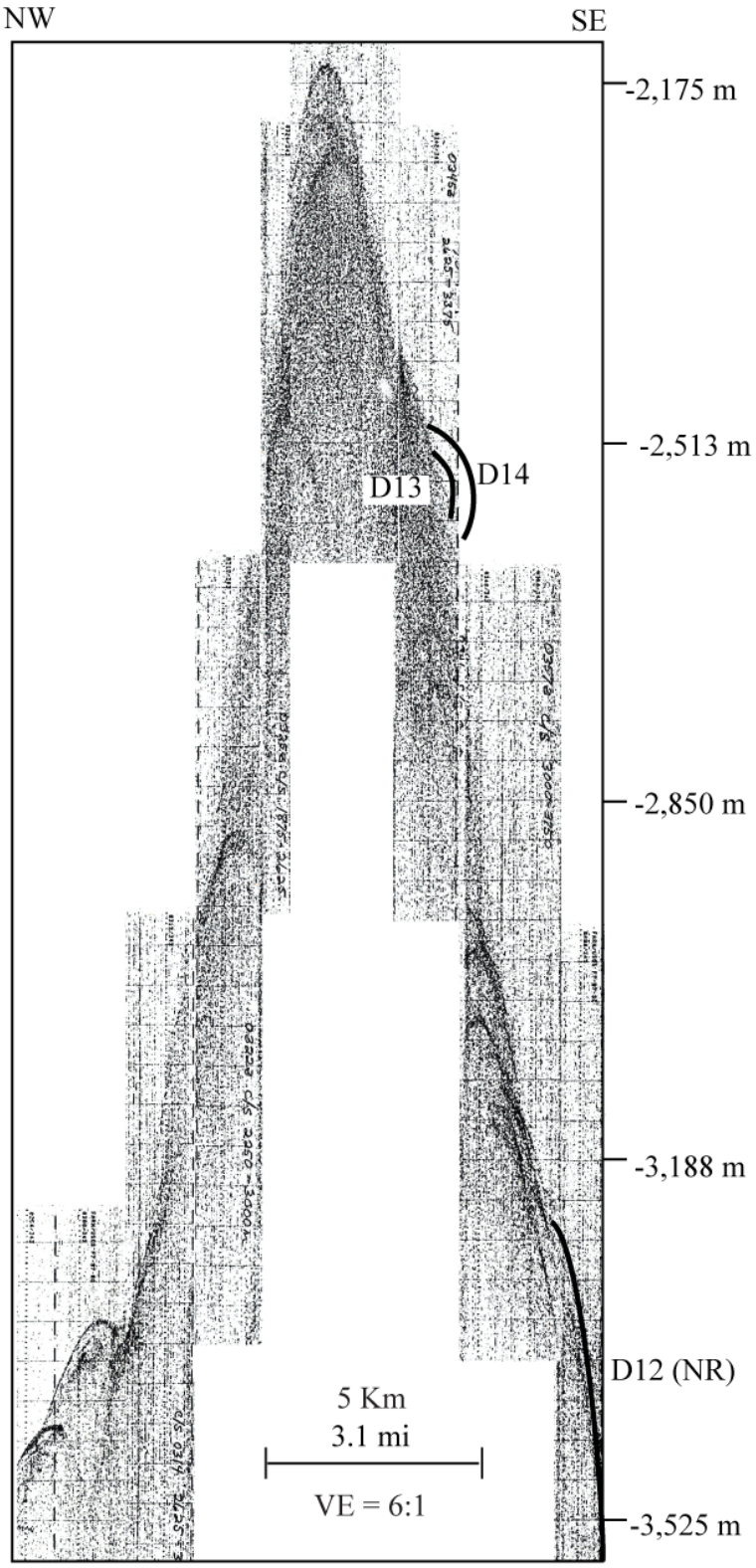

Figure 21. Little Joe Seamount 3.5 kHz bathymetry line LJ1 with D, dredges 12-14; NR, No Recovery; VE, vertical exaggeration.

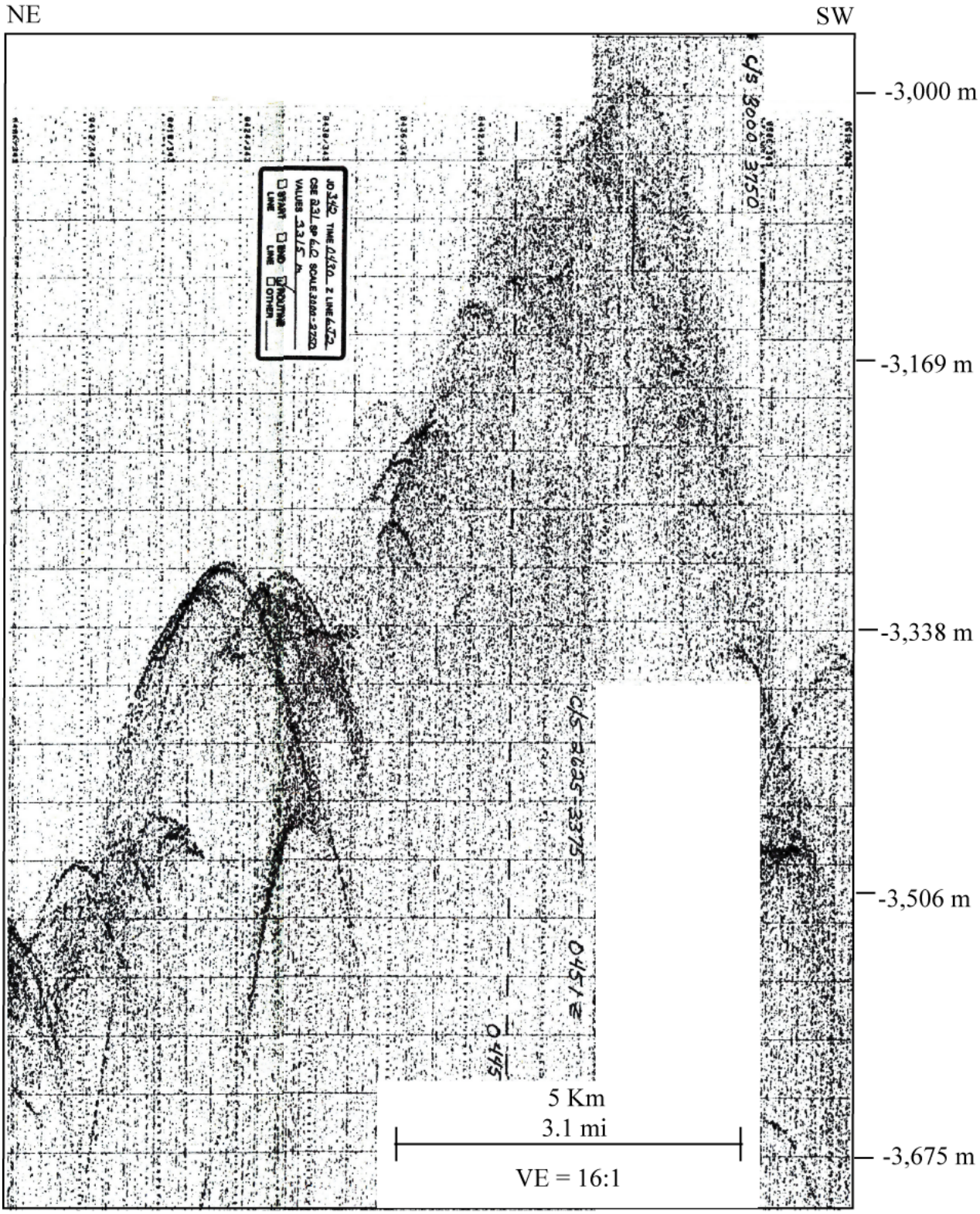

Figure 22. Little Joe Seamount 3.5 kHz bathymetry line LJ2; VE, vertical exaggeration.

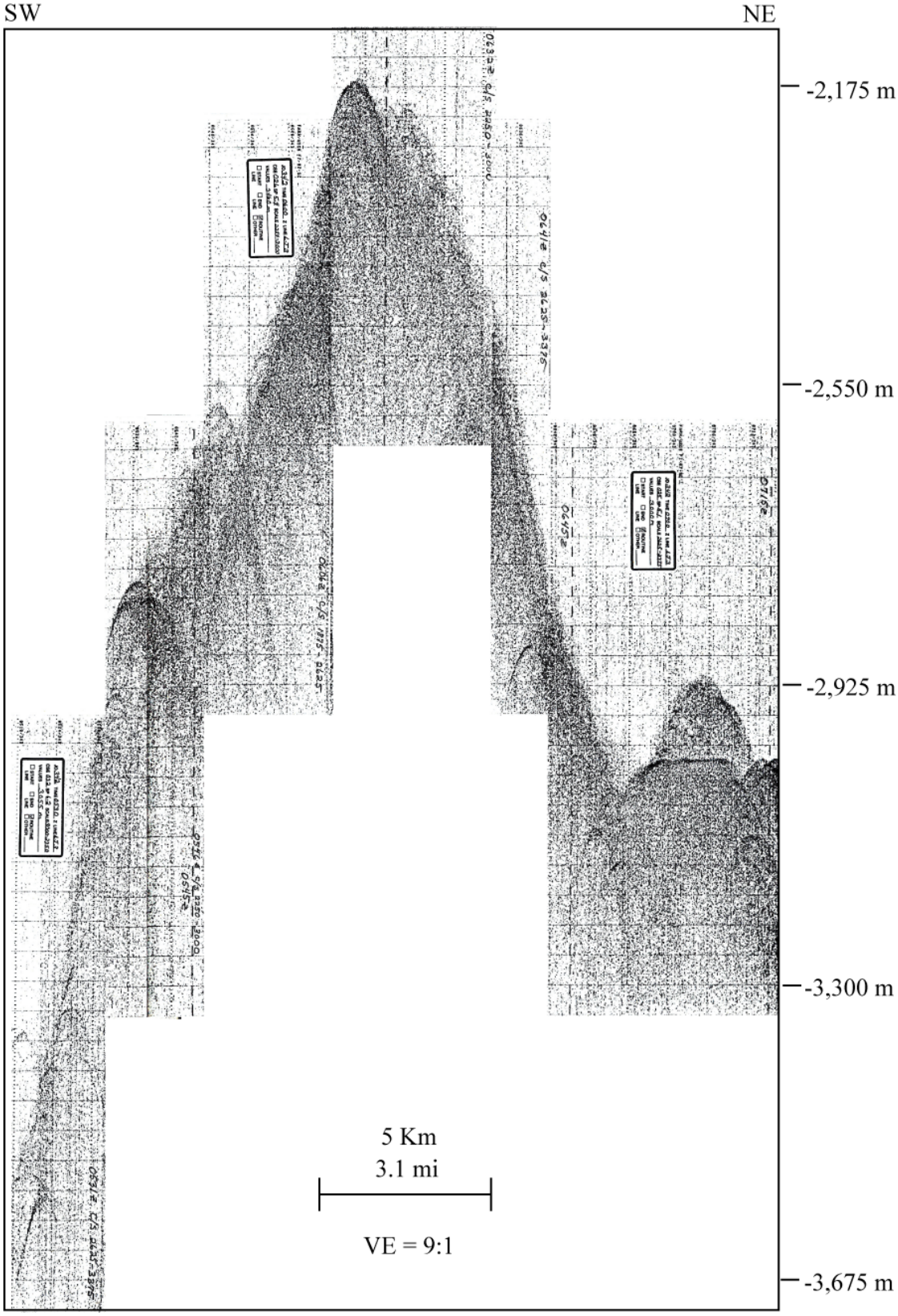

Figure 23. Little Joe Seamount 3.5 kHz bathymetry line LJ3; VE, vertical exaggeration.

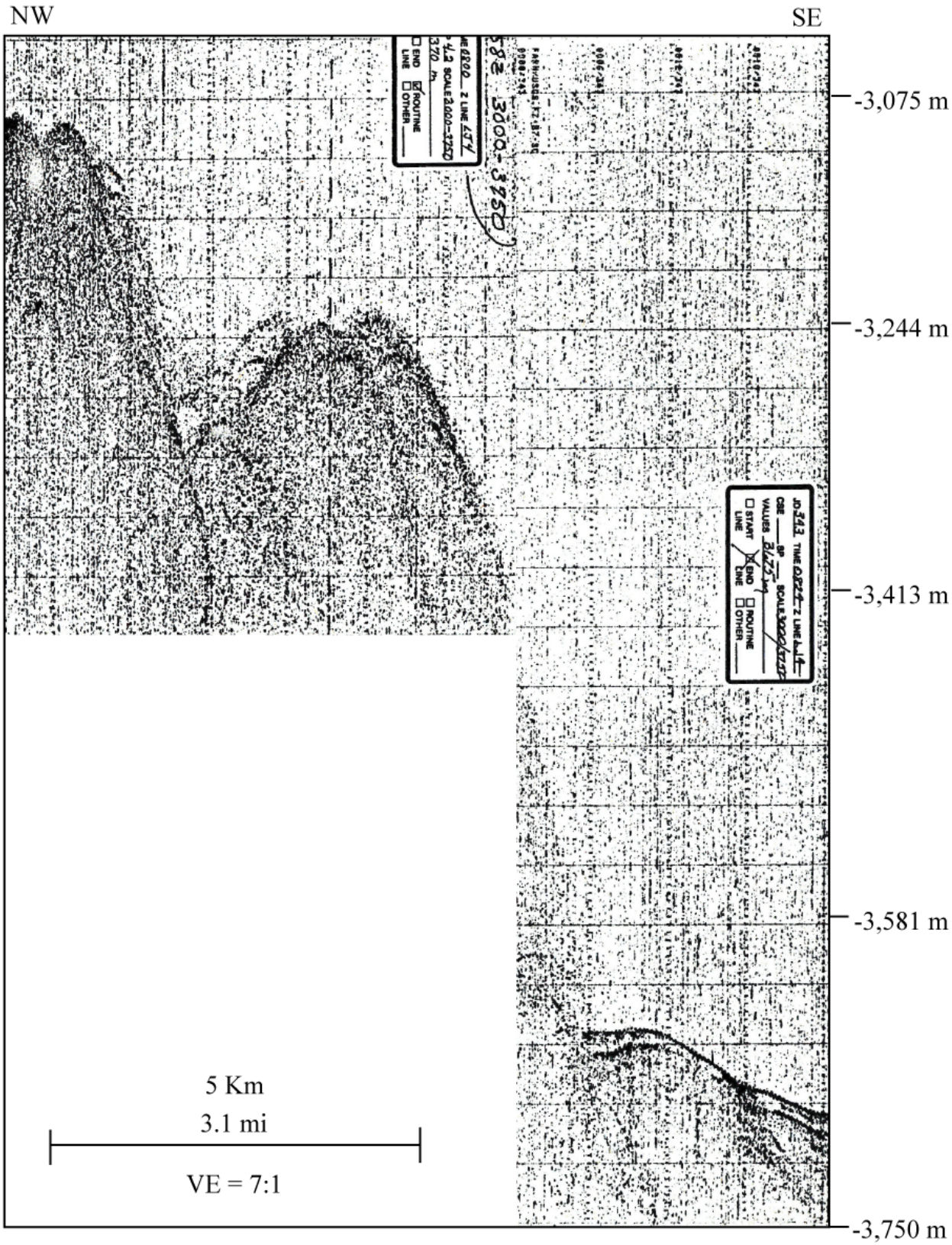

Figure 24. Little Joe Seamount 3.5 kHz bathymetry line LJ4; VE, vertical exaggeration.

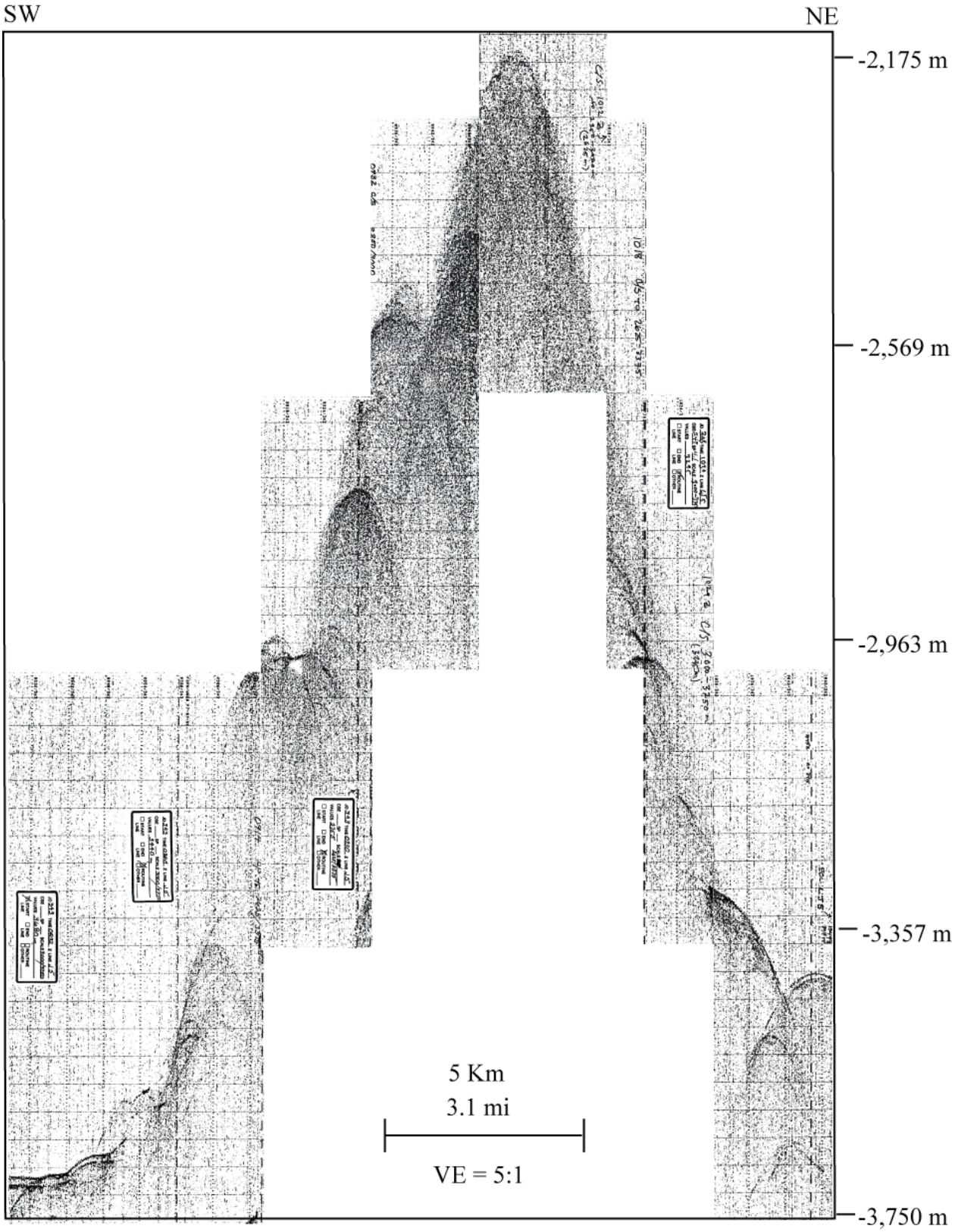

Figure 25. Little Joe Seamount 3.5 kHz bathymetry line LJ5; VE, vertical exaggeration.

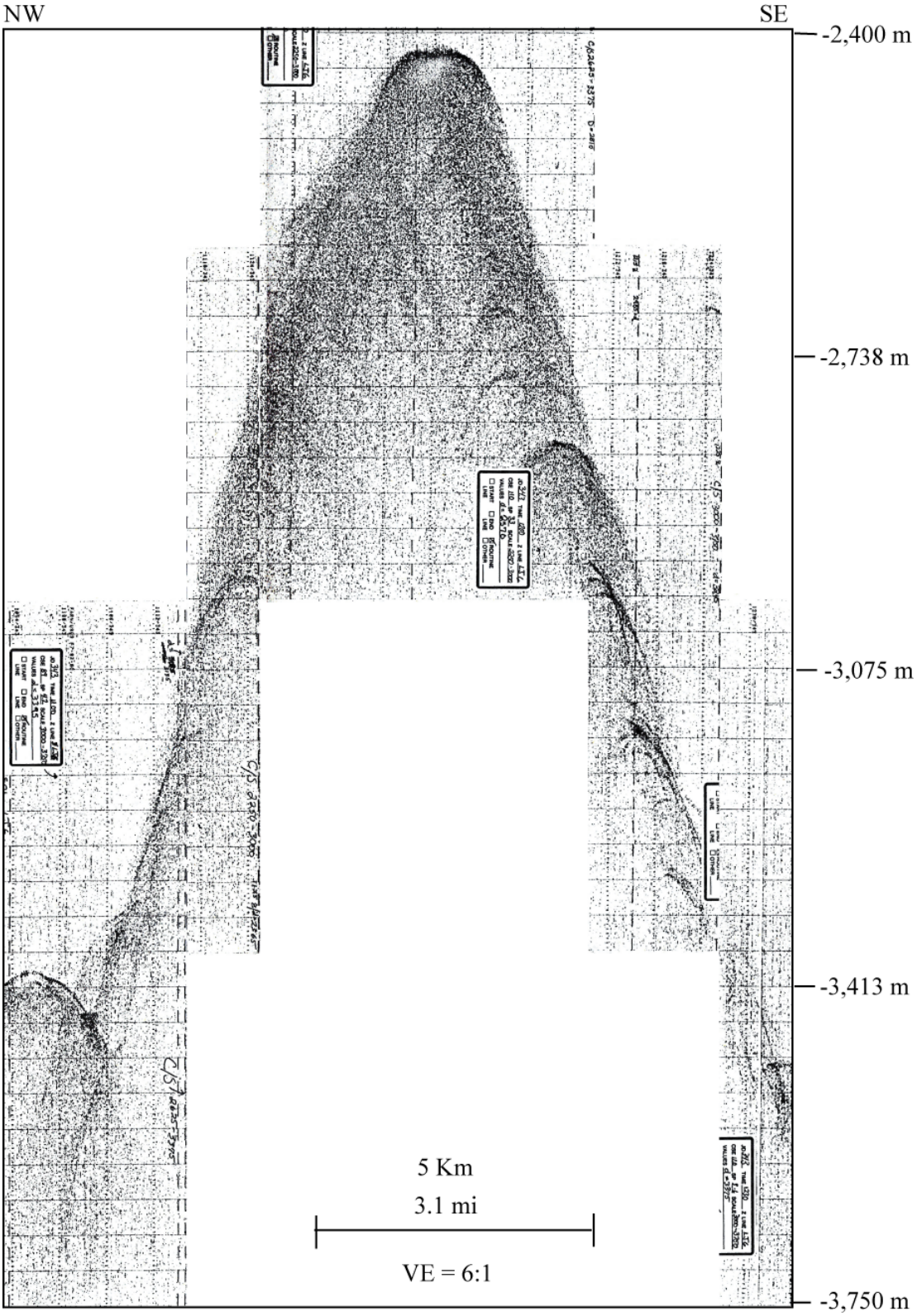

Figure 26. Little Joe Seamount 3.5 kHz bathymetry line LJ6; VE, vertical exaggeration.

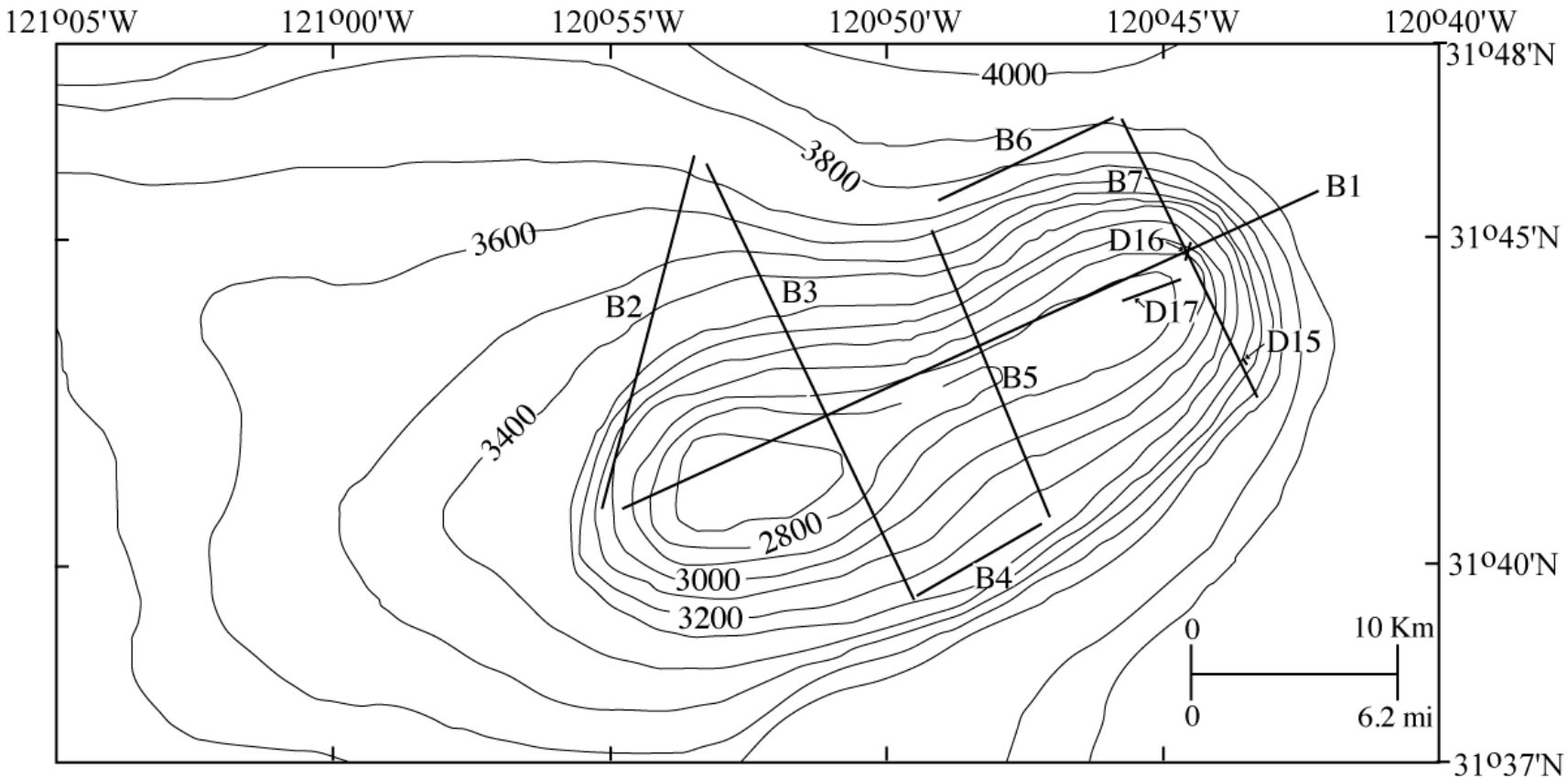

Figure 27. Map showing Ben Seamount bathymetry, D, dredge; and B, geophysical line locations; contour interval is 100 m.

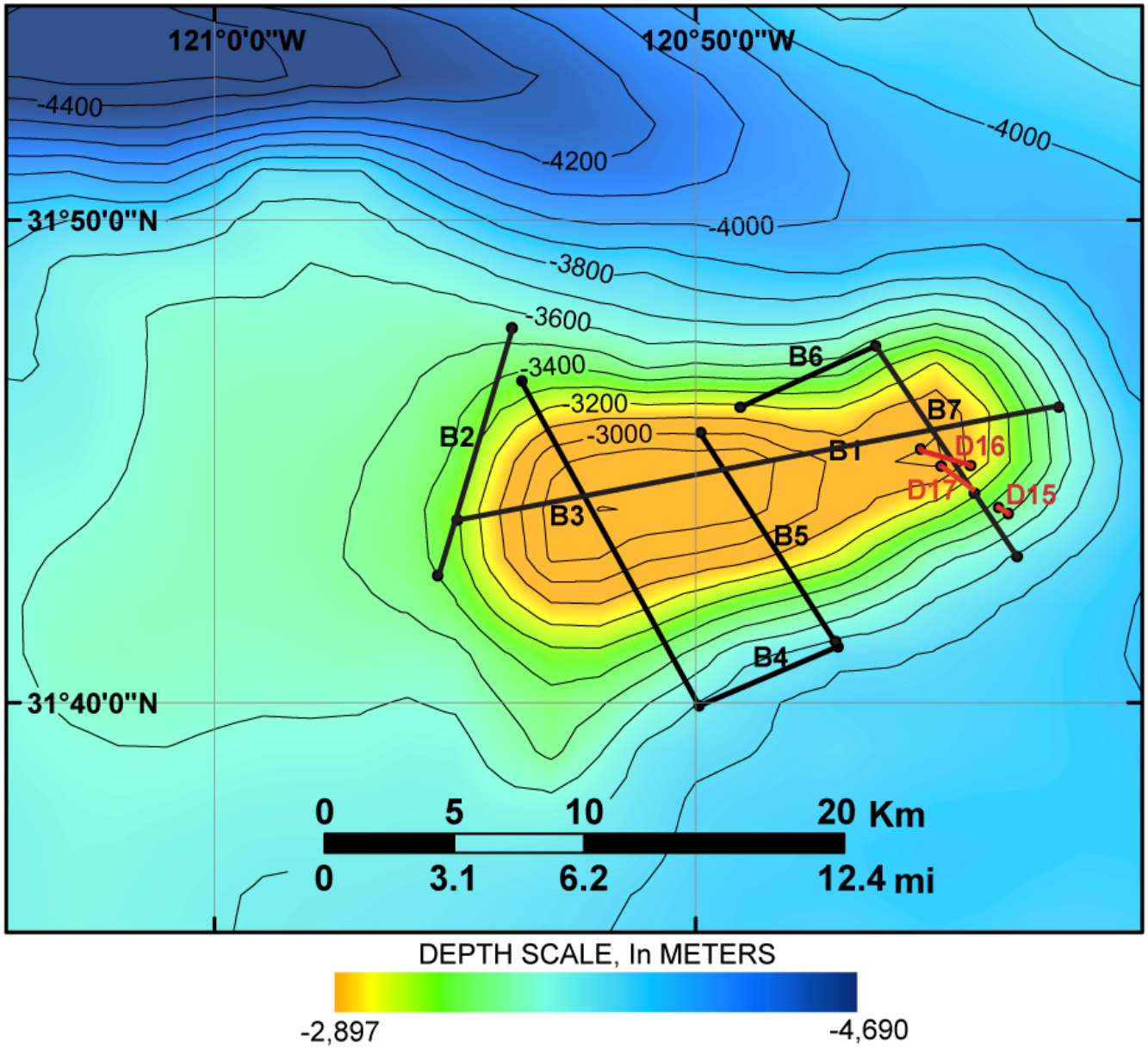

Figure 28. Map showing Ben Seamount bathymetry, D, dredges in red; and B, geophysical lines in black; contour interval is 100 m.

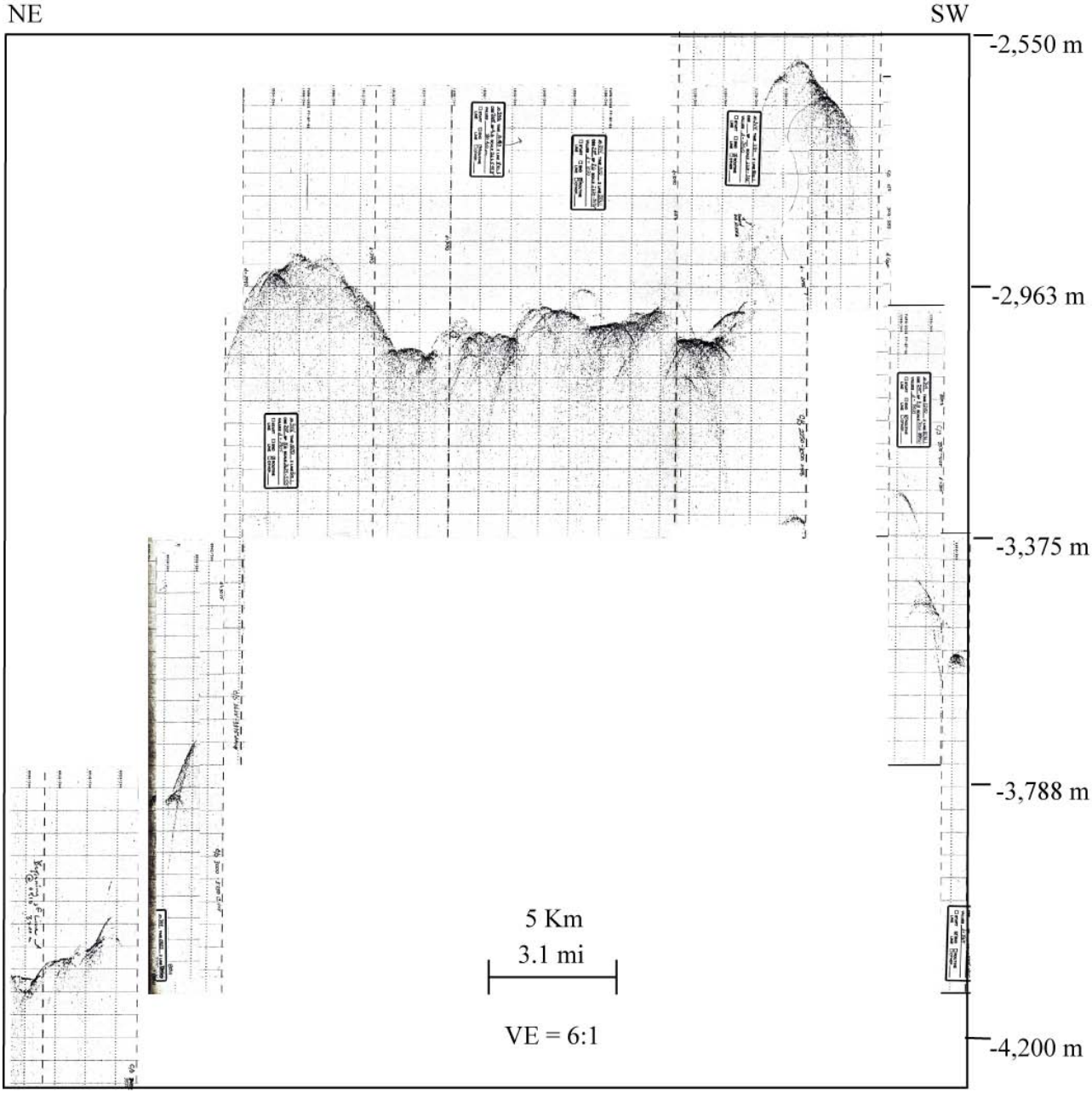

Figure 29. Ben Seamount 3.5 kHz bathymetry line B1; VE, vertical exaggeration.

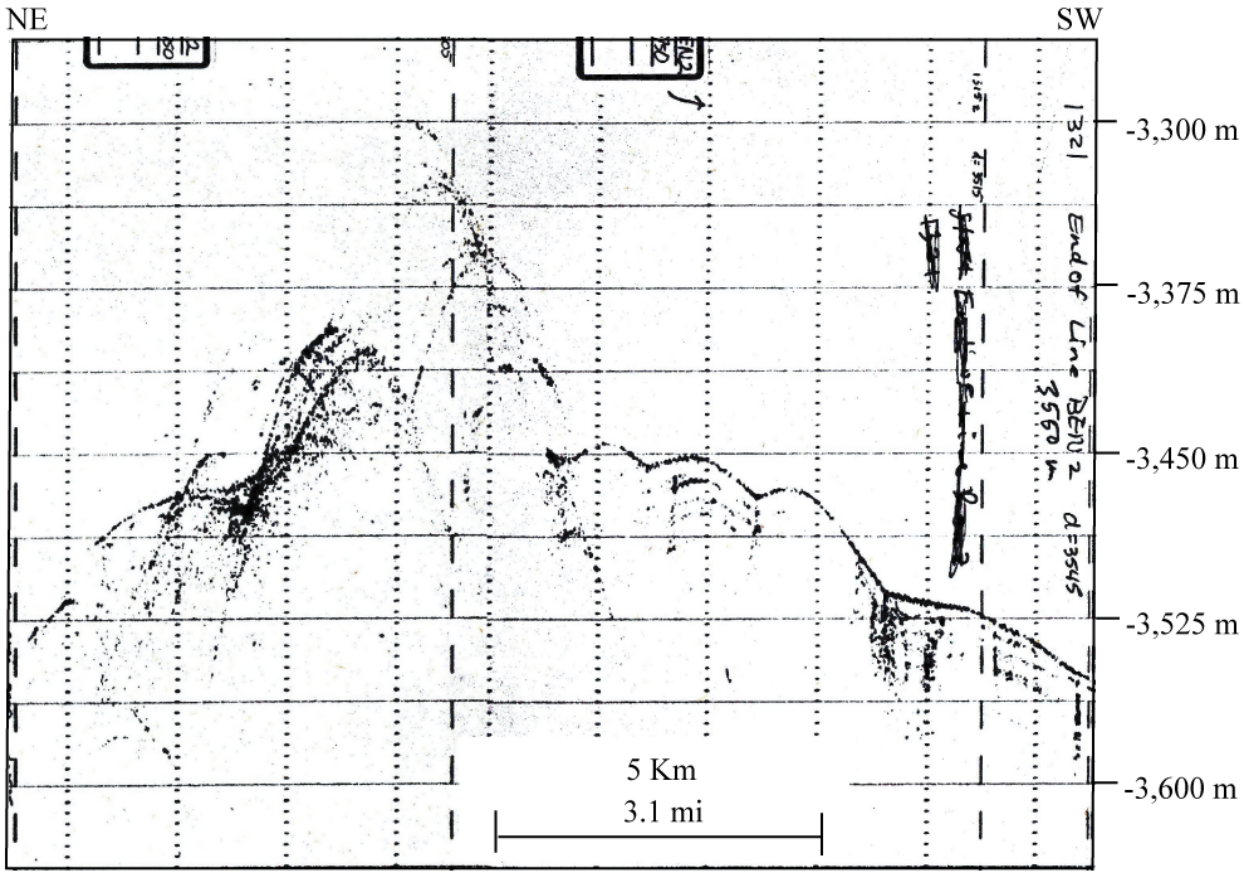

Figure 30. Ben Seamount 3.5 kHz bathymetry line B2.

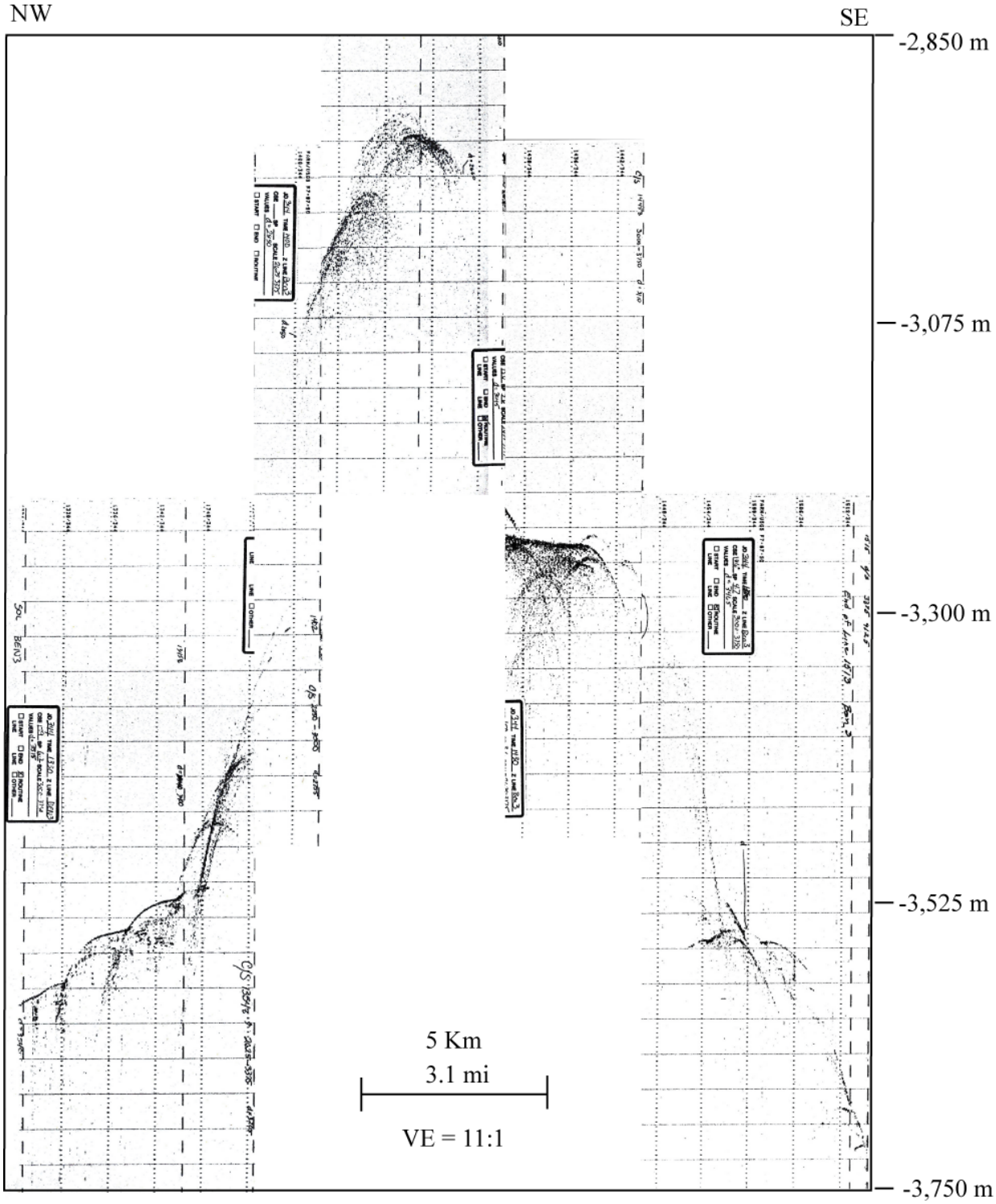

Figure 31. Ben Seamount 3.5 kHz bathymetry line B3; VE, vertical exaggeration.

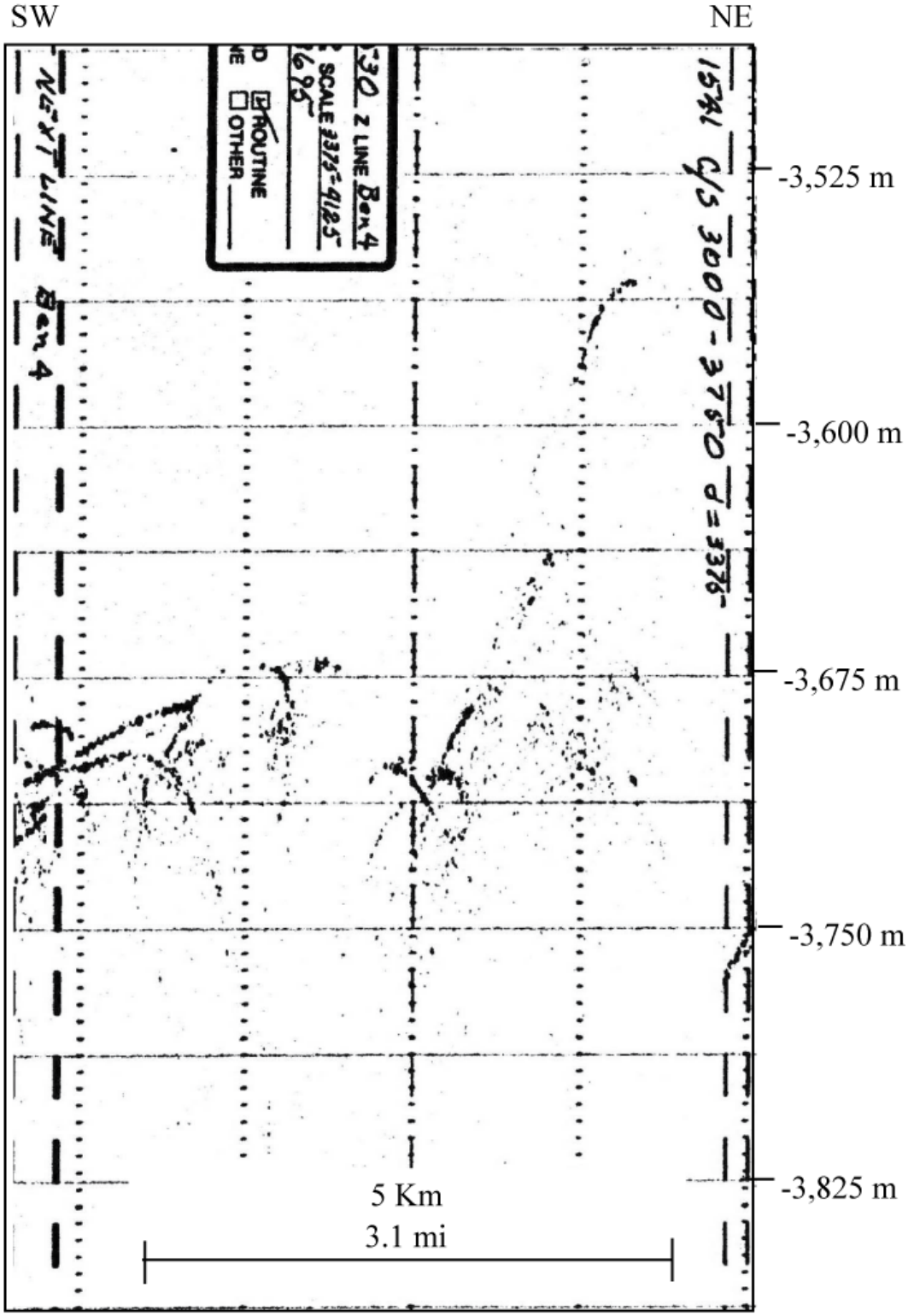

Figure 32. Ben Seamount 3.5 kHz bathymetry line B4.

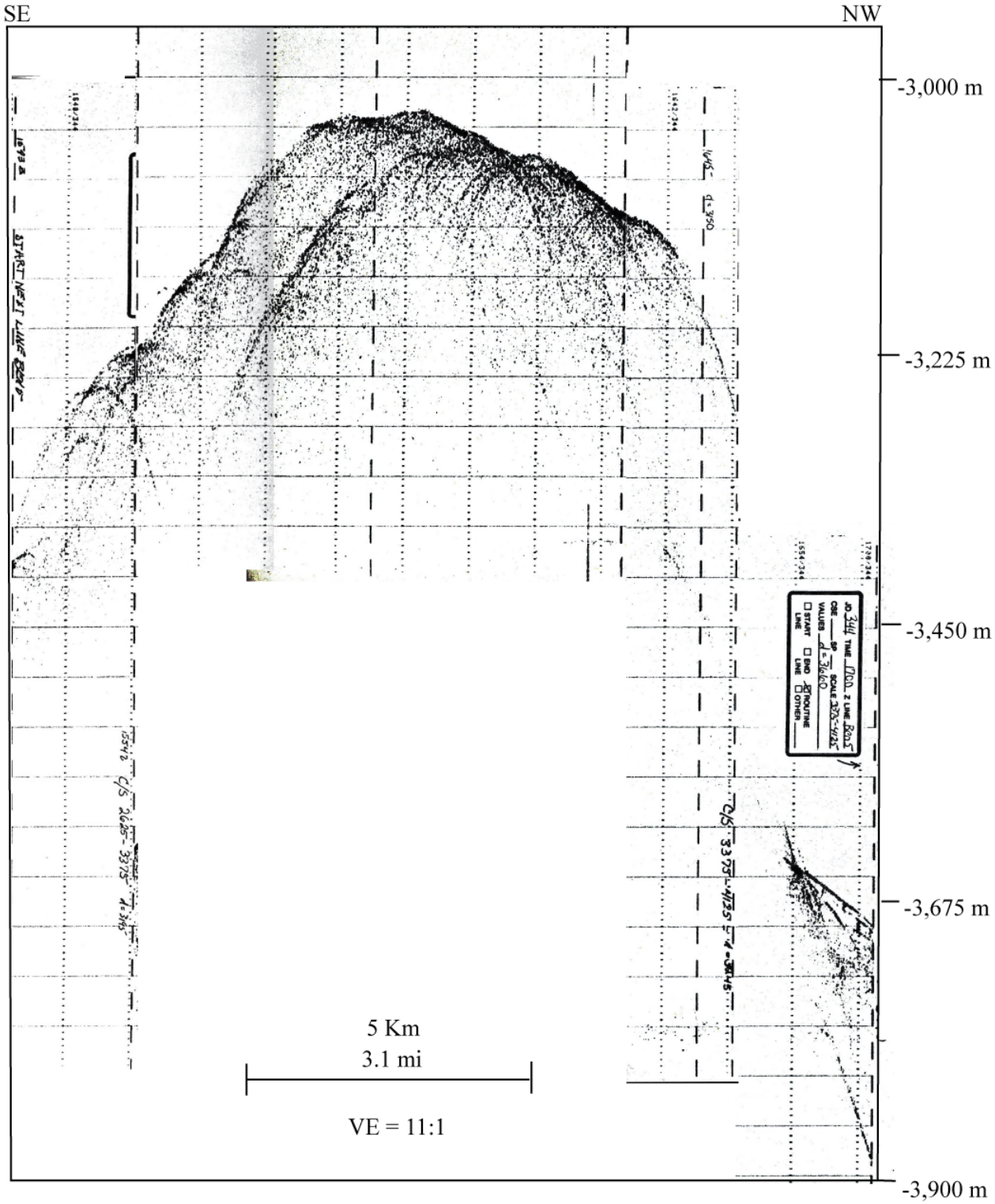

Figure 33. Ben Seamount 3.5 kHz bathymetry line B5; VE, vertical exaggeration.

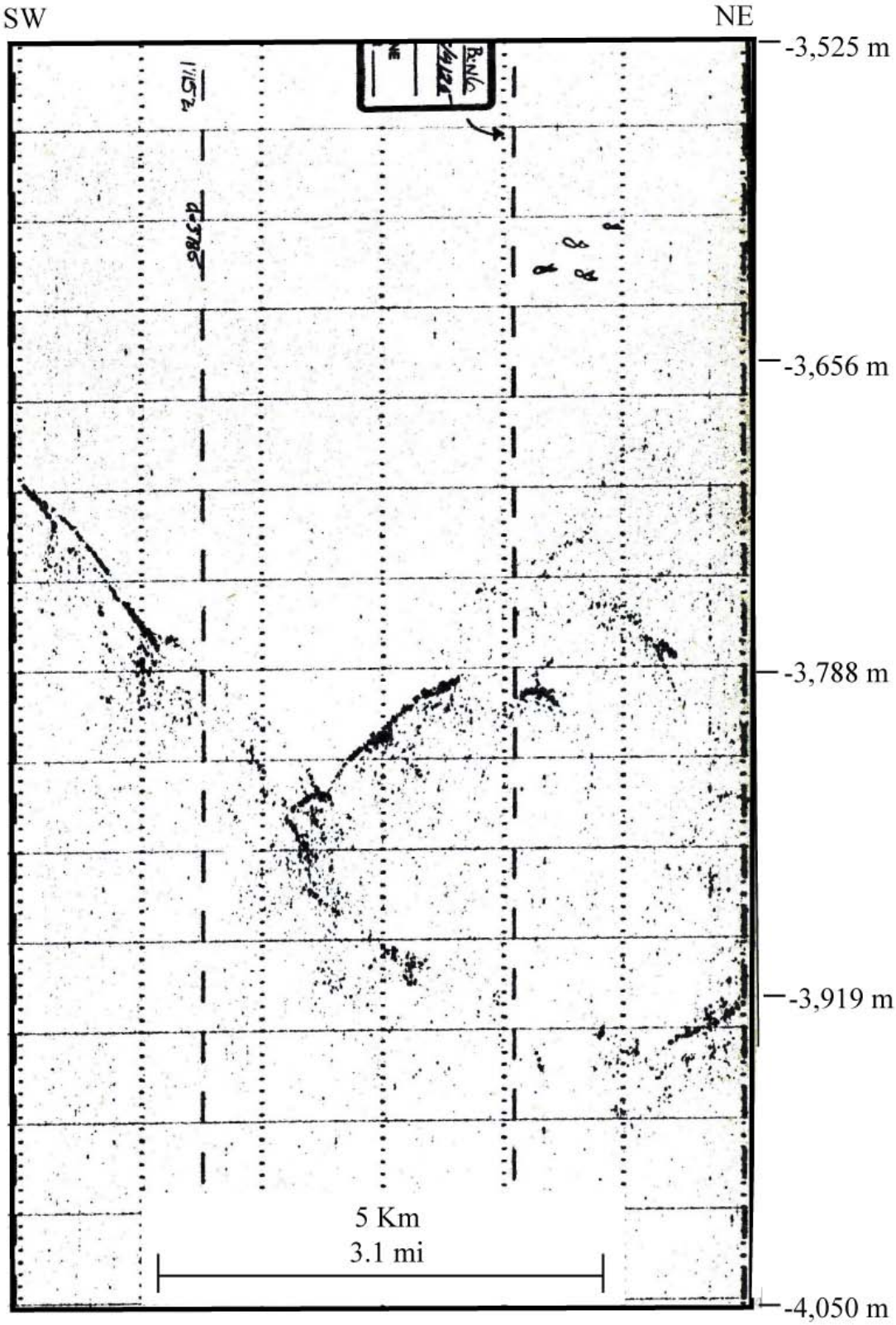

Figure 34. Ben Seamount 3.5 kHz bathymetry line B6.

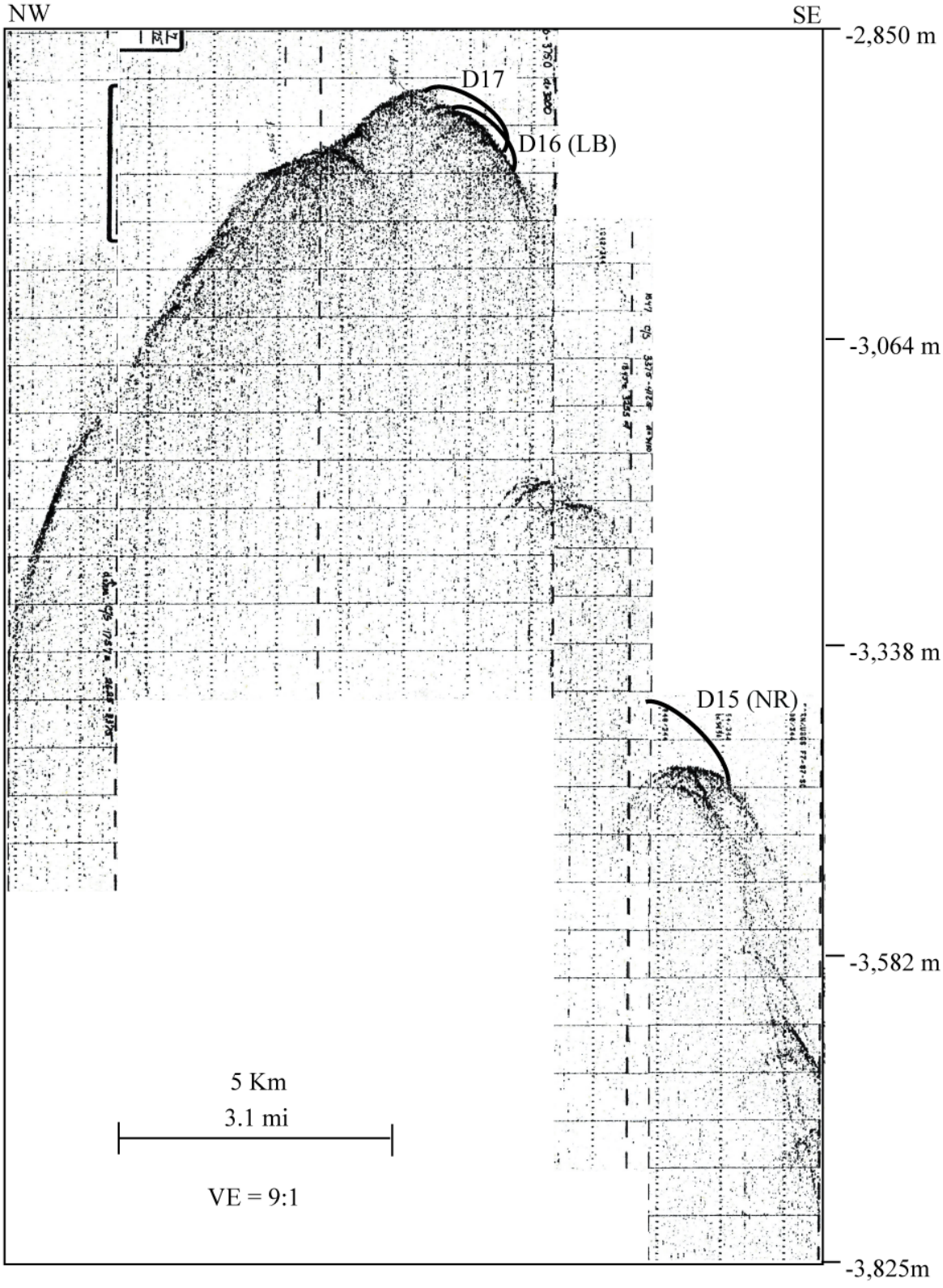

Figure 35. Ben Seamount 3.5 kHz bathymetry line B7 with D, dredges 15-17; NR, No Recovery; LB, Lost Bag; VE, vertical exaggeration.

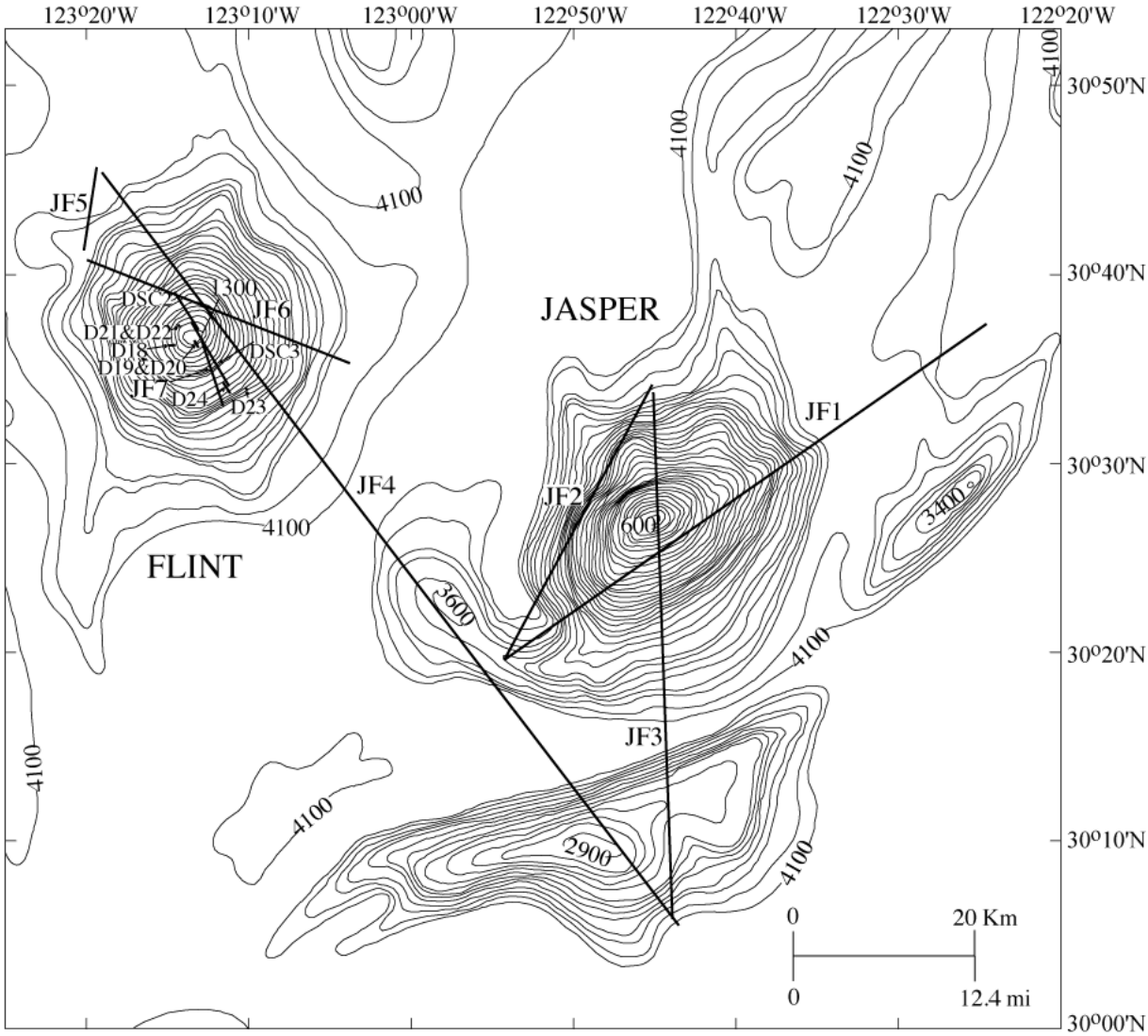

Figure 36. Map showing Jasper and Flint Seamounts bathymetry. D, dredge; DSC, deep-sea camera; and JF, geophysical line locations; contour interval is 100 m; see Figure 37 for close-up of Flint Seamount.

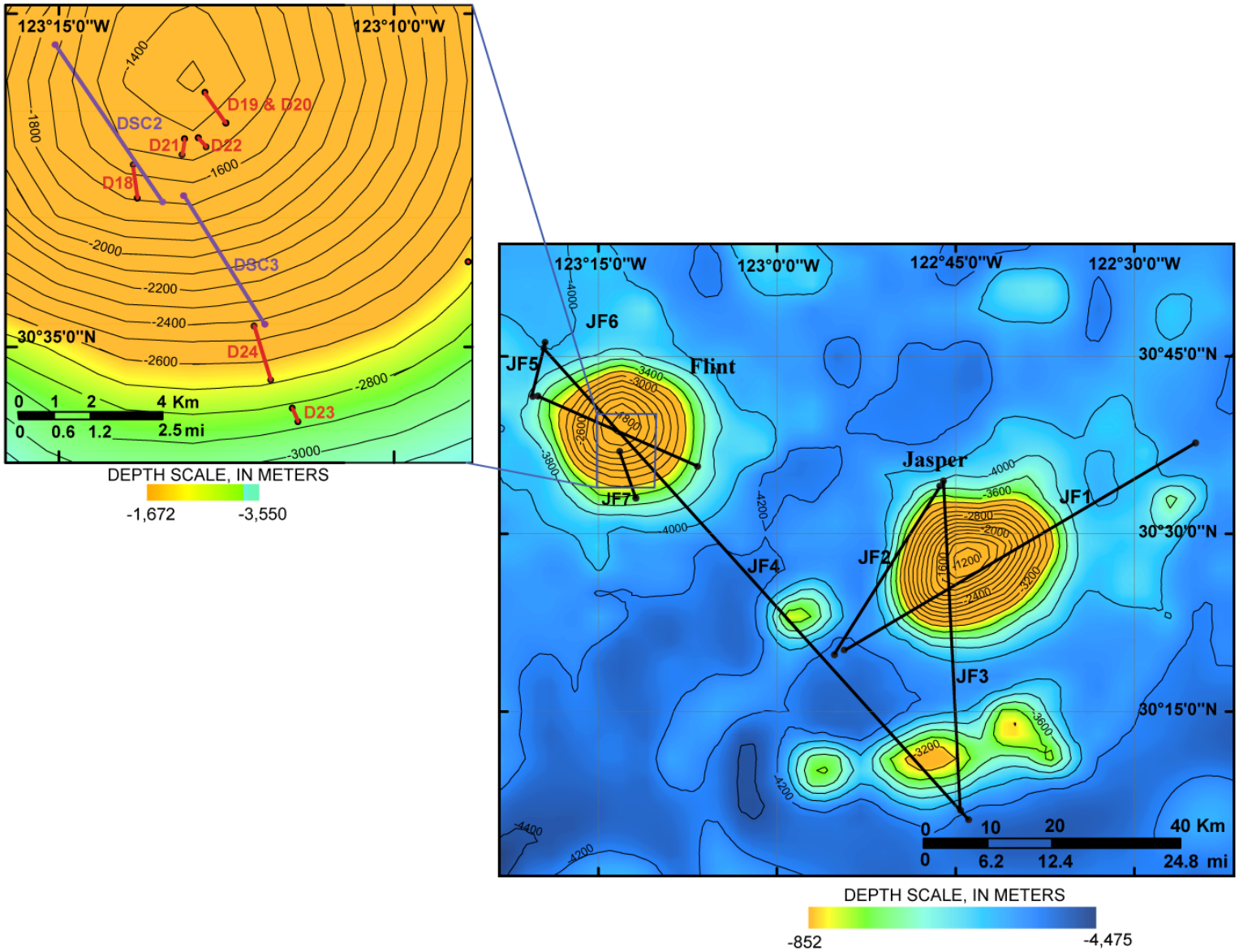

Figure 37. Maps showing Jasper and Flint Seamounts bathymetry. D, dredges in red; DSC, deep-sea camera in purple; and JF, geophysical line locations in black; contour interval is 200 m for the seamount map and 100 m for the close-up of Flint Seamount.

Figure 38. Jasper Seamount 3.5 kHz bathymetry line JF1; VE, vertical exaggeration.

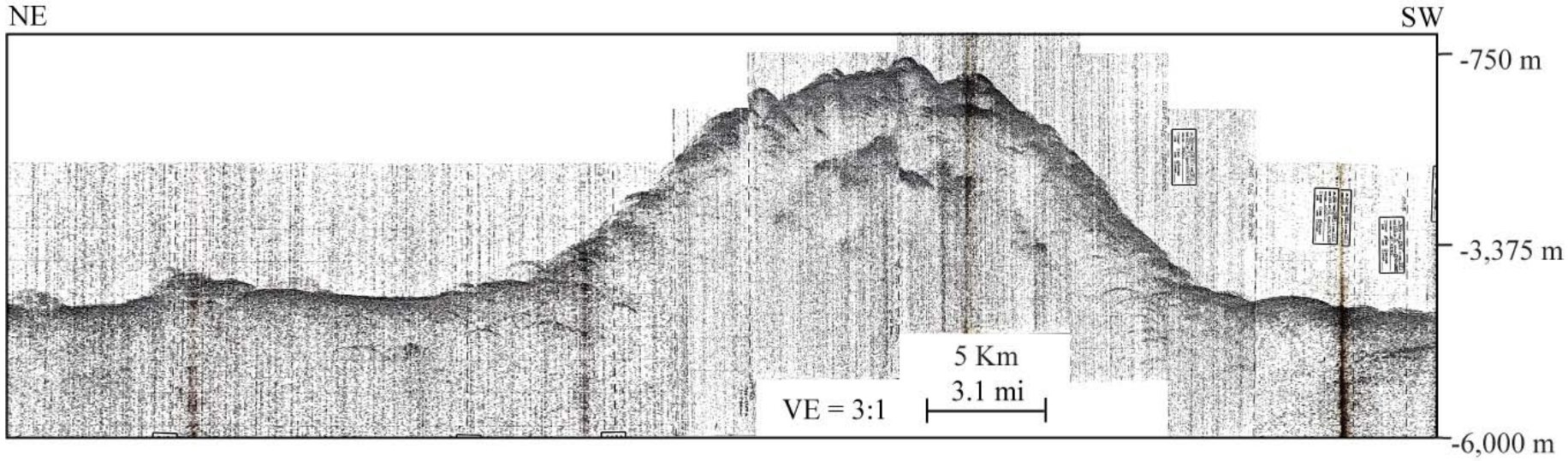

Figure 39. Jasper Seamount single-channel water-gun line JF1; VE, vertical exaggeration.

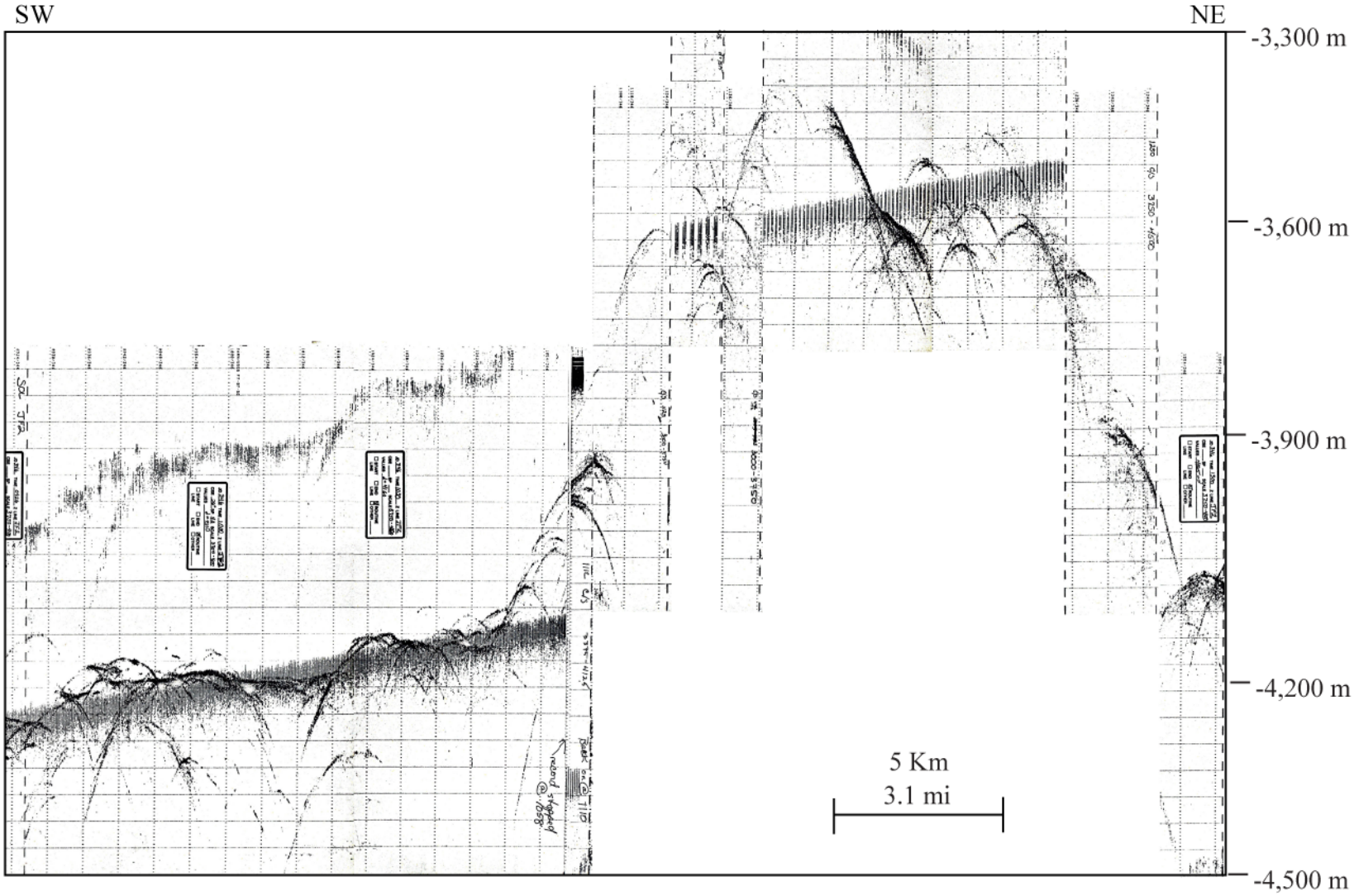

Figure 40. Jasper Seamount 3.5 kHz bathymetry line JF2.

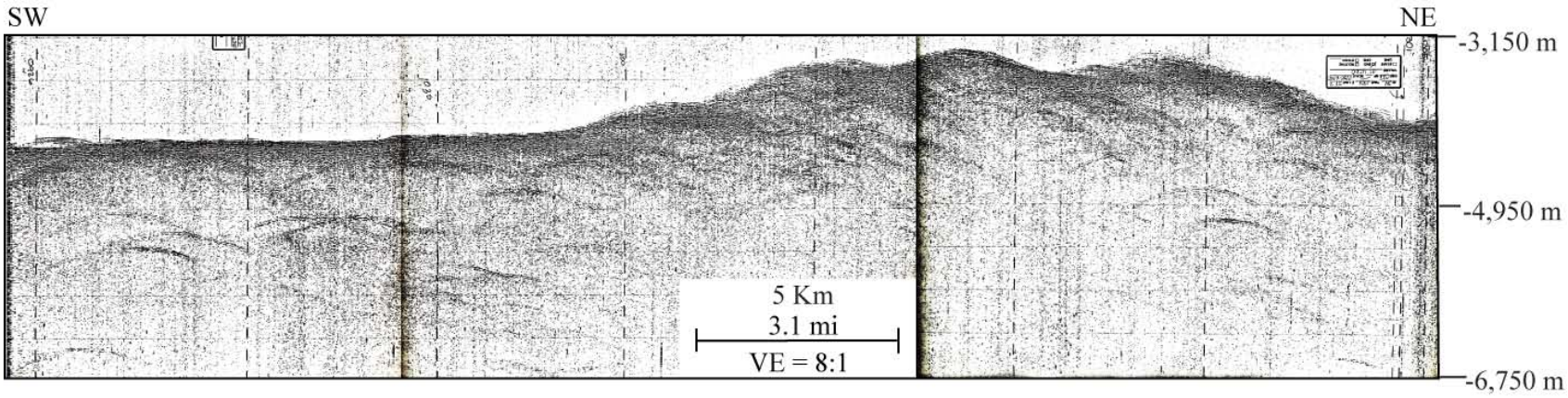

Figure 41. Jasper Seamount single-channel water-gun line JF2; VE, vertical exaggeration.

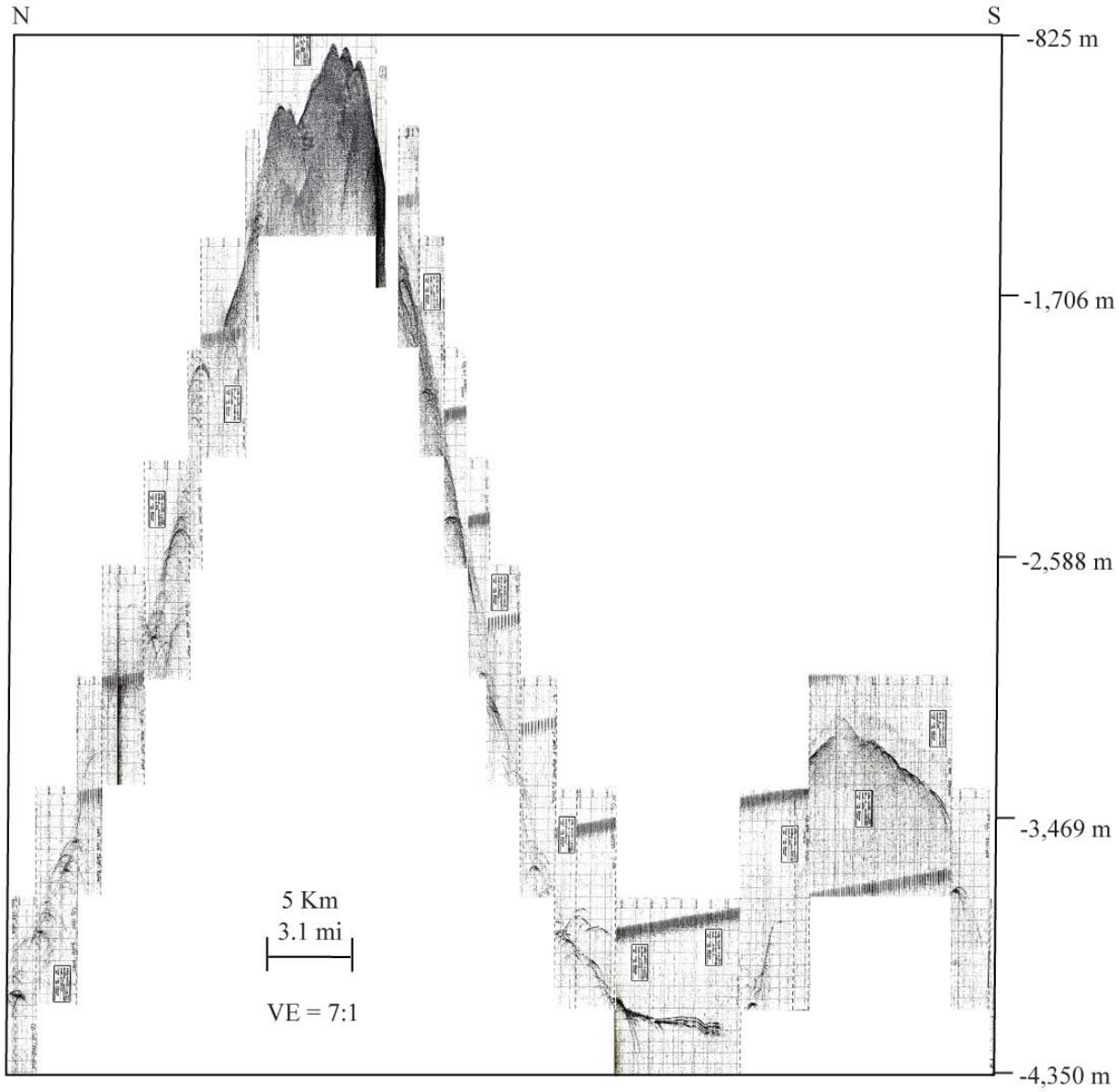

Figure 42. Jasper Seamount 3.5 kHz bathymetry line JF3; VE, vertical exaggeration.

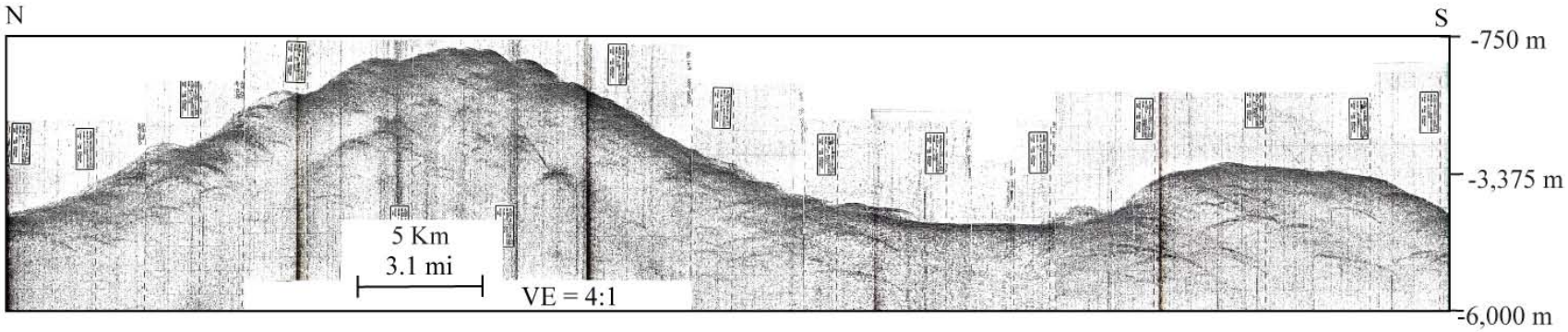

Figure 43. Jasper Seamount single-channel water-gun line JF3; VE, vertical exaggeration.

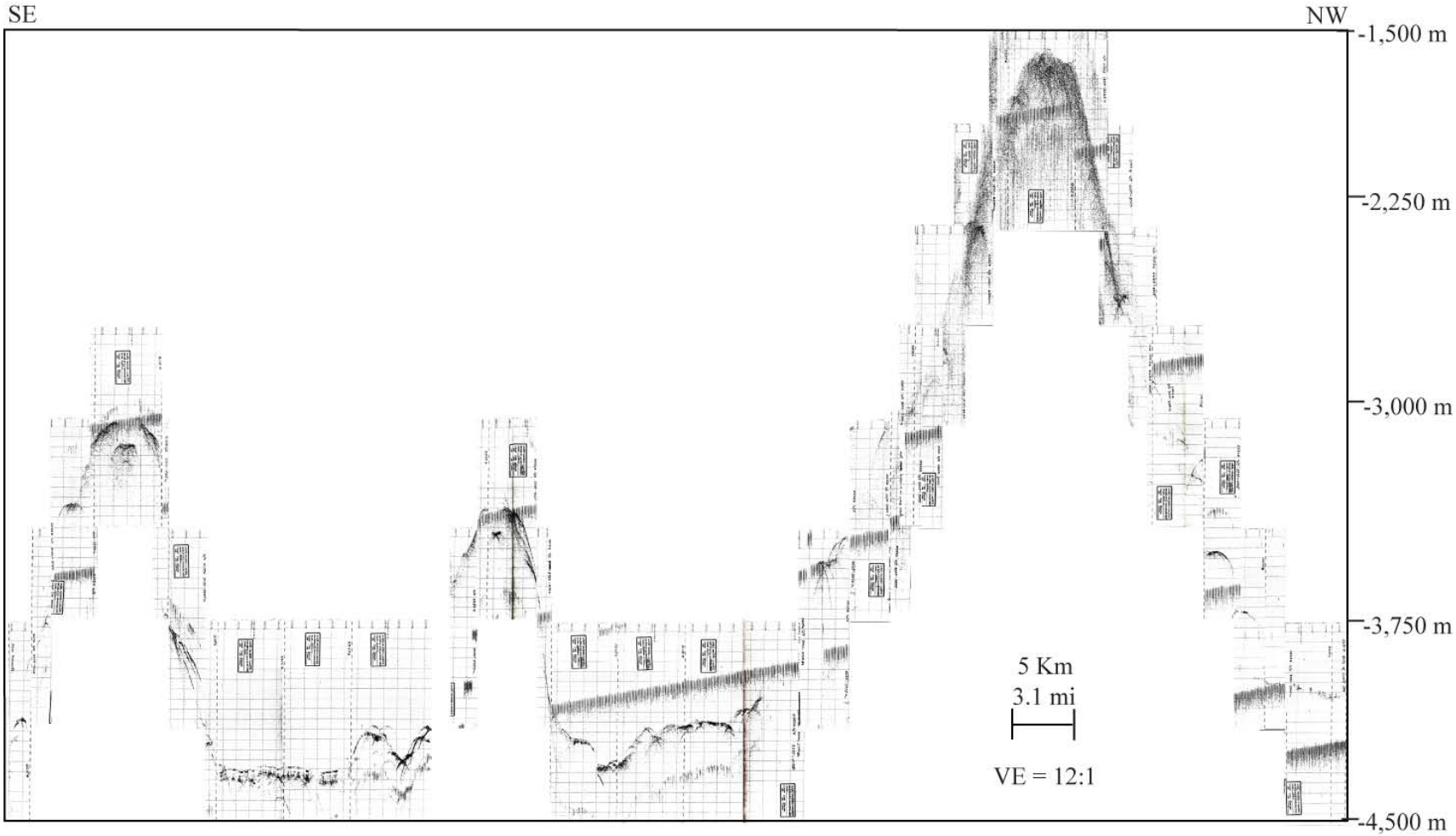

Figure 44. Jasper and Flint Seamounts 3.5 kHz bathymetry line JF4; VE, vertical exaggeration.

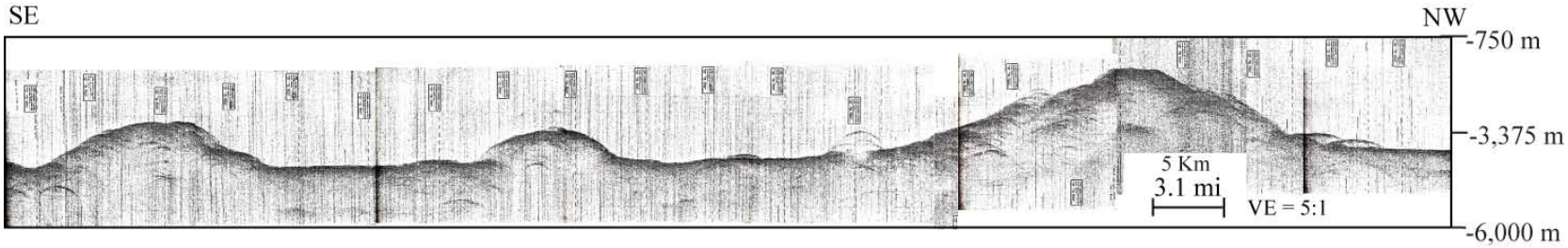

Figure 45. Jasper and Flint Seamounts single-channel water-gun line JF4; VE, vertical exaggeration.

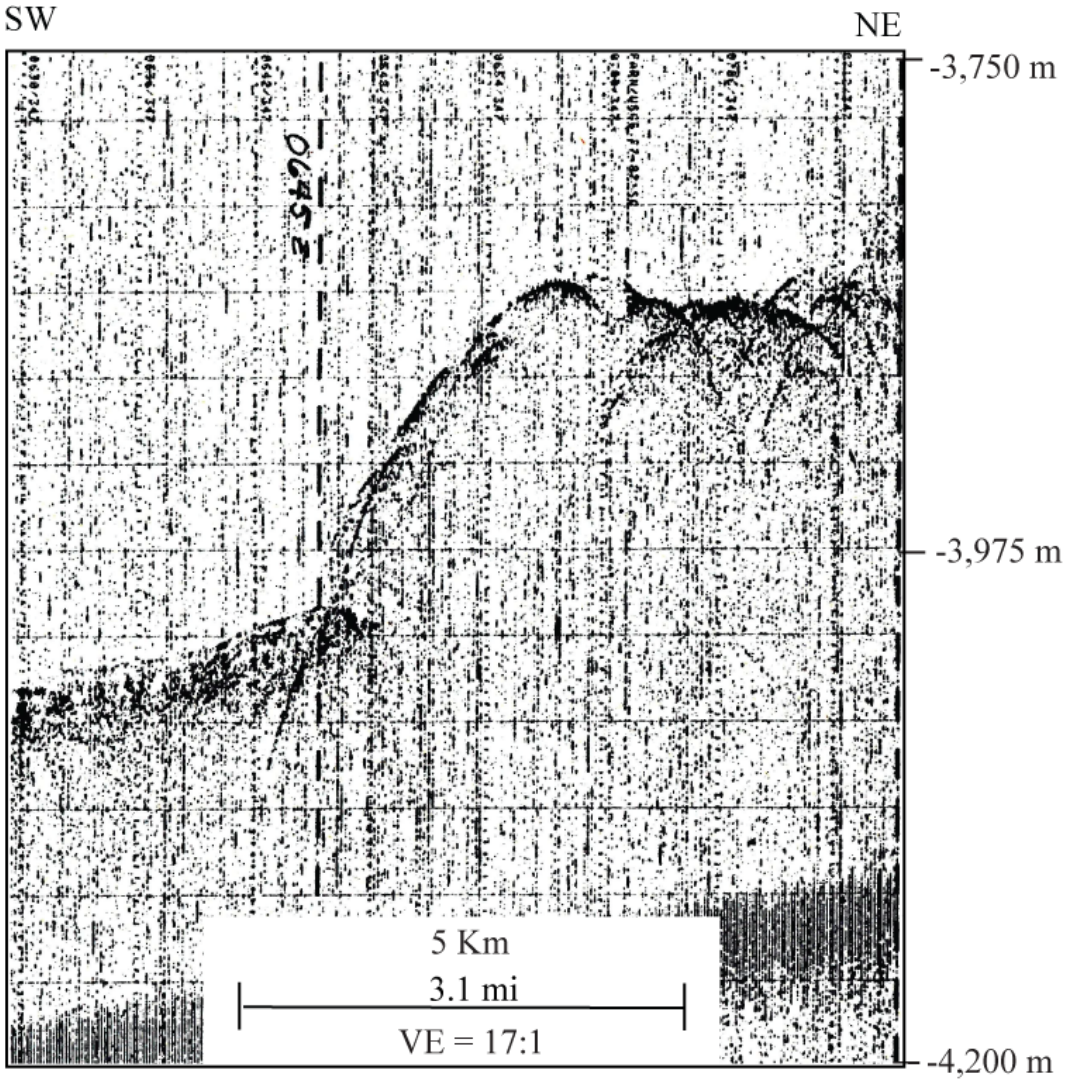

Figure 46. Flint Seamount 3.5 kHz bathymetry line JF5; VE, vertical exaggeration.

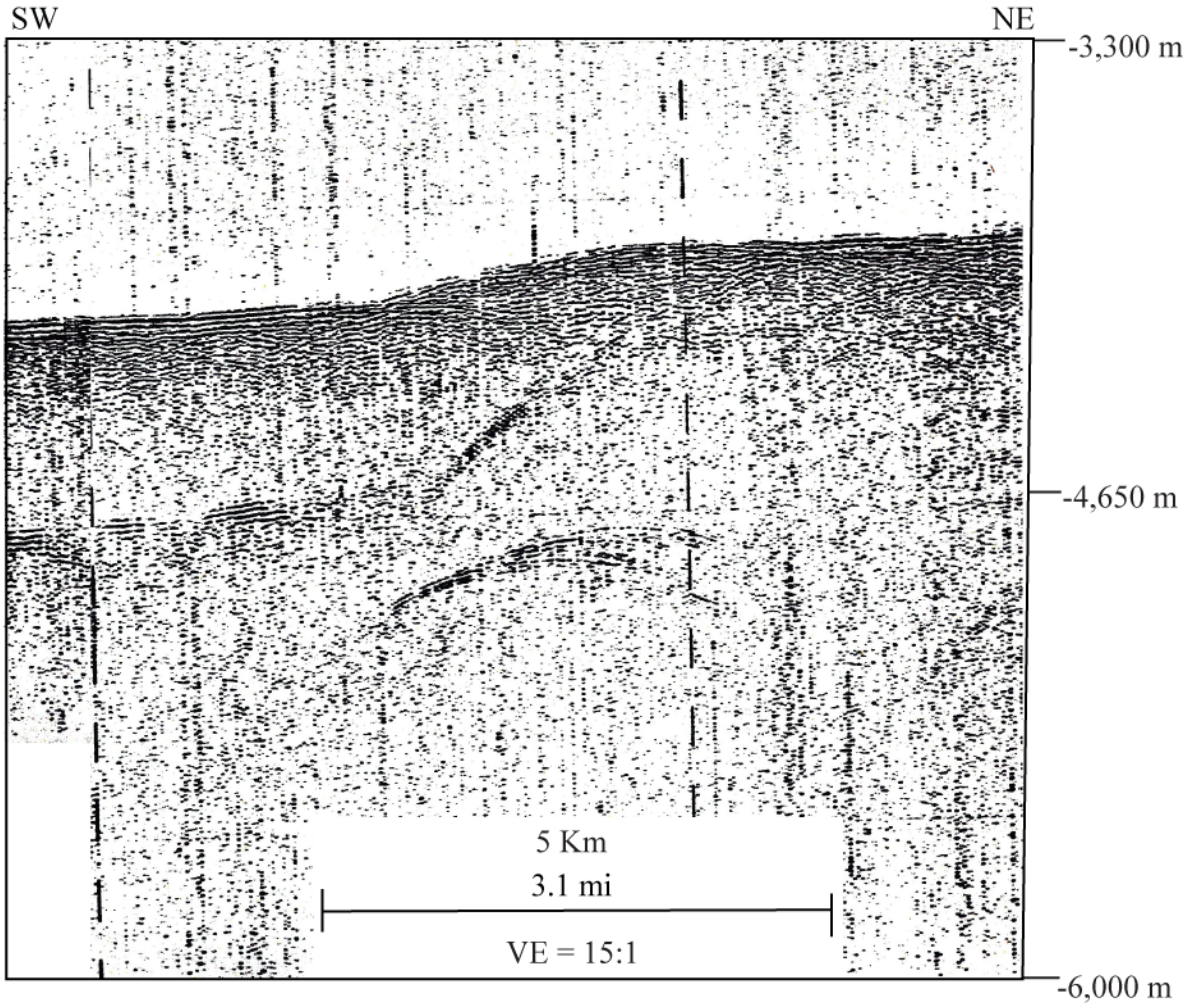

Figure 47. Flint Seamount single-channel water-gun line JF5; VE, vertical exaggeration.

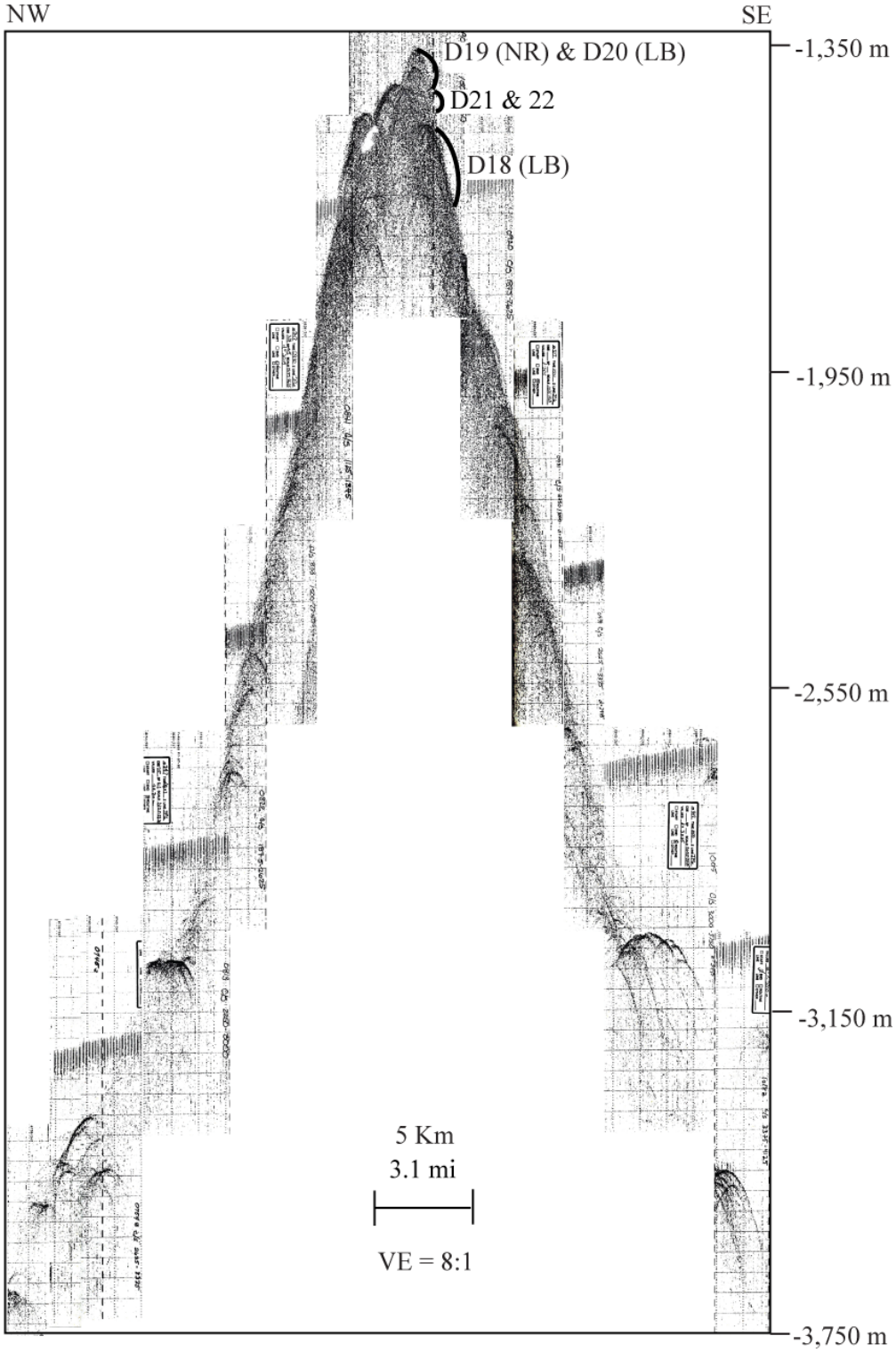

Figure 48. Flint Seamount 3.5 kHz bathymetry line JF6 with D, dredges 18-22; NR, No Recovery, LB, Lost Bag; VE, vertical exaggeration.

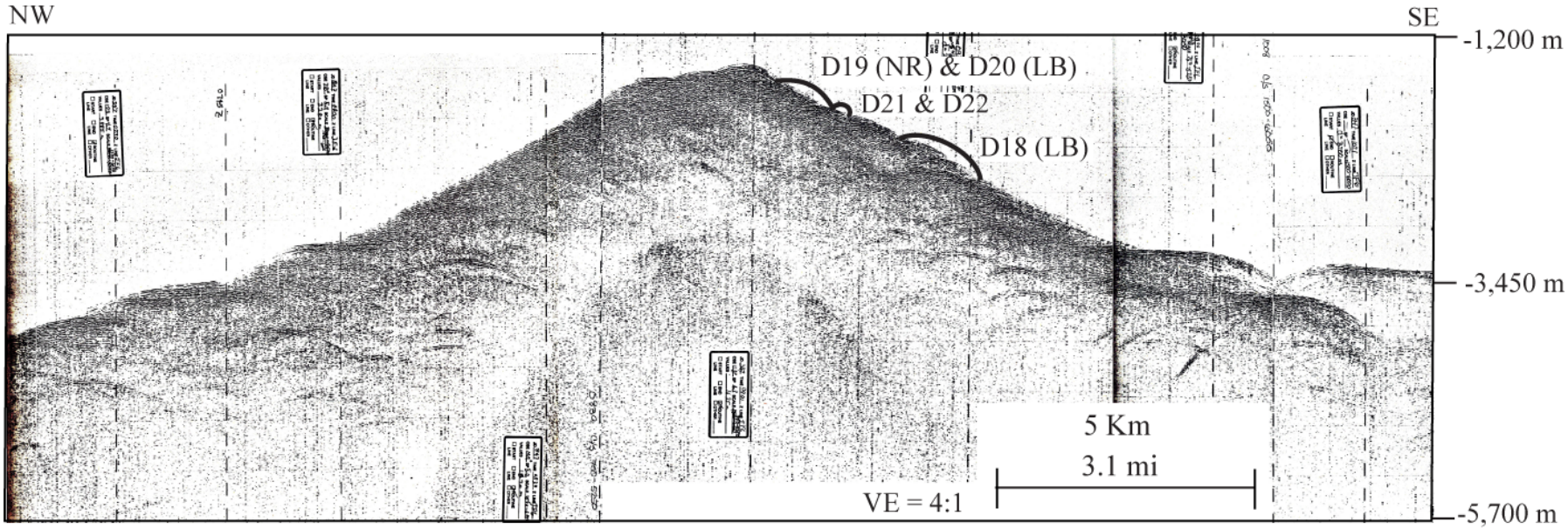

Figure 49. Flint Seamount single-channel water-gun line JF6 with D, dredges 18-22; NR, No Recovery, LB, Lost Bag; VE, vertical exaggeration.

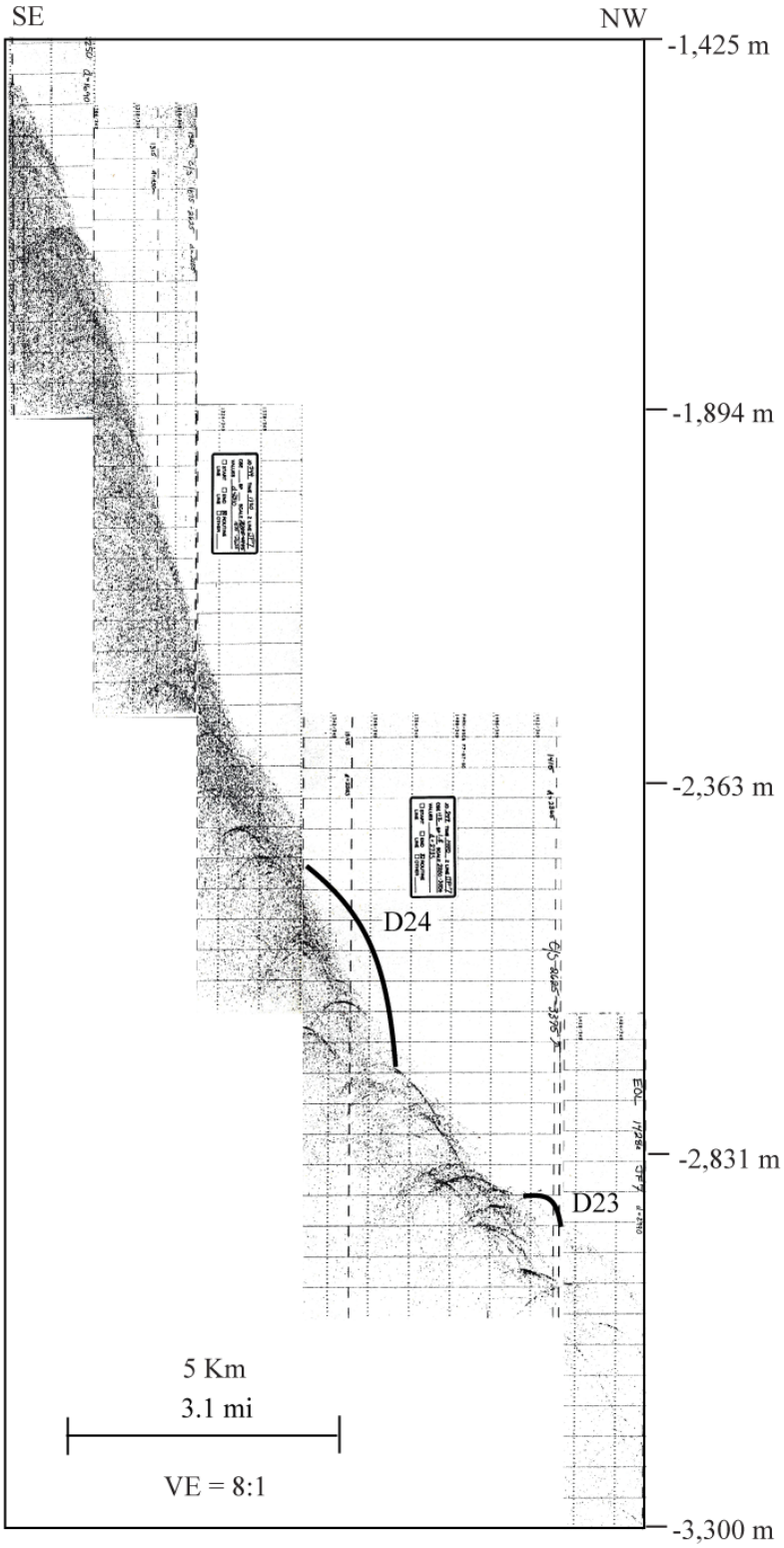

Figure 50. Flint Seamount 3.5 kHz bathymetry line JF7 with D, dredges 23 and 24; VE, vertical exaggeration.

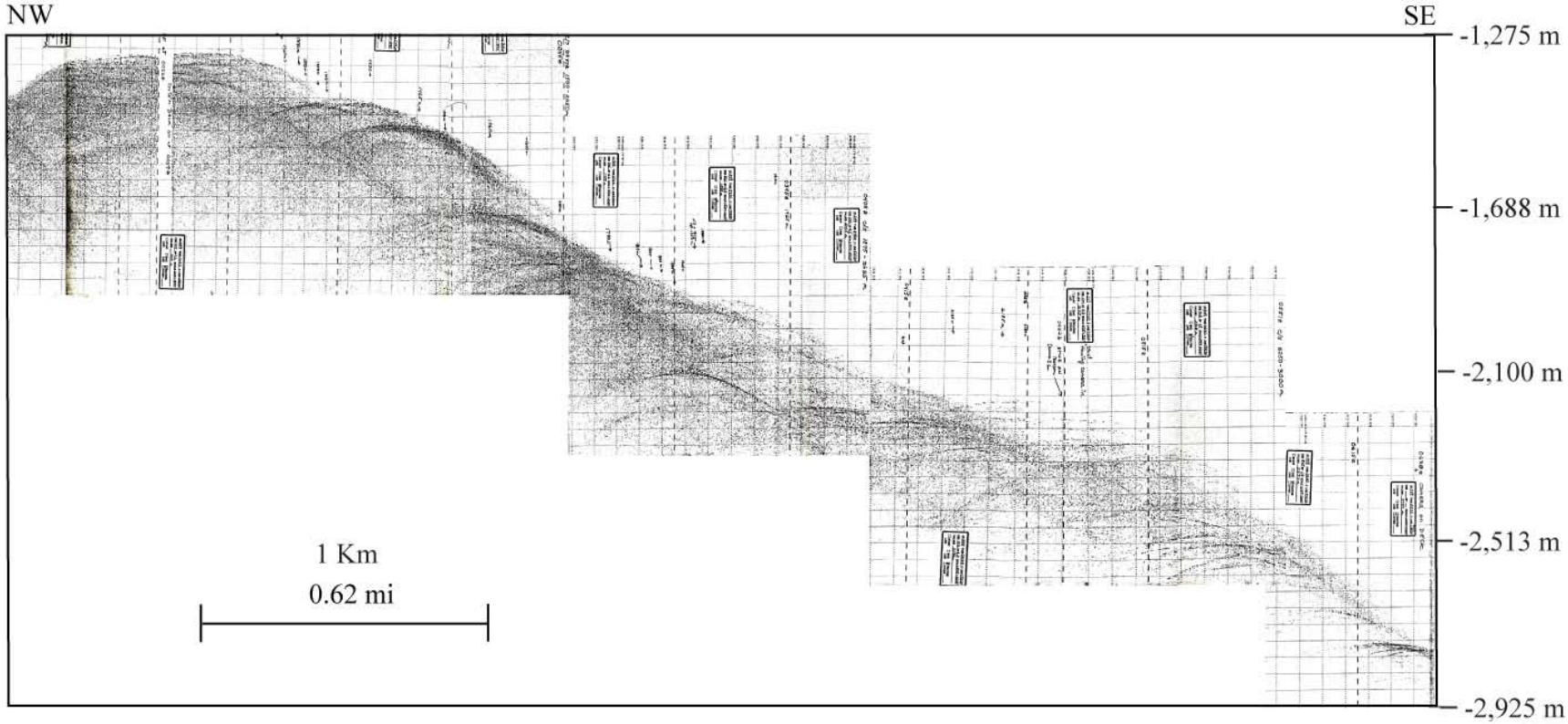

Figure 51. Flint Seamount 3.5 kHz bathymetry DSC2, deep-sea camera line 2.

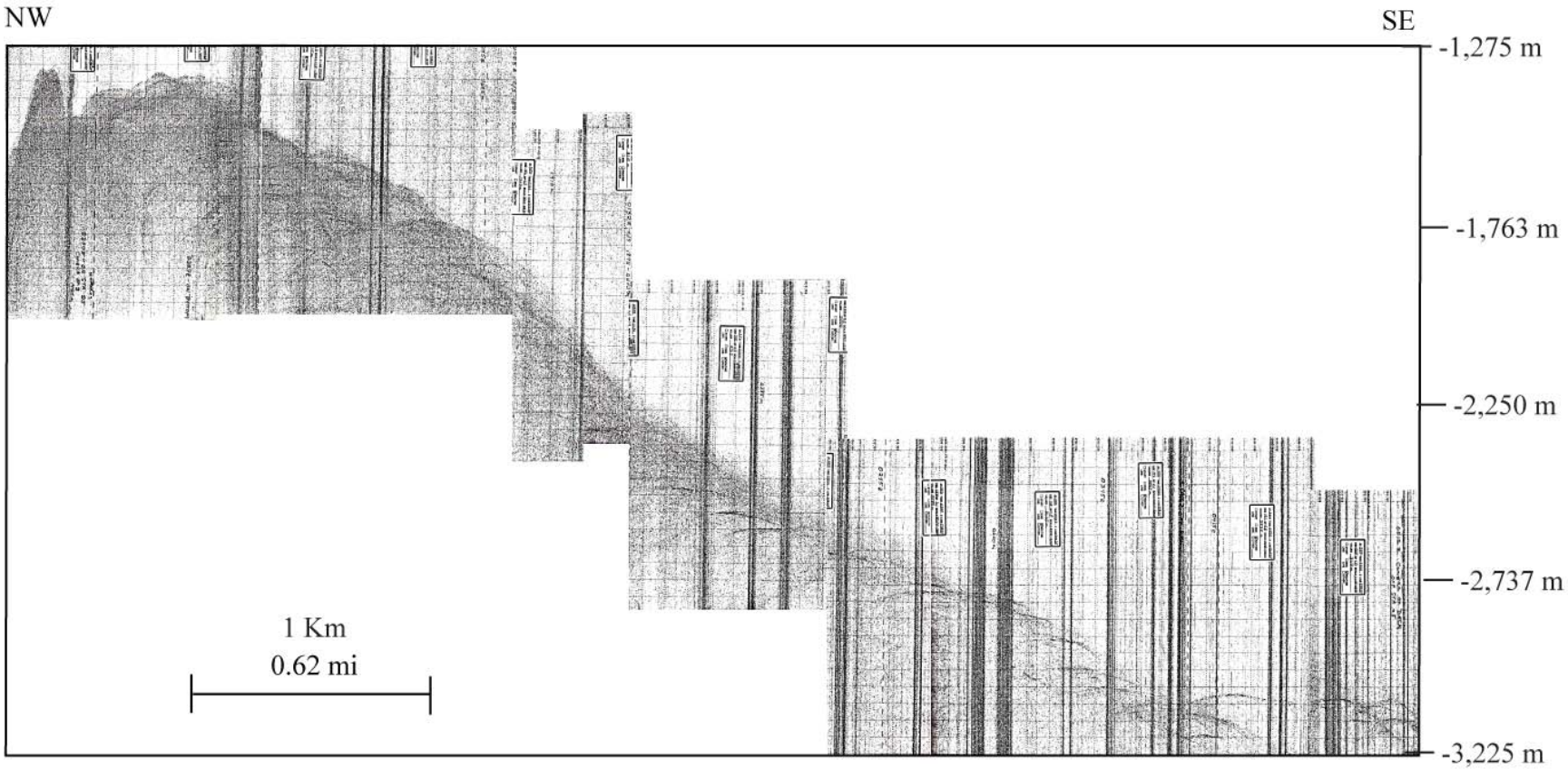

Figure 52. Flint Seamount 3.5 kHz bathymetry DSC3, deep-sea camera line 3.

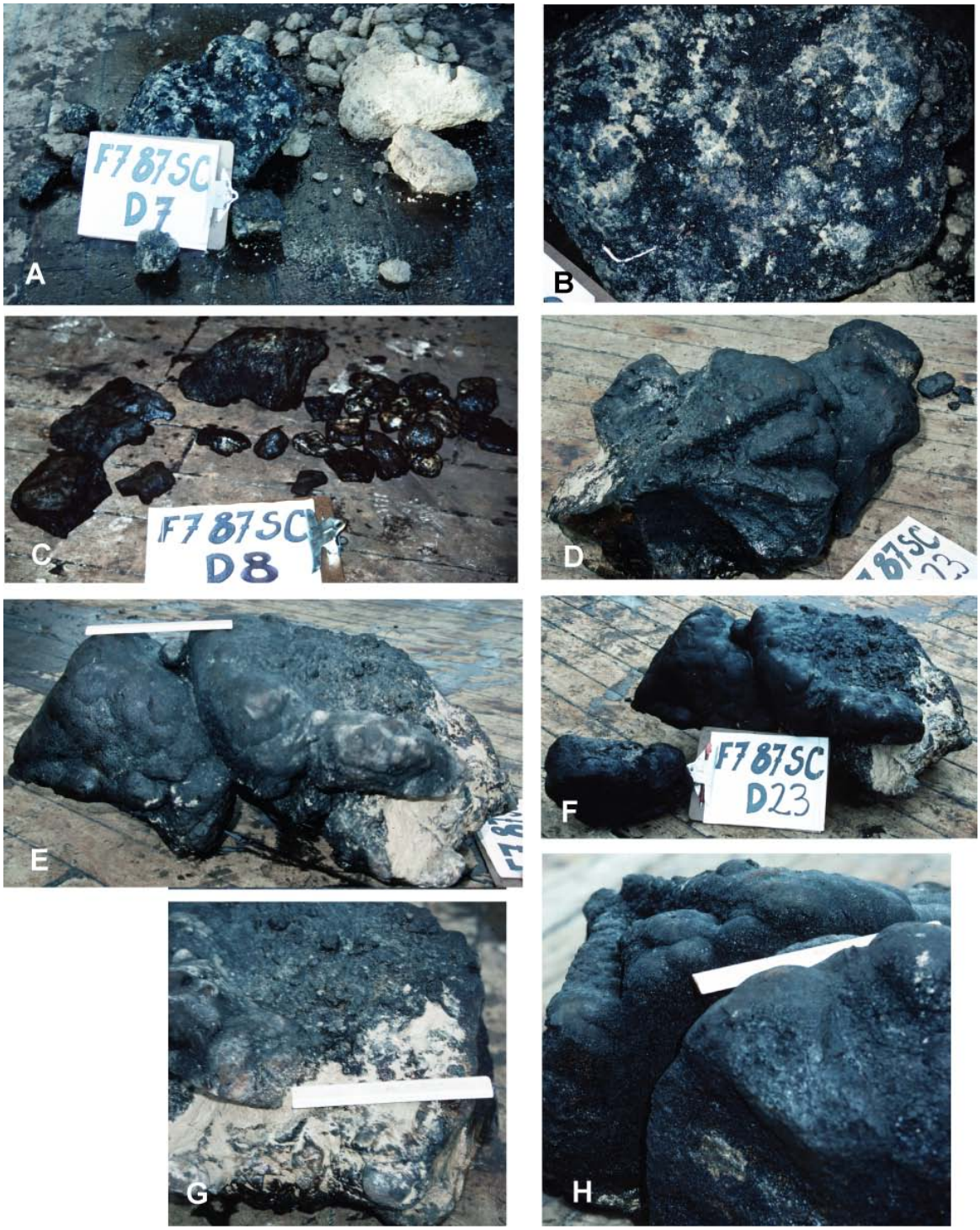

Figure 53. Photographs of dredge hauls. *A*, Dredge D7, Adam Seamount, showing mudstone and Fe-Mn crusts. *B*, Close-up of large center sample from dredge D7 (in *A)* showing Fe-Mn crust coated in places with calcareous mud. *C*, Dredge D8, Adam Seamount, with small rounded Fe-Mn nodules (right half) and basalt with Fe-Mn crust. *D-H*, Dredge D23, Flint Seamount, primarily basalt including pillow fragments with thick Fe-Mn crust, smoothed in places by bottom currents, such as in *E*; the Fe-Mn crust is coated in places with silty mud.

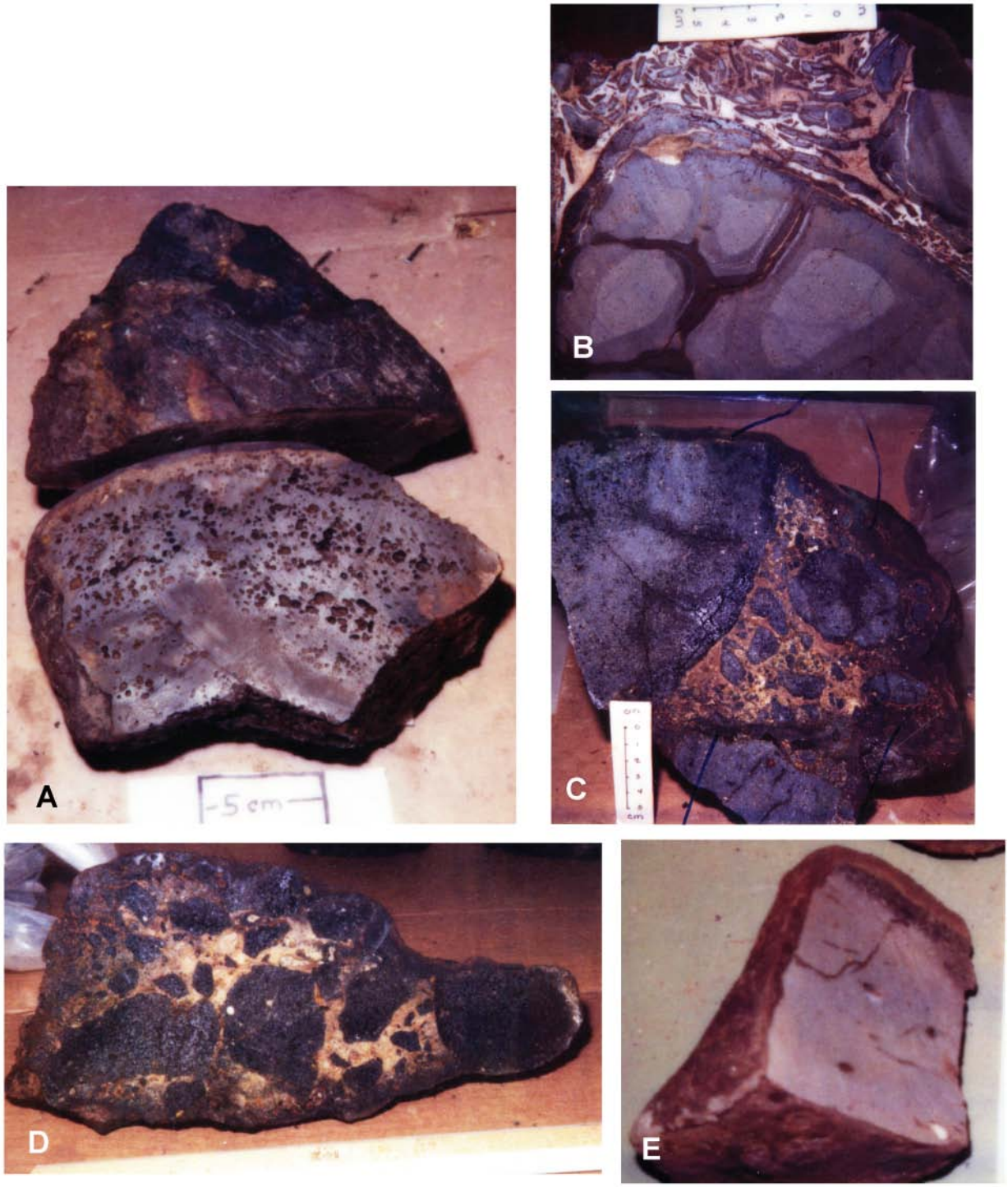

Figure 54. Sample photos from Rodriguez (*A*) and San Marcos Seamounts (*B-E*). *A*, D4-1 vesicular basalt with common vesicles. *B*, D5-3B fractured basalt with alteration rims along the fractures, encrusted by cement supported phosphatized carbonate breccia. *C*, D6-32 breccia with vesicular basalt in a phosphate matrix. *D*, D6-30 breccia. *E*, D5-17 basalt with a glass rim.

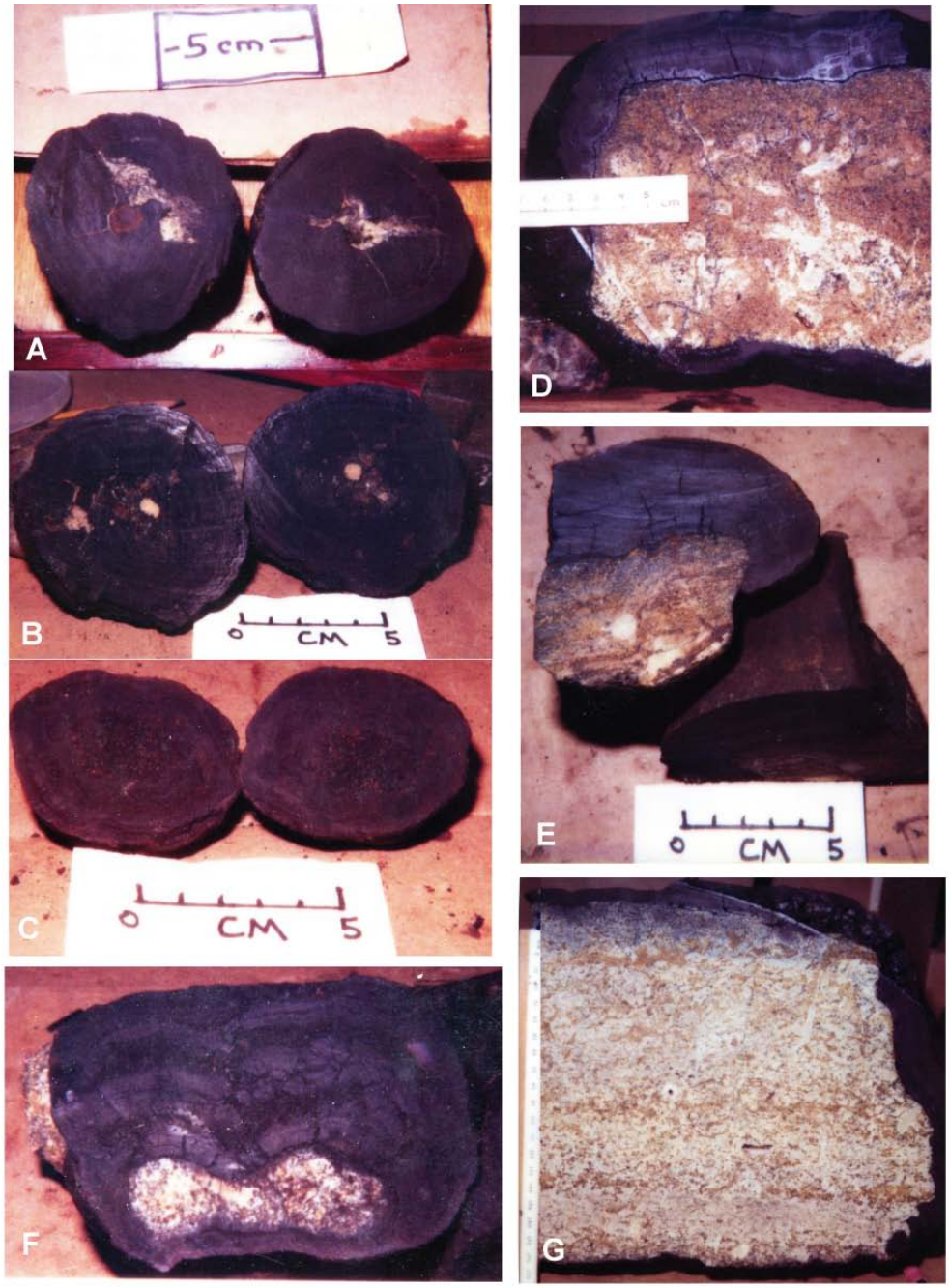

Figure 55. Photographs of cut samples from Adam Seamount. *A*, D8-5, Fe-Mn nodule with a fracture filled with sediment. *B*, D9-25, spherical Fe-Mn nodule with old nodule fragment nucleus and zeolites. *C*, D9-23, nodule with granular Fe-Mn nucleus. *D*, D9-3, volcanic tuff or hyaloclastite mixed with phillipsite-cemented basalt-clast microbreccia; laminated dark-brown Fe-Mn crust averages about 22 mm thick. *E*, D9-9E, 30-mm thick layered Fe-Mn crust on altered hyaloclastite. *F*, D9-9B, 35-mm thick layered Fe-Mn crust on hyaloclastite; a thinner crust occurs on the underside of the sample. *G*, D9-1, crudely bedded, extensively bioturbated, altered (to phillipsite and smectite) volcanic tuff or hyaloclastite.

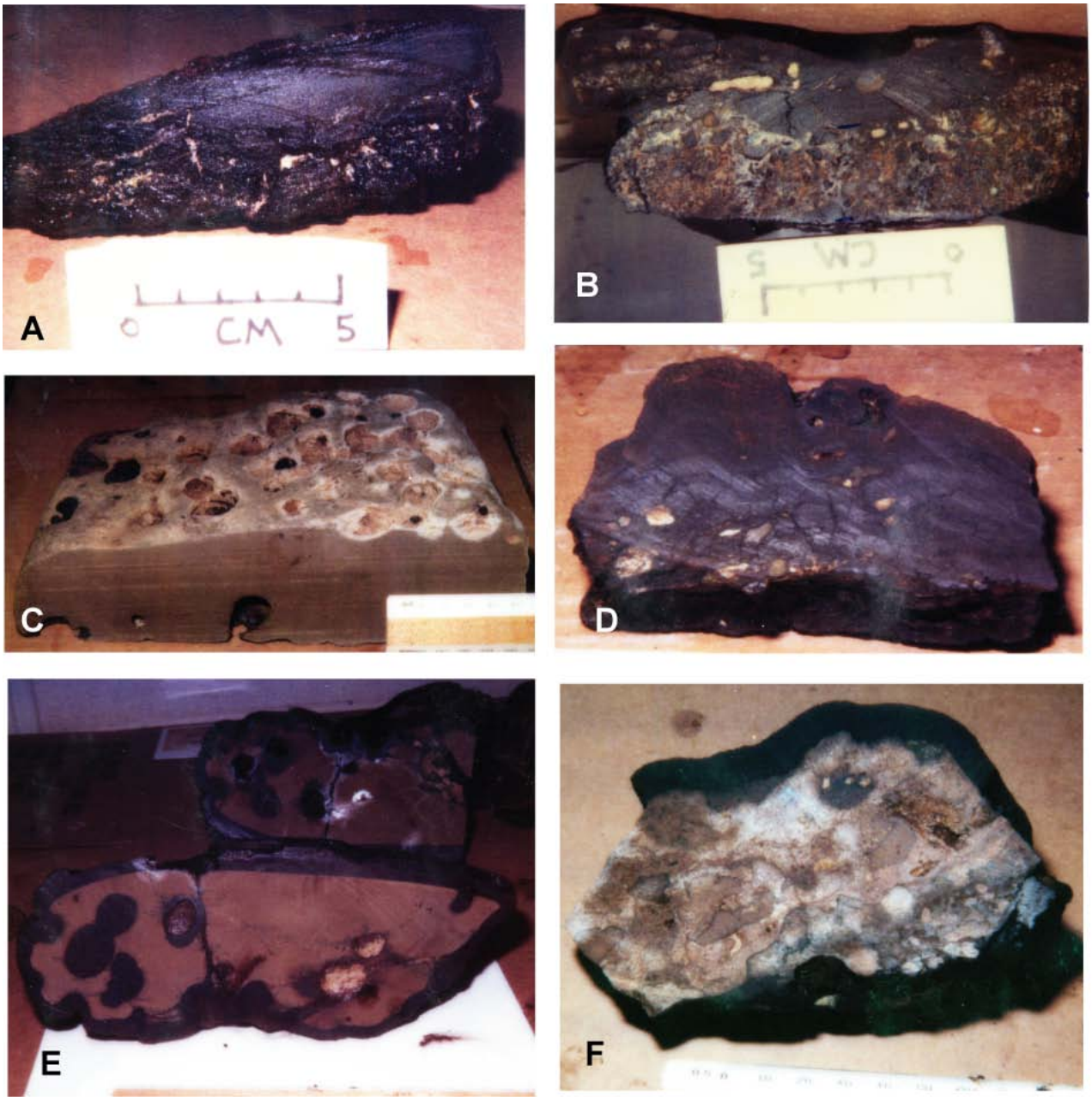

Figure 56. Photographs of cut samples from Hoss (*A-D*) and Little Joe (*E,F*) Seamounts. *A*, D10-3, 25- to 52-mm thick Fe-Mn crust fragment with zeolitic hyaloclastite inclusions. *B*, D10-4, massive 20-mm thick Fe-Mn crust with clasts of hyaloclastite phillipsite and breccia, resting on an altered breccia with Mn cement. *C*, D11-1, laminated and bored calcareous porcellanite. *D*, D11-7, 35- to 55-mm thick Fe-Mn crust with hyaloclastite clasts. *E*, D14-2, massive brown dolomitic mudstone with local dendritic Mn-oxide lining burrows; Fe-Mn crust averages 10 mm thick. *F*, D14-3, phosphorite breccia with a 10-mm thick black Fe-Mn crust.

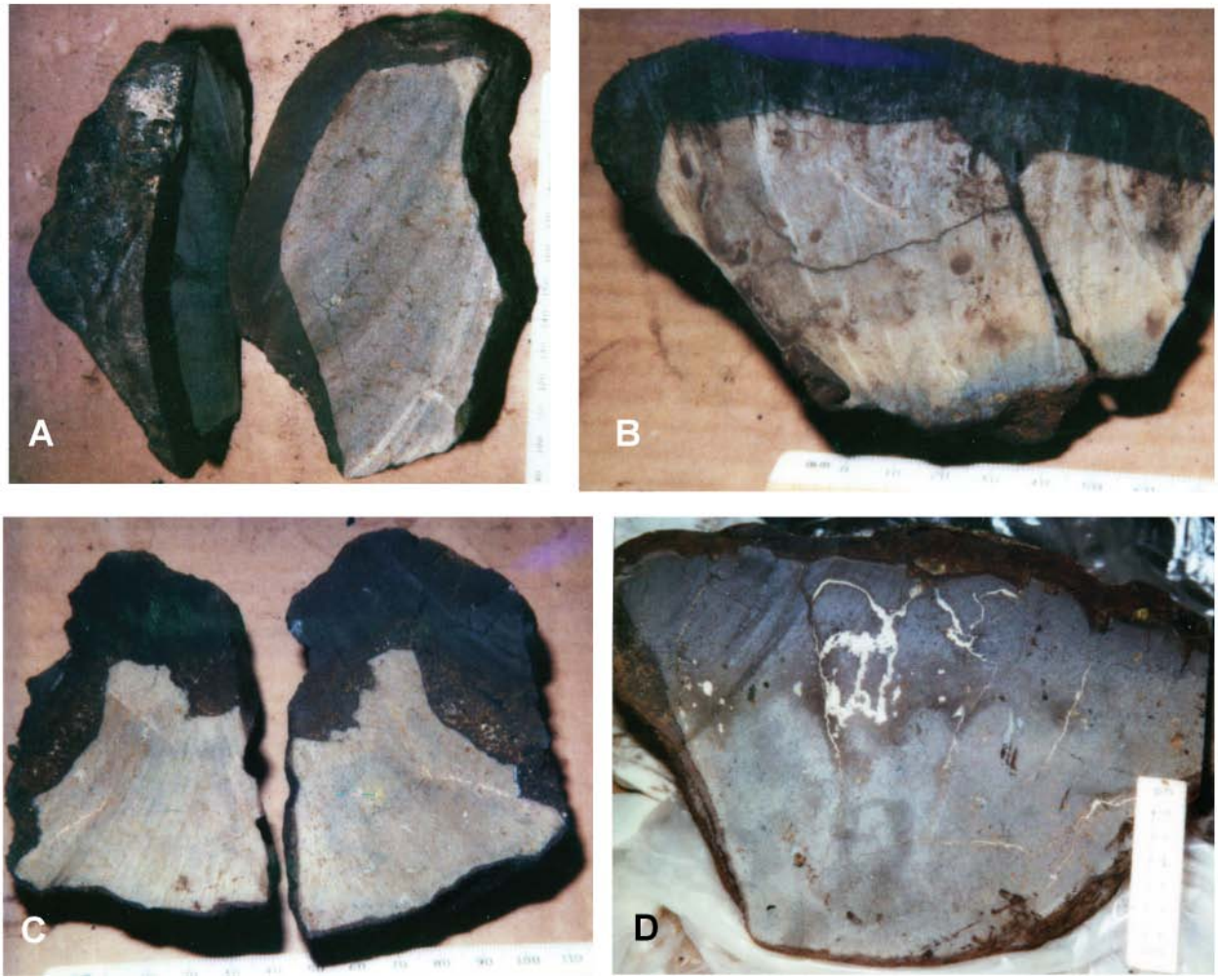

Figure 57. Photographs of cut samples from Ben (*A*-*C*) and Flint (*D*) Seamounts. *A*, D17-9, porphyritic basalt with 15-mm thick Fe-Mn crust. *B*, D17-14, massive basalt with 16-mm thick Fe-Mn crust. *C*, D17-13, massive basalt with 23- to 35-mm thick Fe-Mn crust. *D*, D23-3C, large massive pillow-basalt fragment with glass rind and 10- to 40-mm thick Fe-Mn crust.

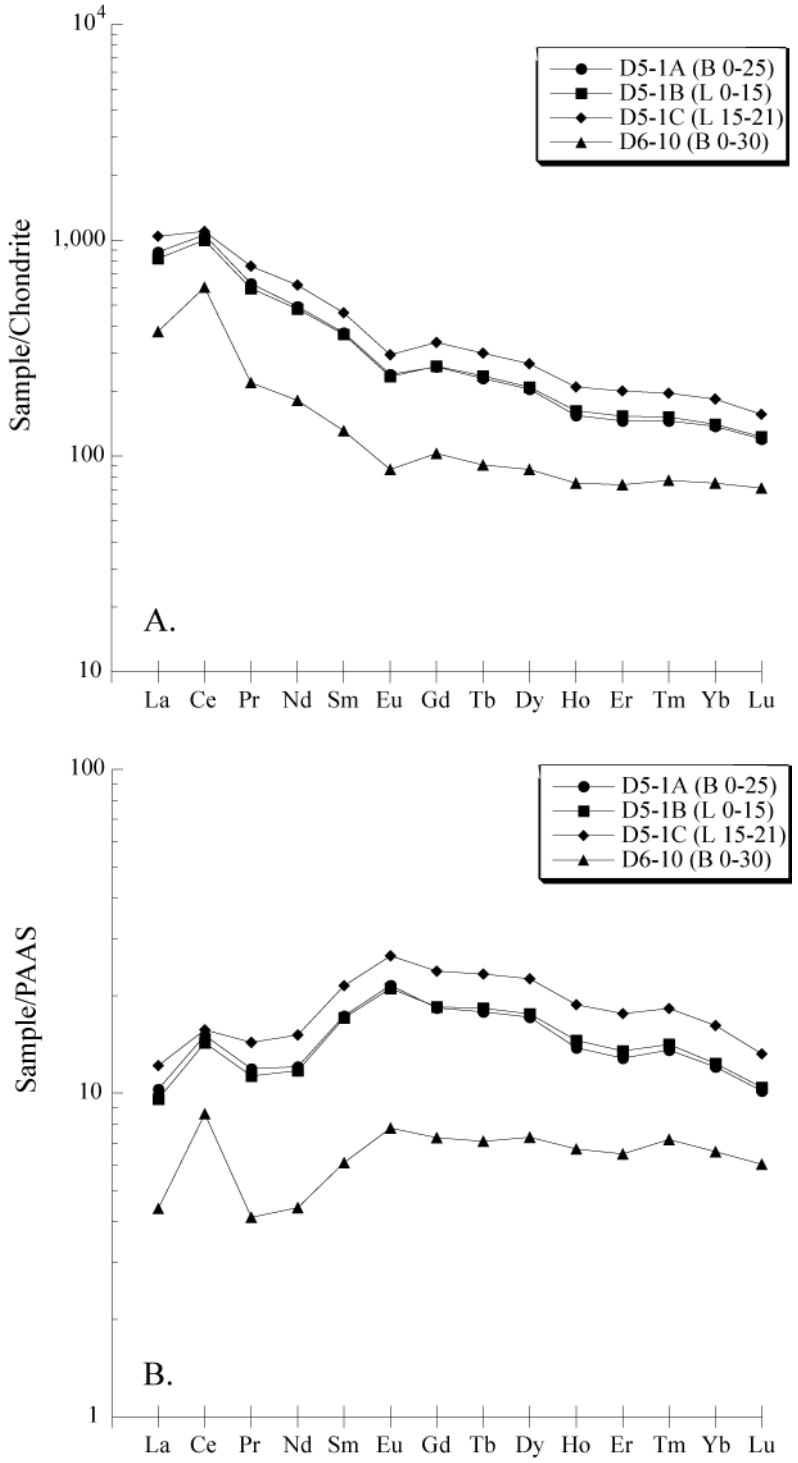

Figure 58. REE plots of 2 B, bulk crusts and 2 L, crust layers from dredges D5 and D6, San Marcos Seamount: *A*, Chondrite (Anders and Ebihare 1982) normalized and *B*, PAAS (McLennan 1989) normalized; interval in mm.

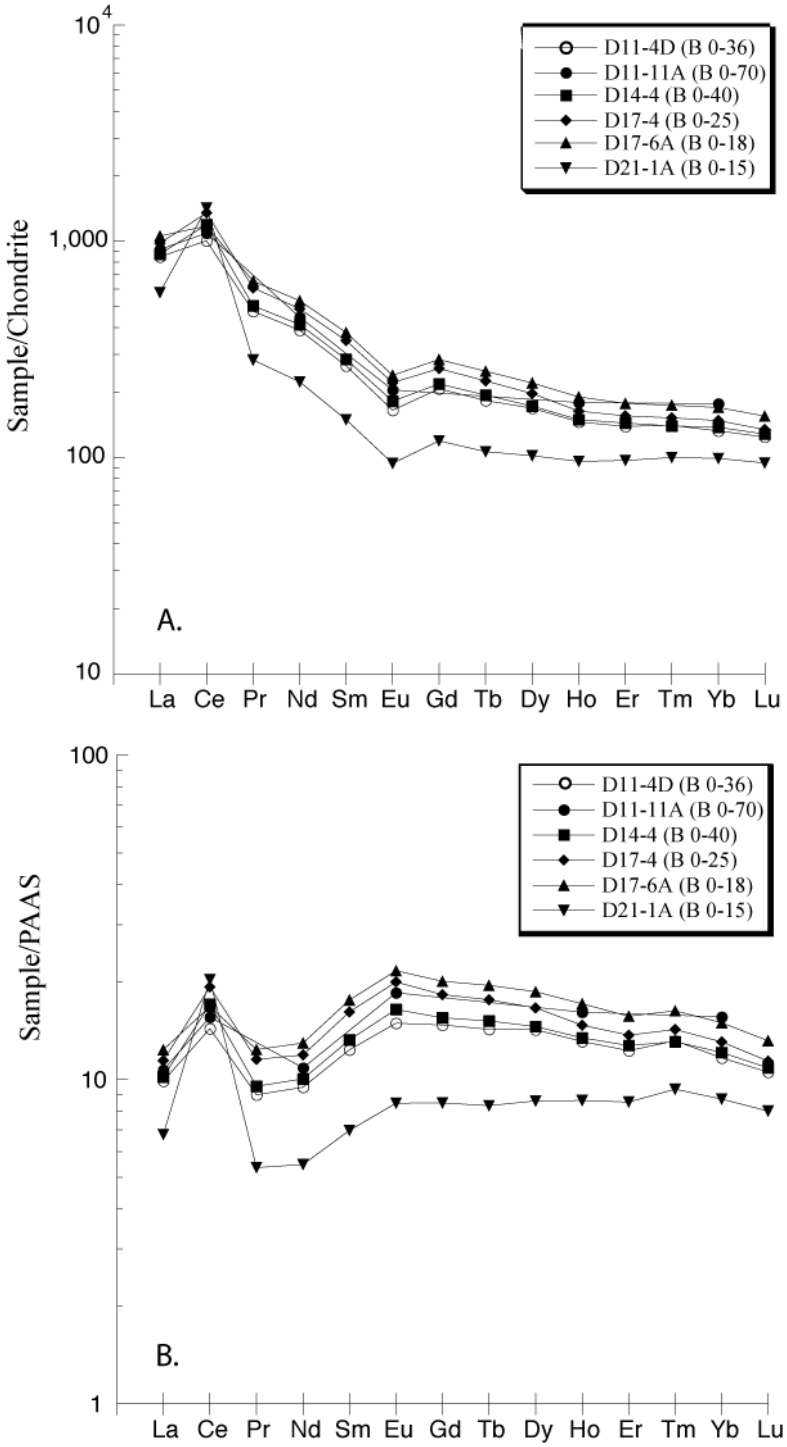

Figure 59. REE plots of B, bulk crusts from dredges D11, Hoss Seamount; D14, Little Joe Seamount; D17, Ben Seamount; and D21, Flint Seamount; *A*, Chondrite (Anders and Ebihare 1982) normalized and *B*, PAAS (McLennan 1989) normalized; intervals in mm.

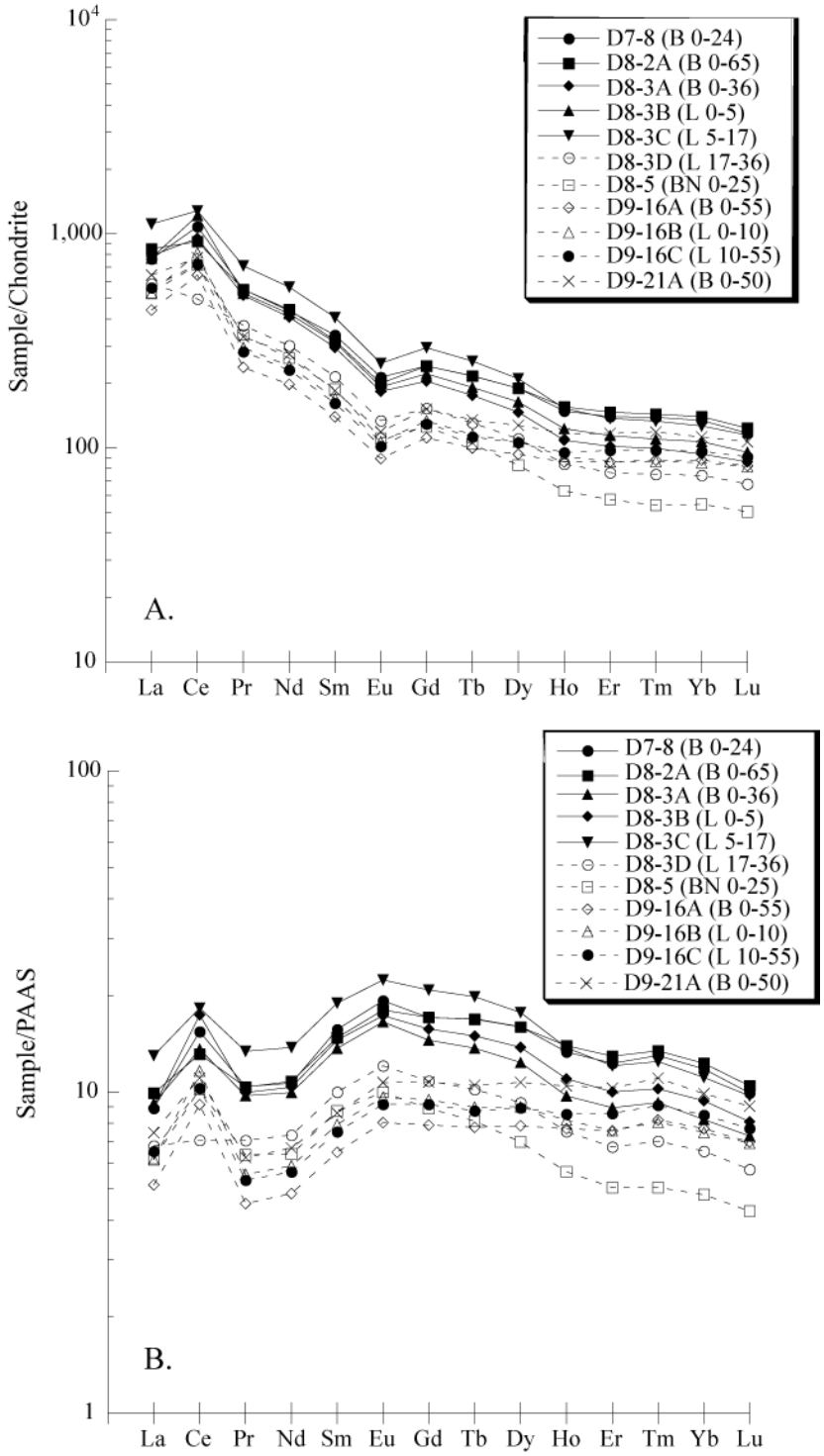

Figure 60. REE plots of B, bulk crust and L, crust layer samples from dredges D7, D8, and D9, Adam Seamount; *A*, Chondrite (Anders and Ebihare 1982) normalized and *B*, PAAS (McLennan 1989) normalized; (BN, bulk nodule; interval in mm.

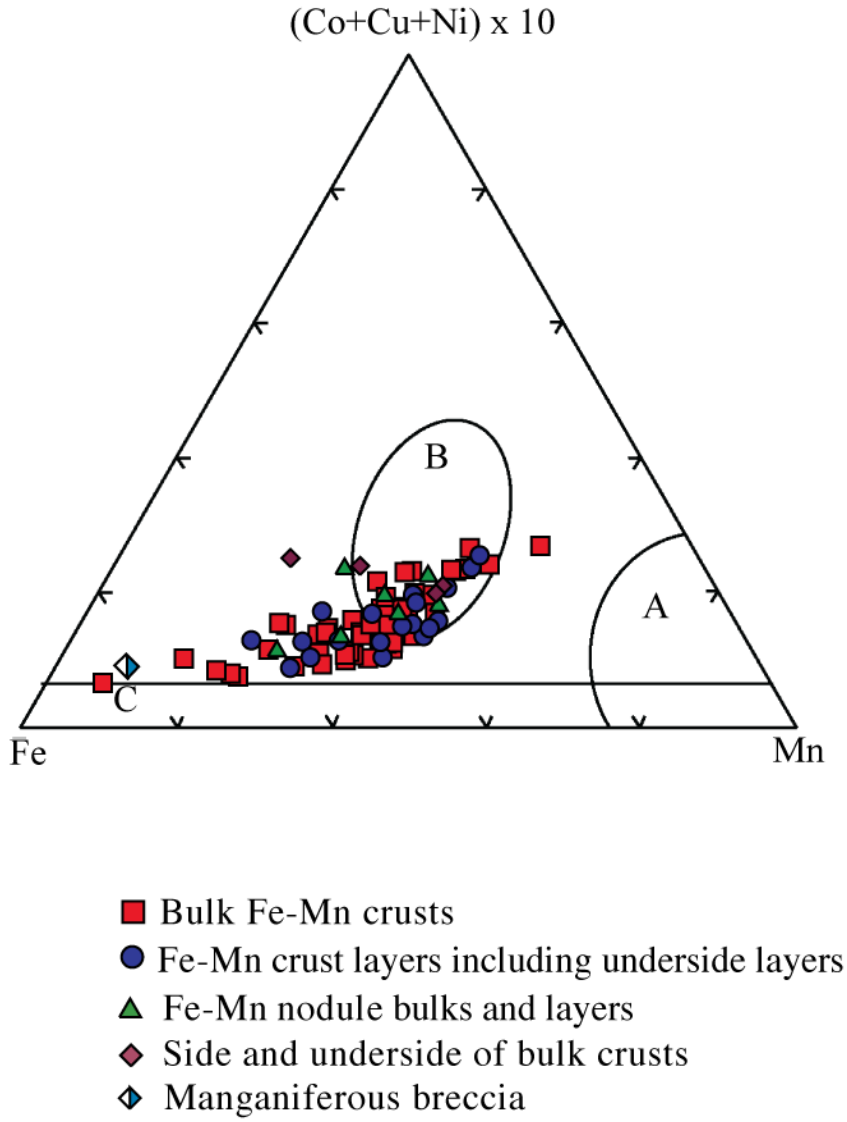

Figure 61. Ternary diagram showing A, diagenetic; B, hydrogenetic; and C, hydrothermal fields.